**An-Najah National University**

**Faculty of Graduate Studies**

# Purification of Water in Palestine from Persistent Pesticides Using New Synthesized Cellulose Nanoparticles

**By**

**Bayan Mohamad Mahmoud Khalaf**

**Supervisor**

**Prof. Shehdeh Jodeh**

**Co-Supervisor**

**Prof. Othman Hamed**

**This Thesis is Submitted in Partial Fulfillment of the Requirements for the Degree of Ph. D of Chemistry, Faculty of Graduate Studies, An-Najah National University, Nablus, Palestine.**

**2021**

# Purification of Water in Palestine from Persistent Pesticides Using New Synthesized Cellulose Nanoparticles

**By**

**Bayan Mohammad Mahmoud Khalaf**

**This Thesis was defended successfully on 3/3/2021 and approved by:**

| **Defense Committee Members** | **Signature** |
|---|---|
| – **Prof. Shehdeh Jodeh / Supervisor** |  ……. |
| – **Prof. Othman Hamed / Co-Supervisor** |  ..…….. |
| – **Prof. Ibrahim Kayali / External Examiner** |  ……. |
| – **Dr. Ibrahim Abu Shqair / Internal Examiner** |  ..……. |

# Dedication

I dedicate this thesis to my family for supporting and encouraging me all the way, and to my friends who have been supporting me and believing in my abilities.

# Acknowledgments

I would like to express my extreme gratitude for my supervisors at An-Najah National University, Prof. Shehdeh Jodeh and Prof. Othman Hamed. As well as for the Professors in Forschungszentrum Jülich in Germany, Prof. Erwin Krumpp, Dr. Roland Bol and Dr. Birte Drewes. They all didn’t keep any effort in encouraging me to do a great job, providing me with valuable information and advices to be better each time. Many Thanks for the kind communication and continuous support which had a great effect regarding to feel interesting and very proud about what I am working on.

Furthermore, I would love to thank my family members especially my mother and my father for believing in me, and I wish that I made them proud.

In addition, I would like to thank both Palestinian Water Authority and MEDRC for their financial funding for my PhD degree works.

Many Thanks to the Palestine Academy of Science and Technology and Forschungszentrum Jülich for their support and cooperation to do part of my project in Germany.

Finally, I won't also forget to present my special thanks for my friends who have been in my side during this research.

# الإقرار

أنا الموقعة أدناه مقدمة الرسالة التي تحمل العنوان :

**Purification of Water in Palestine from Persistent Pesticides Using New Synthesized Cellulose Nanoparticles**

أقر بأنّ ما اشتملت عليه هذه الرسالة إنما هي نتاج جهدي الخاص ، باستثناء ما تمّت الإشارة إليه حيثما ورد ، و أنّ هذه الرسالة ككل ، أو أي جزء لم يُقدّم لنيل أي درجة أو لقب علمي أو بحثي لدى أي مؤسسة تعليمية أو بحثية أخرى.

## Declaration

The work provided in this thesis, unless otherwise referenced, is the researcher's own work and has not been submitted elsewhere for any other degree or qualification.

**Student's name:** **اسم الطالبة: بيان خلف**

**Signature:**  **التوقيع :**

**Date:** **3 / 3 / 2021** **التاريخ:**

# List of Contents

# List of Tables

# List of Figures

# List of Abbreviations

| Symbol | Abbreviation |
|---|---|
| OISW | Olive Industry Solid Waste |
| OILW | Olive Industry Liquid Waste |
| BOD | Biological Oxygen Demand |
| COD | Chemical Oxygen Demand |
| MCC | Cellulose Microcrystalline |
| CNC | Cellulose Nanocrystalline |
| AGU | D-anhydroglucopyranose Unit |
| Lpcd | Liters per capita per day |
| POPs | Persistent Organic Pollutants |
| PCB | Polychlorinated Biphenyls |
| PCDF | Polychlorinated Dibenzofurans |
| PCDD | Polychlorinated Dibenzo-p-dioxins |
| t ½ | Half-time |
| $t_e$ | Equilibrium Time |
| DT50 | Disappearance time 50 |
| DMAc | Dimethyl Acetamide |
| TLV | Threshold Limit Value |
| WHO | World Health Organization |
| Ppm | Part Per million (mg/L) |
| Ppb | Part Per Billion (µg/L) |
| SEM | Scanning Electron Micrograph |
| UV-Vis | Ultra-Violet Visible |
| FT-IR | Fourier Transform Infrared |
| TGA | Thermogravimetric Analysis |
| HPLC | High Performance Liquid Chromatography |
| $^1$H NMR | Proton Nuclear Magnetic Resonance |
| $C_e$ | The equilibrium concentration of the adsorbate (mg/L) |
| $C_o$ | The initial concentration of the adsorbate (mg/L) |
| $R^2$ | Correlation Coefficient |
| $Q_e$ | The amount of adsorbate divided to adsorbent unit mass (mg/g) |
| $R_L$ | Dimensionless Constant Separation Factor |
| B | Constant that represents Langmuir affinity (L/mg) |
| $Q_o$ | The adsorption capacity at equilibrium (mg/g) |
| V | The volume of the solution (L) |
| M | The mass of the adsorbent (g) |
| $K_F$ | Constant in Freundlich Isotherm that related to the adsorption capacity (mg/g). |
| N | The heterogeneity Freundlich coefficient which used as indication of how feasible and favorable the process of |

| | |
|---|---|
| | adsorption (g/L) |
| $Q_t$ | The mass of adsorbate divided to the adsorbent unit mass at time t (mg/g) |
| $K_1$ | The rate constant for pseudo-first-order kinetic adsorption model with unit of ($mg.g^{-1}.min^{-1}$) |
| $K_2$ | The equilibrium rate constant for pseudo-second-order adsorption kinetic model with unit of ($g.mg^{-1}.min^{-1}$) |
| $K_p$ | The rate constant for diffusion Kinetic model ($mg.g^{-1}.min^{0.5}$) |
| C | Constant which used as an indication for the boundary layer thickness (mg/g) |
| $\Delta G$ | Gibbs free energy change (J) |
| $\Delta H$ | Enthalpy change (J) |
| $\Delta S$ | Entropy change (J/K) |
| T | The absolute temperature (K) |
| R | The universal gas constant with a value of (8.314 J/mol.K) |
| $K_d$ | Constant for thermodynamic equilibrium that equals ($Q_e/C_e$) with a unit of (L/g) |
| Cel-F | Cellulose functionalized with 2-Furan carbonyl chloride |
| Cel-P | Cellulose functionalized with 2,6-pyridine dicarbonyl dichloride |

**Purification of Water in Palestine from Persistent Pesticides Using New Synthesized Cellulose Nanoparticles**

**By**
**Bayan Khalaf**
**Supervisor**
**Prof. Shehdeh Jodeh**
**Co- Supervisor**
**Prof. Othman Hamed**

## Abstract

As the need of water increases annually in Palestine, and the available water resources are barely sufficient to meet the demands of the current quality life and the economy. There is a huge necessity of purifying water from different pollutants including pesticides. This research involves synthesis of the cellulose based adsorbents modified with 2-furan carbonyl chloride and cellulose modified with 2,6-pyridine dicarbonyl dichloride. Cellulose nanocrystalline (CNC) was also evaluated as a reference. The prepared cellulose-based adsorbents were characterized by SEM, FT-IR spectroscopy, $H^1$ NMR and TGA. Obtained SEM images showed that the adsorbent has an amorphous morphology, which made them ideal as adsorbents. They also showed good thermal stability as shown by TGA.

The adsorbent efficiencies of cellulose based adsorbents in addition to CNC were evaluated toward adsorption of the pesticides difenoconazole and tetraconazole in water.

The maximum extent of removal of difenoconazole and tetraconazole from water was shown by the cellulose modified with 2-furan carbonyl chloride, the adsorption efficiency reached 96.63% for 10 ppm Difenoconazole

concentration at 30 °C, pH 8, 20 minute contact time and 20 mg adsorbent dose. For 8 ppm Tetraconazole concentration, the percentage removal was 98.51% at 20 °C, pH 4, 15 minute shaking time and 20 mg adsorbent mass. The cellulose modified with 2,6-pyridine dicarbonyl dichloride derivative showed a removal efficiency about 95% for both difenoconazole and tetraconazole. Nanocellulose bio adsorbent showed a removal efficiency of 93.08% and 91.73% for Difenoconazole and Tetraconazole, respectively.

Adsorption isotherms, kinetics and thermodynamics were also investigated. Adsorption parameters detect that these adsorptions fitted with the Langmuir isotherm of adsorption and all reaction mechanisms fitted with pseudo-second-order adsorption kinetic model. The thermodynamic parameters proved that these reactions are favorable at room temperature, in which they are both spontaneous ($\Delta G < 0$) and exothermic ($\Delta H < 0$)

The synthesized adsorbents was also regenerated, and the percentage removal before and after adsorbent recovery was determined. The results showed a promising percent of removal for Difenoconazole and Tetraconazole.

# CHAPTER ONE

# INTRODUCTION

## 1.1 Background

### 1.1.1 Global Need for Clean Water

Water covers around 70% of our planet, but only 2.5% of this water is freshwater. This limited resource will need to support a projected population of about 9.7 billion by the year 2050; this means that an estimation by 3.9 billion will live by that date in severely unsafe water conditions [1, 2].

The pressure in using water resources results not just because of the population numbers but also due to excessive use. The global population tripled in the 20th century, however using water resources increased six-fold [3]. By the year 2050, water demands are expected to increase by 130% from household use and by 400% from manufacturing use [4].

The importance of water is very critical, but more importantly is the issue of having clean water for all people in the world. In general, clean water is the water that has an acceptable level of useful minerals, without any toxic substances, pathogenic organisms, taste, color and turbidity [4].

According to the World Health Organization (WHO), there are more than 1.1 billion persons cannot get any access to improved water supply. The results of inadequate water sources are catastrophic with 2.2 million deaths due to diarrheal diseases each year as an example. Generally, there are many

infectious agents detrimental to human health that grow in unsanitary/contaminated water and causing number of waterborne illnesses, such as typhoid, cholera, diarrhea and hepatitis. There are approximately 10–20 million people die each year due to waterborne diseases, and nonfatal infection causes death of more than 200 million people annually. [5–7].

Continuing coordination and cooperation between nations is so crucial for ensuring adequate and clean water is available for human, environmental and economic requirements [7].

### 1.1.2 Water Pollution

Toxins transferred by water can be regarded as one of the most harmful factors to humankind and environment. Water can be polluted with many toxic chemical substances including pesticides. These days, pesticides usage has been increased because of diversification of plant pests and agricultural development. The passage of water through heavily sprayed and fertilized agricultural lands has serious impacts leading to pollution of groundwater and surface water [8–10].

As a result of the uncontrolled pesticides practices for industrial and agricultural purposes, wastewater containing pesticides of high toxicity considers a worldwide public health issue [11]. Pesticides can be synthetic or natural compounds that are used to control pests. One of the most significant and earliest studies of the environmental effects of pesticides was published in 1962 [12]. In general. There are several studies performed in the past decades indicate that pesticides typically used at the ground surface

penetrate underground and leading to water pollution [13]. These toxic materials remain in underground resources due to environmental conditions and chemical structure. There are no comprehensive information on pesticide residues in the environment. However, many factors including chemical and physical characteristics of pesticides, as well as, weather conditions, can play an important role in toxin residues in the environment. The amount of these pollutants is determined to be under the permissible limits of pesticides in water (0.1 – 0.5 µg/L) [14].

## 1.2 Pesticides

### 1.2.1 Persistent Organic Pollutants

Persistent organic pollutants (POPs) are defined as organic compounds that resist biological, chemical, and photolytic degradation. These compounds are characterized by their semi-volatile, persistence, biomagnify and bioaccumulative properties. The presence of physicochemical characteristics in POPs permits them to occur either in the vapor phase or adsorbed on the atmospheric particles (aerosol), and hence enabling POPs to move for very long distances in the atmosphere before deposition occurs. Thus, they are supposed to be found in all over the world and in measurable concentrations [15].

The Stockholm Convention initially addressed twelve priority POPs; since then, these have been extended to 28 POPs by the year 2017. Despite the fact that many of these toxic materials were banned in the 1970's and 1980's, and others have been restricted in several countries, Persistent Organic

Compounds are still found in our air, soil and water in considerable amounts [15, 16].

POPs are classified into organochlorine pesticides that have been proven to be the widest production, use and release characteristics; as well as, they have the most resistant to degradation. Examples of Organochlorine pesticides are DDT and Aldrin. Persistent Organic Pollutants also include industrial chemicals, such as polychlorinated biphenyls (PCB). Additionally, some unintentional by-products of many industrial processes, especially polychlorinated dibenzofurans (PCDF) and polychlorinated dibenzo-p-dioxins (PCDD) [16].

POPs persistency can be measured by their half-life duration ($t_{½}$) or which can be also called Disappearance time 50 (DT50). For example; organochlorine DDT pesticide has a DT50 ranges from 2 to 15 years depending on the environment. The presence of POPs in the environment also affects human health through polluted drinking water, bio-accumulate in organisms and bio-magnify throughout the food chain [16–18].

Humans can be exposed to POPs through the direct exposure, occupational accidents and through the environmental pollution (including outdoor and indoor pollution). Short-term exposures to high concentrations of POPs may result in death. Chronic exposure to POPs; even to low levels, may be associated with a wide range of adverse health effects; such as cancer, endocrine disruption, reproductive and immune system alteration, neurobehavioral and developmental disorders. Furthermore, exposure of

humans to POP can eventually occur, via leaching of pollutants from treated soil into aquifers. As the majority of POPs are semi-volatile compounds, they are able to cycle among soil, air and water [16–18]. Characteristics of POPs include subcooled liquid vapor pressure, octanol-water (log $K_{ow}$) partition coefficients, that give information about molecule hydrophilicity. As well as, temperature of condensation. These characteristics enable the determination of the mobility of a persistent pollutant through a transportation cycle in the water, atmosphere, or soil [18, 19].

### 1.2.2 Persistent Pesticides in Groundwater

Pesticides have been increasingly and widely used due to the high nutritional demand by the world's population which significantly increases year by year. These organic compounds used for controlling agricultural pests, such as insects, weeds, rodents, and plant pathogens. Based on their chemical structure, pesticides are divided into four general categories: Organochlorine, Organophosphorus, Pyrethroid and Carbamate [20–22].

The persistence property of a Pesticide is often expressed in terms of half-life ($t_{½}$), that is defined as the length of time required for one-half of the original quantity to break down, pesticides can be divided into three categories based on half-lives: non persistent ($t_{½} < 30$ days), moderately persistent (30 days $< t_{½} <$ 100 days), or persistent pesticides ($t_{½} >$ 100 days). As a result of the mobility of many persistent pesticides in soil, groundwater becomes more susceptible to pesticide contamination [23, 24]. Pesticides mobility can be affected by several factors, such as; distance of water sources

from the area of application as shown in (Figure 1.1), vapor pressure of pesticide and its solubility in water. In addition, site and environmental factors have a significant effect on pesticides mobility, for example; weather, topography, canopy and ground cover, soil organic matter, soil structure and texture (percent sand, silt, and clay). Pesticide contamination of groundwater is of vital, especially in Palestine, where the main source of drinking water is groundwater aquifers [25–28].

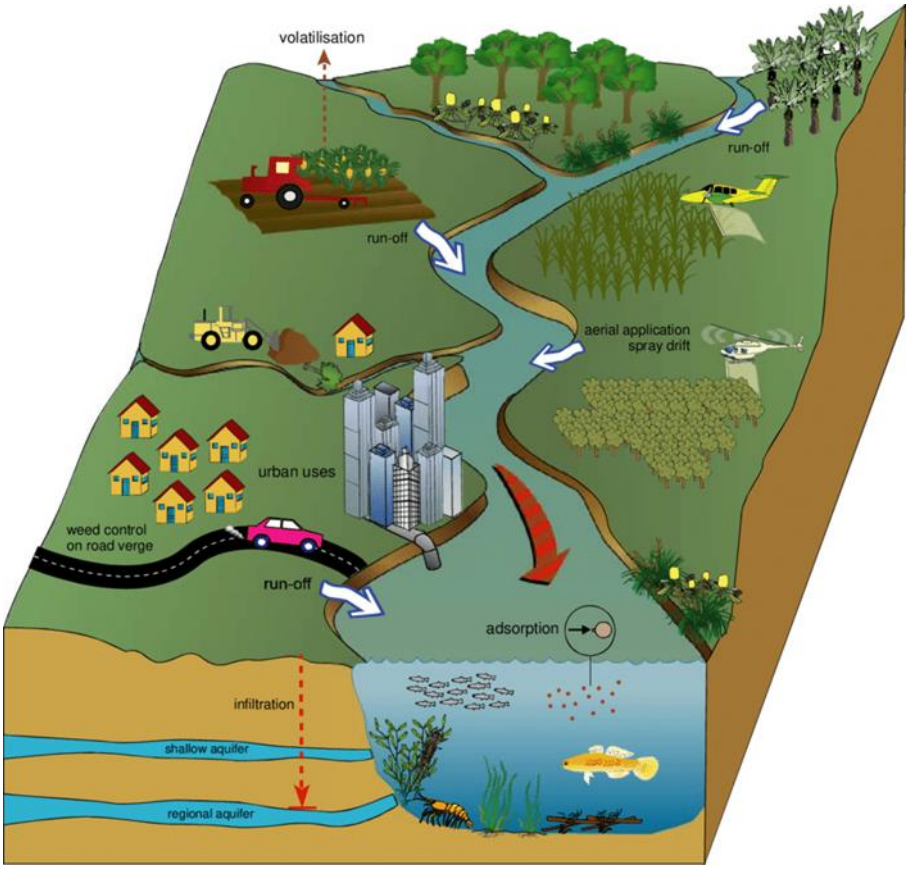


**Figure 1.1:** Sources and transport of pesticides in the environment [28].

There are many toxic pesticides that are used in Palestine, examples of these organic pollutants include Malathion, Oxadiazon, Endosulfan, Difenoconazole, Tetraconazole and others [29].

### 1.2.3 Difenoconazole

Difenoconazole, [1-((2-(2-Chloro-4-(4-chlorophenoxy)phenyl)-4-methyl-1,3-dioxolan-2-yl)methyl)-1H-1,2,4-triazole] has a solubility in water of (15 mg/L) at room temperature. In addition, it is very persistent pesticide with half-life in soil of more than 7 months. The chemical structure of Difenoconazole is shown in (Figure 1.2). This synthetic fungicide is used to prevent fungal diseases in plants owing to its systemic and broad-spectrum antifungal activities, for instance; basidiomycetes, ascomycetes and deuteromycetes. It is also an ergosterol biosynthesis inhibitor which is used during the entire growing season of crops [30, 31].


**Figure 1.2:** Chemical structure of Difenoconazole (C19H17Cl2N3O3).

Difenoconazole considered as an inhibitor of aromatase activity in human adrenocortical carcinoma cell line H295R. Due to its different molecular configurations, enantiomers of this pesticide probably exhibit stereoselectivity in the process of distribution, toxicity, absorption and degradation in the environment. Since previous studies on the fungicidal activity of difenoconazole implied that the biological activities of difenoconazole had enantioselectivity with the (2R,4S)-difenoconazole with a more pronounced fungicidal activity more than other forms [31–33].

Comparing difenoconazole with other triazole fungicides, it possess relatively high acute toxicity, so the contamination of aquatic ecosystems by difenoconazole is of a great environmental concern. In addition, exposure of water polluted by the pesticide difenoconazole has hazardous effects on human health that may cause death in case of high concentrations [31–33].

Removing of Difenoconazole by remediation was investigated in previous studies. As well as; several adsorbents for Difenoconazole extraction from water was suggested, such as; cyclodextrin-bases adsorbents, mesoporous activated carbon and graphene-based compounds [34–38].

### 1.2.4 Tetraconazole

Tetraconazole, [(RS)-2-(2,4-dichlorophenyl)-3-(1H-1,2,4- triazole-1-yl)propyl 1,1,2,2-tetrafluoroethyl ether] considers as a systemic fungicide containing a triazole group. This pesticide was introduced in the year 1973. Tetraconazole considers relatively soluble in water (156.6 $mg.L^{-1}$). In addition, it is highly effective in controlling and decreasing the adverse effect of a wide range of diseases; such as, powdery mildew and scab on the fruits, powdery mildew on the cucumbers and vines, as well as; powdery mildew and rust on the vegetables. Its chemical structure is shown in (Figure 1.3) [39].

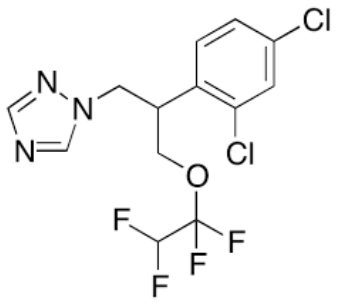


**Figure 1.3:** Chemical structure of Tetraconazole ($C_{13}H_{11}Cl_2F_4N_3O$).

As a result of the presence of the tetrafluoroethoxy group in Tetraconazole pesticide, it can act either as a lipophilic material or a hydrophilic material. Furthermore, the well-balanced ratio of hydrosolubility/ liposolubility will result with excellent systemic activity. Tetraconazole can rapidly enter the plant and distributes equally throughout the treated plant tissues; resulting with very good level in plant protection even in the vegetation grown after the spray or in the untreated section [39, 40].

Microbial degradation, photolysis and hydrolysis for tetraconazole fungicide move and proceed slowly in soil. Several field and laboratory studies estimate the half-time ($t_{1/2}$) of tetraconazole that depends on its application, concentration and soil texture, to be in the range from 69 days to more than 1688 days [40].

The persistency and bioaccumulation for tetraconazole affects adversely on environment and humankind, for instance, causing liver damage, kidney failure, and nervous system disorder. In order to reduce usage of this pesticide, the EU authorizes the limited use of tetraconazole pesticide for crops on the same field every third year [41–43].

Previous literatures suggested several methods of removing tetraconazole from water. Among them, light Induced Degradation and mesoporous alumina. Additionally, magnetic graphene nanoparticles and nanomembranes have been used successfully as adsorbents for the process of extracting tetraconazole pesticide from aqueous solutions [44–46].

### 1.2.5 Water Treatment

In order to minimize the adverse effect of pesticides, there are some strategies available for the removal of pesticides in wastewater, such as; solid phase extraction [47], photocatalytic degradation [48], ozonation [49], combined photo-Fenton and biological oxidation [50], advanced oxidation processes [51], fluid extraction [52], aerobic degradation [53], Nano filtration membranes [54], coagulation [55] and adsorption. Among the various methods, adsorption is the most promising one due to its high efficiency, flexibility, simplicity, ease of operation and low consumption [56–58].

In addition, purification of water using nanomaterials, such as Nano-powders, Nano-filters, Nano-adsorbents and others, has been considered to have a good treatment potential. Effective nanomaterials production with less waste and little resources in order to reduce pollution are becoming more and more available in the world. Using Nano-particles and Nano-adsorbents is considered a promising and useful method for reducing the potential risks of various pesticides in water because of large surface area, porous size, optical and electronic properties [58].

### 1.2.6 Situation of Water in Palestine

Palestine considers as one of the scarcest water availability ‘per capita supply’ in the whole world, with average domestic water consumption of just 70 liters per capita per day (lpcd), falling short of the ‘absolute minimum’ standard of 100 lpcd, that is recommended by the World Health Organization. This water scarcity results from both natural and man-made constraints, such as, increasing population numbers and industry, but above all reasons, occupation practices and restrictions imposed on both the water resources and its sector's development [59–61].

Palestine considers an agriculture country with excessive daily use of pesticides. Generally, any pesticide should be used just for the targeted pests with limited and suitable amounts. However, as a result of the knowledge gap about pesticides correct use, many farmers follow the rule “if little is good, a lot more will be better” that hence played very havoc effect on both humankind and environment [62–64].

## 1.3 Adsorption

### 1.3.1 Adsorption Features and Types

Adsorption technique is important process of utilitarian significance. It has practical applications in industry, biology, technology, and environmental protection. The efficiency of this treatment method depends on a number of factors. For instance, the nature of adsorbate and adsorbent, the surface area of the adsorbent and its activation. Also, it depends on experimental

conditions, such as; pH, temperature and pressure [65].

Adsorption is a surface phenomenon that refers to the adhesion of the adsorbate on the adsorbent surface. The adsorbate is an atom, ion or molecule that adsorbs on the pores of the surface, while the substance on which adsorption occurs is called the adsorbent. Adsorbate can be gas, liquid, or dissolved solids. Whereas, adsorbent may be a liquid or a solid [66].

Adsorption is more effective and suitable purification method for removing different pollutants over other conventional treatment techniques. This is because of its low cost, simplicity, possibility of adsorbent recovery, high efficiency in minimization of many chemical and biological wastes, and successful operation over a wide range of temperatures and pH values [67].

This treatment method results in forming a new intermolecular attraction forces between the adsorbate and the adsorbent. Depending upon the type of these forces, adsorption can be classified into two types.

**Physical Adsorption (Physisorption)**

Physical adsorption is characterized by weak intermolecular forces of bonding usually as dipolar interaction. It also has low heat of adsorption so it requires a little or no activation energy at all. Physisorption forms multi–molecular layers and it is not very specific. In addition, this type of adsorption is reversible, as the adsorbate molecule does not remain fixed on a specific location on the adsorbent surface, so it will be free to move from one position to another, and hence making adsorbate recovery is possible.

Physisorption usually takes place at low temperatures and can be easily reversed by heating or by decreasing the pressure [67, 68].

**Chemical Adsorption (Chemisorption)**

Chemisorption is irreversible, specific adsorption and taking place at high temperatures. The forces of interaction in chemical adsorption are strong chemical bond forces, such as covalent and ionic bonds. Also, it has relatively high adsorption enthalpy, so that; this adsorption usually requires high activation energy to be happened [68].

### 1.3.2 Equilibrium Isotherm Models

Adsorption process can be investigated and studied using the adsorption isotherm, that relates the amount of adsorbate on the adsorbent surface as a function of concentration (for liquid materials) or its pressure (for gases) for isothermal adsorption process (constant temperature). The data analysis for an Adsorption isotherm is very vital in order to determine the parameters of the adsorption equation that hence detects the observed results [68].

The most common studied adsorption isotherms in which they are usually applied for Liquid / Solid systems, include the theoretical equilibrium adsorption isotherm models that are Freundlich and Langmuir isotherms [68].

#### 1.3.2.1 Langmuir Adsorption Isotherm

Langmuir Isotherm is usually called “ideal monolayer localized adsorption model”; it was developed for representing chemisorption. Langmuir

isotherm based on the following assumptions: adsorption is limited into monolayer coverage, in which the adsorbed molecules cannot move or migrate across the adsorbent surface or interact with other neighboring molecules. Furthermore, the adsorbent surface in Langmuir adsorption model is uniform such that the adsorption sites are all have the same energy amount (i.e. energy equivalent of all adsorbent pores) [69].

Langmuir adsorption equation detects the coverage of adsorbate on the adsorbent solid surface to the amount of concentration for the medium above adsorbent solid surface, in which the process occurs at fixed temperature. Langmuir equation (1.1) can be represented as the following [69]:

$$\frac{C_e}{q_e} = \frac{1}{bQ_o} + \frac{1}{Q_o} C_e \qquad (1.1)$$

Where;

- $C_e$ is the equilibrium concentration of adsorbate (mg/L).

- b is a value represents the Langmuir affinity constant (L/mg).

- $Q_o$ is a value represents the adsorption capacity at equilibrium (mg/g).

- $q_e$ represents the adsorbate amount divided to the adsorbent mass with the unit of (mg/g), $q_e$ can be calculated using the following relation (1.2):

$$\mathbf{q_e = (C_o - C_e)\frac{V}{m}} \qquad (1.2)$$

Where;

- $C_o$ is the initial concentration of the adsorbate (mg/L).

- V is solution volume (L).

- m is the mass of the adsorbent (g).

- ($C_o$ – $C_e$) is the adsorbed amount (ppm).

Using equation (1.1), a plot for ($C_e/q_e$) values versus $C_e$ values for each adsorption can be used to detect the Langmuir isotherm parameters which are ($1/Q_o$) as slope and ($1/bQ_o$) as y-intercept [69].

### 1.3.2.2 Freundlich Adsorption Isotherm

Freundlich isotherm model has been described by adsorption to surfaces supporting sites with different affinities values or to adsorption on adsorbent heterogeneous surfaces. This isotherm model depends on a phenomena that stronger adsorbents binding sites will be occupied in the beginning of the adsorption, such that; the binding strength decreases with increasing the degree for site occupation [70].

According to Freundlich isotherm, the adsorbed mass divided to the mass of adsorbent can be expressed using equation (1.3) [70].

$$\boldsymbol{logq_e = logK_F + \frac{1}{n} logC_e} \qquad (1.3)$$

Where;

- $K_F$ is constant for Freundlich isotherm detects the adsorption capacity (mg/g).

- n value is the Heterogeneity coefficient and it can be used as an indication parameter to determine if the adsorption process is favorable or not (g/L).

1/n value represents the adsorption intensity, if values of (1/n) < 1, this indicates a normal adsorption. In case that, 1 < (1/n) < 10, this is indication of having a favorable adsorption.

Depending of equation (1.3), a plot of $\log q_e$ on y-axis versus $\log C_e$ on x-axis can be used to detect the parameters for Freundlich isotherm including $\log K_F$ as the plot y-intercept and slope of (1/n) value [70].

### 1.3.3 Adsorption Kinetic Models

Adsorption kinetic is the measure of the adsorption uptake with respect to time at a constant concentration or pressure and is employed to measure the diffusion of adsorbate in the pores. The adsorbate particles are transferred from bulk solution reaching the boundary layer of water molecules surrounding the adsorbent depending on molecular diffusion through water stationary layer. Adsorbate molecules are then transported to an available adsorbent site and hence forming an adsorption bond between the adsorbent and the adsorbate [71, 72].

There are many kinetic adsorption models that are suggested for describing the adsorption kinetics and reaction rate-limiting step. In general, kinetic models give vital information to know the adsorption behavior, as well as; the reaction rate in which such a specific constituent is adsorbed on an

adsorbent. Furthermore, these models detect whether the adsorption is fitted with a chemical or a physical adsorption, and which step in the reaction mechanism is the rate-determining-step [72].

Examples for the kinetic adsorption models including but not limited; , first-order-reversible-reaction-kinetic-model, external-mass-transfer-model, pseudo-first-order model, pseudo-second-order-model, Weber and Morris sorption kinetics, first-order equation of Bhattacharya, Venkobachar and Elovich's kinetic adsorption models, Adam–Bohart–Thomas kinetic adsorption relation. [73, 74].

### 1.3.3.1 Pseudo First–Order Kinetics

This kinetic adsorption model is considered the earliest model developed of investigating adsorption kinetics. Equation (1.4) represents the final integrated equation for pseudo-first-order model:

$$\boldsymbol{log(q_e - q_t) = logq_e - \frac{K_1}{2.303}t} \qquad (1.4)$$

Where,

- $q_e$ and $q_t$ represent the masses of adsorbate divided to the adsorbent mass at equilibrium time ($t_e$), and at time (t) respectively (mg/g).

- $k_1$ is pseudo-first-order-kinetic adsorption rate constant with a unit of (mg. $min^{-1}$. $g^{-1}$).

By using equation (1.4), a plot of $\log(q_e - q_t)$ on y-axis versus time values (t) on x-axis will give a straight line of pseudo-first-order-adsorption model

with y-intercept of $\log q_e$ and a graph slope equals ($-k_1/2.303$) [74].

### 1.3.3.2 Pseudo Second–Order Kinetics

This adsorption kinetic model detects that the rate-determining-step can be fitting with a chemical adsorption that includes valence forces, such that; electrons will be exchanged or shared between the adsorbate and the adsorbent [75].

Pseudo-second-order-adsorption-kinetic model can be represented by equation (1.5).

$$\frac{\mathbf{t}}{\mathbf{q_t}} = \frac{\mathbf{1}}{\mathbf{k_2 q_e^2}} + \frac{\mathbf{1}}{\mathbf{q_e}}\mathbf{t} \qquad (1.5)$$

Where;

- $k_2$ represents pseudo-second-order-kinetic adsorption rate constant at equilibrium with a unit of ($g.\ min^{-1}.\ mg^{-1}$).

Depending on equation (1.5). The plot of $t/q_t$ on y-axis versus time (t) on x-axis gives a linear relationship that detects the computation of a second-order rate constants including $k_2$ and $q_e$, in which ($1/q_e$) is the graph slope and ($1/K_2\ q_e^2$) as the y-intercept [75].

### 1.3.3.3 Intra-Particle Diffusion Kinetic Model

Intra-Particle Diffusion Adsorption model assumed a theory that was proposed by Morris and Weber scientists. Equation (1.6) is representing the adsorption kinetic model [76].

$$\boldsymbol{q_t = K_p t^{0.5} + C} \qquad (1.6)$$

Where,

- $K_p$ represents Intra-Particle-Diffusion-adsorption-model rate constant with a unit of ($mg/g.min^{1/2}$).

- C is a constant related to the boundary layer thickness with a unit of (mg/g) [76].

Using equation (1.6), a plot of $q_t$ on y-axis versus $t^{1/2}$ on the x-axis gives a linear relationship for intra-particle diffusion adsorption model in which the constant C represented the graph y-intercept and the rate constant $K_p$ is the slope [76].

### 1.3.4 Adsorption Thermodynamics

Thermodynamic studies of any adsorption process are vital to investigate if such an adsorption is a favorable process or not. The thermodynamic adsorption behavior is investigated depending on calculating the thermodynamic adsorption parameters: Change in Entropy (ΔS), Change in Gibbs Free Energy (ΔG), and Enthalpy Change (ΔH) such that; ΔG and ΔH have a unit of (J) and the unit of ΔS is (J/K) [76, 77].

Equation (1.7) represents the general relation between the thermodynamic adsorption parameters [76–78].

$$\Delta G = \Delta H - T\Delta S \qquad (1.7)$$

Where; T represents the absolute temperature with a unit of (K).

The Change in Gibbs Free Energy (ΔG) can be also represented by using

equation (1.8).

$$\Delta G = - RT \ InK_d \quad (1.8)$$

Where;

- R is the Universal Gas Constant that equals a value of 8.314 J/K.mol.

- $K_d$ is thermodynamic equilibrium constant that equals a value of ($q_e/C_e$) with a unit of mol or (L/g).

Combination of the above two equations, equation (1.7) and equation (1.8) will result in the following relation :

$$\mathbf{lnK_d = \frac{\Delta S}{R} - \frac{\Delta H}{RT}} \quad (1.9)$$

Depending on equation (1.9), graph of $InK_d$ values on y-axis versus (1/T) on the x-axis gives a straight line relationship with a slope of (-ΔH/R) and (ΔS/R) as the plot y-intercept. The name of this resulting plot is Van't Hoff graph [78].

An objective of this work is to develop natural-based adsorbent forms for removing pesticides from water. The natural material selected for this work is cellulose.

## 1.4 Cellulose

Cellulose is one of the most abundant biological and renewable compounds worldwide. This polymer consists of $\beta$-D-glucose units linked together by (1→4) glycosidic bonds to form cellobiose residues that are the repeating units in the cellulose chain. Cellulose consists of three hydroxyl groups per

anhydroglucose unit, that giving the molecule a high degree of functionality [79]. Cellulose can be used successfully as an industrial feedstock of many derivative materials and for unlimited numbers of commercial, pharmaceutical and other applications. In addition, modifying of the cellulose polymer surface can be of great interest, as a results of its large range of potential applications that can be applied [80].

Plants contain approximately 33% cellulose, whereas wood and Olive Solid Waste (OSW) contain around 50%, and cotton contains 90%. Extraction of Cellulose from OSW is of great importance, especially in Palestine, where the olive oil industry is one of the most economically important agro-food sectors. In general; there are several methods that can be used for cellulose extraction. The properties of the extracted cellulose and the degree of its purity depend on its raw material and pretreatment methods [81–83].

In particular, for extracting cellulose from its natural source like wood or olive industry solid waste, there are two main processes; Pulping and Bleaching [83].

**Pulping process**

It includes mechanical or chemical pulping. Mechanical pulping usually results in little or no waste, but it requires high energy. While, chemical pulping depends on treatment using chemicals at high temperatures. It can be applied in several methods, for instance; Kraft pulping, Steam explosion and Sulfite process [81–83].

**Bleaching Process**

It aims to improve the cleanliness of the pulp by removing extractives. Bleaching includes many steps, such as; chlorination, hypochlorite bleaching, chlorine dioxide bleaching and others [82, 83].

### 1.4.1 Microcrystalline Cellulose (MCC)

Microcrystalline cellulose is prepared from cellulose by purified depolymerization process, which usually carried out by treating cellulose with mineral acid. In the process of acid hydrolysis, the non-crystalline region is preferentially hydrolyzed. So that, the cellulose crystals are released. In the initial stage of the hydrolysis, the polymerization degree of cellulose decreases dramatically, but it approaches to a constant value, known as the leveling-off degree of polymerization (LODP) [84–86].

### 1.4.2 Cellulose Nanoparticles

Cellulose Nanocrystalline (CNC) or Nanocellulose is highly versatile bio-based renewable and relatively inexpensive material that has many advantageous properties, including biodegradability and nontoxicity. Nanocellulose has low density (1.6 $g.cm^{-3}$) and reactive surfaces of hydroxyl (–OH) sites which facilitates surface functionalization through grafting and click reactions in order to achieve various modifications with different surface properties [87].

Nanocellulose has a numerous potential applications, such as; its usage in the preparation of high-performance composites, it also has attracted much

attention from industry. Owing to the low energy consumption and the addition of significant value, Nanocellulose extraction from agricultural waste is one of the best promising alternatives for waste treatment [87–89].

In general, Nanocellulose can be obtained from concentrated acid hydrolysis of microcrystalline cellulose. Compared to microcrystalline cellulose, nanocrystalline cellulose possesses many advantages, due to high surface area, nano scale dimension, high specific strength and modulus, unique optical properties and many others. These physicochemical properties, as well as, wide application prospects of Nanocellulose have attracted significant interest from both industrialists and research scientists [89, 90].

### 1.4.3 Cellulose Solvents

As cellulose may degrade before melting upon heating; the dissolution and regeneration of cellulose are of vital and importance in order to process native cellulose into various geometries, such as; film, fiber and others. The complex structures of cellulose polymer with both crystalline and amorphous regions making it difficult to be dissolved in most organic and inorganic solvents. It usually be endowed with special functions through solution and graft copolymerization [91].

Cellulose should be dissolved in the homogeneous system of cellulose solvent in order to become a molecule-dispersed system of stable thermodynamic property. The solvents that commonly used to dissolve cellulose include ammonia/ $NH_4SCN$ [91] NaOH/(thio)[92] LiCl/DimethylAcetamide (DMAc) [93] N-methylmorpholine-N-

oxide/water [94] and ionic liquids [95]. Among these solvents, LiCl/DMAc is considered to be a very good solvent system for cellulose with many advantages, including, no chemical degradation during dissolution, as well as; dissolving high molecule weight cellulose (> $10^6$ g/mol) with perfect solution stability and without any chemical degradation. Thus, LiCl/DMAc has been widely used in many scenarios including chemical modifications and analysis processing [96–98].

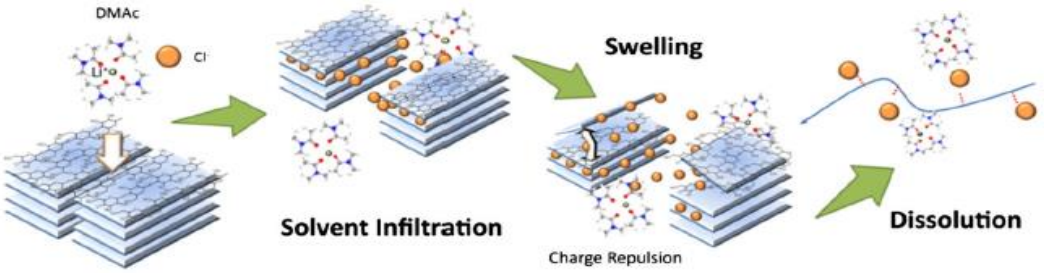


**Figure 1.4:** Dissolution of cellulose in LiCl/DMAc solvent system [98].

LiCl/DMAc solvent system was found to be the only functioning lithium salt-organic solvent combination for dissolving cellulose in 1980 by McCormick [99].

The dissolution of cellulose in LiCl/DMAc, is shown in (Figure 1.4). There are many studies investigated that chloride anions interact strongly with the hydroxyl groups of cellulose, which leads to the ionization of cellulose chains and the following dissolution in LiCl/DMAc. Such that, interaction of chlorine anion with cellulose hydroxyl protons results in the formation of competitive hydrogen bonding and disrupts the original intermolecular hydrogen bonding of cellulose. In addition, it is found that the native cellulose can be dissolved quickly in LiCl/DMAc only after being pretreated

by water, methanol or DMAc. The dissolution of cellulose is also affected by its source, for example; the cellulose from annual plants required longer dissolution time than that from wood due to hemicellulose hindering. As well as, studies have suggested that the dissolution of cellulose in LiCl/DMAc was better at 5 °C than at 25 °C [99, 100].

The dissolution kinetic of cellulose in LiCl/DMAc strongly depends on its solvent treatment conditions. By comparison, even though the solvent treatment of cellulose significantly improves its dissolution rate in LiCl/DMAc, studies has obtained nano-sized pores of 1 nm that are created after dissolution and the inter-molecular hydrogen bonding (O3–O6) becomes weaker. In addition, the mobility of cellulose is enhanced and the characteristic length is shortened. For the solvent treatment, the solvent type has strong influence on the dissolution of cellulose. Such that, DMAc treated cellulose could be dissolved much faster (in few hours) than untreated cellulose (more than 1 year) [100–102].

### 1.4.4 Cellulose based Derivatives

As known, Cellulose is the most important and abundant organic and renewable biopolymer produced by plants worldwide, as well as, the most predominant basic structural component of all plant fibers. The molecular structure of cellulose is of prime importance, as it explains many of its characteristic properties, such as; biodegradability, high functionality, hydrophilicity and chirality. As a renewable material, cellulose polymer and its derivatives have been widely studied, focusing on their chemical,

biological, as well as; mechanical properties. Resource of cellulose in the nature increases by means of annual biosynthesis of 75 billion tons. Therefore, production of cellulose nanomaterials can be inexpensive source with so many applications [103–106].

Derivatizing cellulose interferes with the orderly crystal-forming hydrogen bonding, so that even hydrophobic derivatives may increase the apparent solubility in water [103–106].

Carboxymethylcellulose, Methylcellulose, Cellulose acetate, Ethylcellulose and native cellulose have been used in various industrial applications that included but not limited to; emulsifier, lubricant, glue and binder, barriers films, optical and biomedical devices, pharmaceutical raw materials, flame retardants, resins and filters, blends and composites. The unlimited applications of cellulose derivatives are because of their low cost, softness, comfort, toughness, natural feel, transparency and many other favorable aesthetic properties [107, 108].

### 1.4.5 Applications of Nanotechnology

Nanotechnology is the understanding and controlling matter at dimensions about 1-100 nm that can used in many novel applications. Nanomaterials from cellulose and lignocelluloses are very important in nanotechnology field. Nanocellulose derivatives have received a lot of interest in the last few decades because of unique characteristics, such as; having high tensile strength, low coefficient of thermal expansion, and high surface area to volume ratio [109–111].

Nanocrystalline cellulose is the individual nanocrystalline regions of elementary nanofibrils of crystalline cellulose obtained after the amorphous regions have been removed via hydrolysis with strong acids, in which their particle size depending on temperature, acid concentration and time. Nanocrystalline cellulose in the range of 100–300 nm long has been isolated and it is anywhere from a tenth to a quarter of the strength of carbon nanotubes. A decreased in the size of a nanoparticle leads to a fractional increase in the surface atoms and consequently, it increases reactivity and makes them highly reactive [111, 112].

Cellulose nanocrystals can be used as a starting material for the next generation of cellulose based materials of high mechanical strength, toughness, load bearing potentials, light weight, low density, low cost, biodegradability, enhanced energy recovery and chemical property stability. Under careful selection of reaction conditions, highly crystalline rod-like hydrophilic cellulose nanocrystals with properties comparable to other Nano reinforcement materials can be obtained. Cellulose nanocrystals have low cost compared to other nanoparticles and have high aspect ratio (length / diameter) varying between 30–150 depending on the source, and the processing method from which it is obtained [111–113].

Nanocrystalline cellulose materials have been used as strong template for impregnation for a wide range of different nanomaterials to form composites. For example, mineral ($Ca_x(PO_4)_y$, $CaCO_3$ and montmorillonite), metals (Au, Ag, Pd, Ni, …, etc.), and carbon (carbon nanotube and graphene)

nanomaterials have been incorporated into nanocellulose, and materials with extraordinary optical electrical and catalytic properties were also obtained [111–113].

Generally, ultra-small nanomaterials have many unique physicochemical properties; for example, high bonding ability, developed specific surface and high degree of reactivity, which are different from macroscopic materials of the same composition. These properties significantly expand the application areas of nanomaterials. The main technical applications of nanomaterials include nanochips, nanosensors, nanocomposites, nanoscale labels and indicators. In pharmaceutics and medicine, nanomaterials can also be used as carriers for drug delivery, as well as; for advanced treatment and diagnostic methods. Furthermore, nanomaterials can be used for water treatment from different pollutants with high degree of efficiency [112, 113].

## 1.5 Research Objectives

### 1.5.1 General Objectives

1. Design and synthesize cellulose based novel adsorbents for Pesticides.
2. Evaluate the efficiency of the target adsorbents toward pesticides removal from water.
3. Develop a method for regenerating the adsorbents and reuse them.

### 1.5.2 Specific Objectives

1. Synthesis of novel environmental friendly compounds including Cellulose nanocrystalline, Cellulose functionalized with 2-furan carbonyl chloride, and Cellulose functionalized with 2,6-pyridine dicarbonyl dichloride.
2. Removal of Difenoconazole and Tetraconazole pesticides from water using the new synthesized adsorbents.
3. Study the several solution factors such as; pH, time, concentration, temperature and adsorbent dose, to investigate the extent and the efficiency of each adsorption process.
4. Study the adsorption isotherms, kinetics and thermodynamics of the adsorption of pesticides on cellulose derivatives.
5. Recovery of cellulose-based derivatives after adsorption process and finding the efficiency of multiple reusing of each adsorbent.

## 1.6 Research Questions

1. What are the optimum conditions of pH, temperature, contact time, concentration of adsorbate and amount of adsorbent for the synthesized materials to adsorb persistent pesticides efficiently?
2. To which extent the new synthesized cellulose compounds can tolerate and adsorb pesticides in water?
3. Can cellulose derivatives be used to clean up polluted water to high degree of purification?

## 1.7 Novelty of Thesis

Finding out ideal and novel treatment technique which is ready to uptake persistent pesticides such as, tetraconazole and difenoconazole from the water.

# CHAPTER TWO

# EXPERIMENTAL PART

## 2.1 Chemical Materials

Chemicals were of analytical grade, materials were purchased from Sigma Aldrich Companies for chemical substances in Munich, Germany and Jerusalem, Palestine. All materials were used without any further treatment unless otherwise specified. The chemicals for this project were: ethanol, anhydrous lithium chloride (LiCl), sulfuric acid ($H_2SO_4$), triethylamine ($Et_3N$), Argon gas, Nitrogen gas, anhydrous dimethylacetamide (DMAc), acetonitrile, sodium hydroxide (NaOH), hydrochloric acid (HCl), dimethyl sulfoxide, 2-furan carbonyl chloride, 2,6-pyridine dicarbonyl dichloride, difenoconazole and tetraconazole.

## 2.2 Instrumentations

The analytical instruments include: pH meter (JENWAY model: 3510,) Glassware, Mechanical Ultrasonic Cl, : Water shaking Bath (Daihan Labtech (20 to 250 rpm Digital Speed Control), Thermometer, Thermogravimetric analysis (TGA) (rate of increasing temperature =10 °C/min, $N_2$ is used as gaseous atmosphere), Proton Nuclear Magnetic Resonance using a Bruker 600 MHz spectrometer and equipped with a 5 mm broadband CryoProbe Prodigy (Forschungszentrum Jülich), Scanning Electron Microscope (SEM, Tubney Woods, JEOL 7400F Oxford Instruments Inca, Abingdon, Oxon OX13 5QX, UK), Ultraviolet-Visible Spectrophotometer (UV-1601 model,

SHIMADZU), Fourier-Transform Infrared Spectrophotometer (Nicolet iS5, iD3 ATR, Thermo-Scientific), High Performance Liquid Chromatography (HPLC) instrument (Waters 1525 Binary HPLC Pump ,Waters, Singapore) with Waters 2998 Photodiode Array Detector (PAD).

## 2.3 Extraction of Cellulose from OISW

### 2.3.1 Kraft pulping

Kraft pulping was conducted on the extracted pulp in a 2.0 L beaker covered with a watch glass (it is usually better if carried out in a high Parr Reactor of one liter capacity at 160 °C). In all experiments, the liquor to Olive Industry Solid Waste (OISW) ratio, cooking temperature, temperature rising time, holding time, and operational pressure were 4:1, 100 $^{o}$C, 30 min, 90 min, and 50 psi, respectively. Active alkali charge is defined as [NaOH+$Na_2S$], and sulfidity is defined as [$Na_2S$ / (NaOH+$Na_2S$)], where the concentrations are expressed as g/L $Na_2O$. At the end of pulping, the produced pulp 'cellulose left over after the pulping process' was collected using suction filtration, then washed for many times with tap water, air dried at room temperature, and stored in plastic bags for further use [114].

### 2.3.2 Pulp Bleaching

Bleaching of pulp obtained from OISW was performed using bleaching sequence DEHP, for which the individual stages were carried out as follows:

- D-stage: Conducted in plastic container at 10% consistency, for 1 hour at 70 $^{o}$C, and 1.0% $ClO_2$ (based on the pulp weight), with an end pH of approximately 2.5.
- E-stage: Conducted in a plastic bag at 10% consistency for 90 min at 60 °C and with 5% NaOH (5% based on pulp weight). After the completion of the treatment, the produced pulp was filtered and washed for several times with distilled water until neutral filtrate was obtained.
- H-stage: Conducted in a plastic bag at 10% consistency for 60 min at 60 $^{o}$C and at a pH of 10, Hypochlorite charge of 2.5% based on pulp weight, NaClO was obtained from a stock solution that contained 5% of NaClO.
- P-stage: Conducted in a plastic bag at 10% consistency, for 60 min, at 60 °C and a pH of 9 to 11 and with 2% $H_2O_2$, 0.5% $MgSO_4.7H_2O$, and 3.0% NaOH (based on pulp weight). The mixture was filtered, washed with water until neutralization, and air-dried [114].

## 2.4 Preparation of Cellulose Nanocrystalline (CNC)

Extracted cellulose was converted to cellulose nanocrystalline as follows: (10.0 gram) cellulose was added to 500 mL beaker containing (180 mL) of distilled water and stirred magnetically for about 30 minutes. Then, 20.0 gram concentrated sulfuric acid $H_2SO_4$ is added in order to produce 10 weight% of sulfuric acid solution. After that, the mixture has been stirred magnetically for 2.0 hours at temperature of 60 °C. The hot reaction mixture

was then diluted using ice-cold distilled water. After that, the colloidal suspension has been centrifuged at 10,000 rpm and decanted. To the residue was added a 100 mL, mixed then centrifuged and after that decanted. This process has been repeated for three times to ensure removing sulfuric acid and the hydrolysis product completely. The final product of cellulose nanocrystalline adsorbent is shown in (Figure 2.1).

**Figure 2.1:** Cellulose Nanocrystalline product.

## 2.5 Synthesis of Cellulose-Based Adsorbents

### 2.5.1 Activation and Dissolution of Cellulose

Before modifying cellulose, lithium chloride/dimethylacetamide solvent system was used for cellulose dissolution. Chains of cellulose polymer were activated using water, methanol, and dimethylacetamide (DMAc) respectively, as initial steps; which are required for having an effective and quick process of cellulose dissolution using LiCl/DMAc [115].

Activation process does not affect the crystallinity of cellulose, but it is used in order to have unfold chains, and hence a relaxed conformation of cellulose by enhancing the solvent diffusion kinetics to the crystalline regions which

are packed tightly. This process of dissolving cellulose has many advantages, for example; it does not lead to thermal runaway reaction, ease of processing since there is no need of additive or specialized equipment's, as well as; there is a possibility of recyclable with a high recovery rate [116, 117].

In the dissolution mechanism (Figure 2.2), chloride ion interacts with cellulose (due to $Cl^-$ basicity), followed by an exchange of DMAc in the lithium coordination sphere by cellulose hydroxyl groups, since $Cl^-$ ions get accumulated along the cellulose polymer chain which results in an anionically charged polymer, and the macro cation (Li–DMAc) acts as the counterion. After that, cellulose molecules are forced apart due to charge repulsion known as a 'polyelectrolyte effect'. As a result of the high osmotic pressure, there is a continuous influx of solvent that disrupts the cellulose binding forces until the polymer is solvated [116, 117].

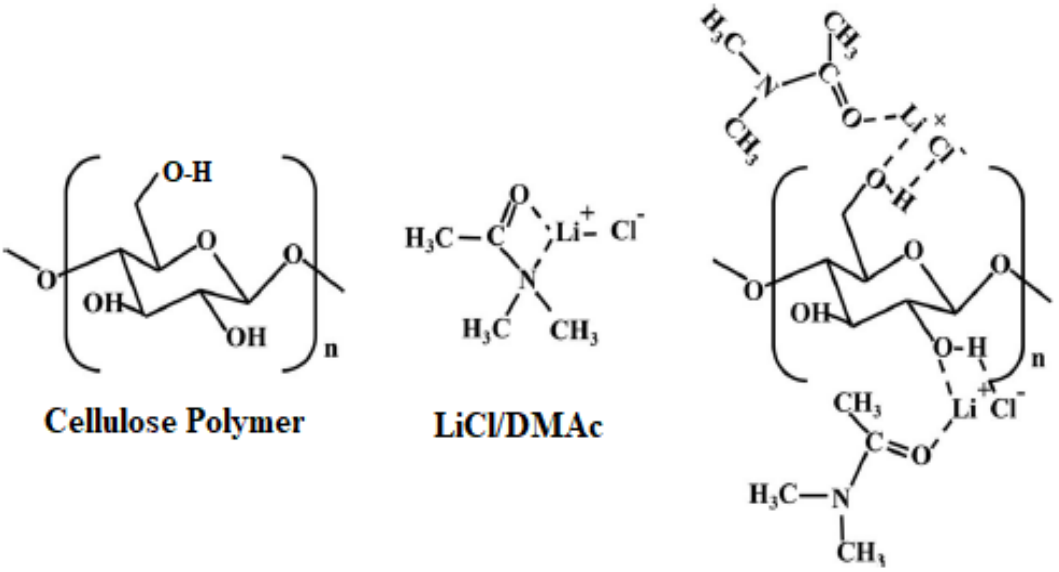


**Figure 2.2:** Mechanism of dissolving cellulose using LiCl/DMAc solvent system.

The experimental part for the dissolution of cellulose was carried out by activation of cellulose (polymer mass = 1.0 g) in (100.0 mL volume) water, the suspension was stirred magnetically for 2.0 hours at room temperature. Then, the cellulose has been removed by suction filtration and suspended for one hour in a 100.0 mL volume of methanol. This procedure was repeated two times, followed with two successive exchanges with 25.0 mL of anhydrous N,N dimethylacetamide (DMAc). The first DMAc solution exchange was carried out for about 1.0 hour and the second one was left for 24.0 hours. After each solvent exchange, solvent was removed by suction filtration under vacuum by using a glass centered funnel. The activated cellulose was then transferred into a two necked round bottomed flask equipped with a magnet stir bar, the flask was connected to a poplar via the condenser. A solution of anhydrous lithium chloride LiCl (6.5 g) in 100.0 ml volume of anhydrous N,N-dimethylacetamide (DMAc) was then added into the mixture in the flask. The reactions mixture was stirred magnetically for around 2.0 hours until a clear gel was appeared.

### 2.5.2 Cellulose Acylation with Furan-2-carbonyl chloride

To the cellulose solution in LiCl/DMAc prepared before (Section 2.5.1) was added trimethylamine solution (volume = 0.5 mL) dropwise under nitrogen gas, followed by a solution of 2-furan carbonyl chloride (2.415 gram, 0.0185 mol) in 10.0 mL volume of anhydrous dimethylacetamide solution DMAc. The produced mixture was then mixed magnetically for about 3.0 hours at a temperature of 70 °C. It was then transferred into a beaker containing 500

mL volume of distilled water. After that, the produced precipitate was collected using suction filtration and washed four times using distilled water, then and with isopropyl alcohol compound, then dried overnight at a temperature of 25° C.

The final product of cellulose modified with 2-furan carbonyl chloride is shown in (Figure 2.3).

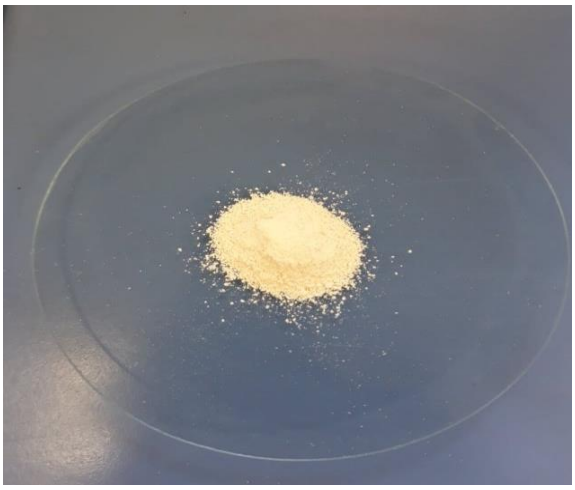

**Figure 2.3:** Cellulose Modified with 2-furan carbonyl chloride Product.

### 2.5.3 Cellulose Crosslinking with Pyridine 2,6-dicarbonyl dichloride

The previous procedure (Section 2.5.2) was repeated exactly except that 2,6-pyridine dicarbonyl dichloride (3.775 g in 10 mL DMAc) was added to the solution of cellulose in LiCl/DMAc solvent mixture. A precipitate of the crosslinked cellulose nanopolymer starts appearing after about 3.0 hours from heating the reaction mixture at a temperature of 70 $^{o}$C. After that, the produced precipitate was collected using suction filtration and washed four times with distilled water, then with ethanol, then dried overnight at room temperature.

Different Adsorbents can be synthesized from MCC or CNC as starting materials by following the previous steps (section 2.5.1, section 2.5.2, and section 2.5.3). However, In the case of using CNC as the basic compound, we should start by suspension of CNC in methanol since CNC bio-adsorbent is totally dissolved in water.

The final product of cellulose modified with 2,6-pyridine dicarbonyl dichloride is shown in (Figure 2.4).

**Figure 2.4:** Cellulose Modified with 2,6-Pyridine dicarbonyl dichloride Product.

## 2.6 Adsorbents Characterization

The synthesized adsorbents have been characterized by different advanced instruments including: Proton Nuclear Magnetic Resonance ($H^1$ NMR), Scanning Electron Microscope (SEM), Fourier-Transform Infrared Spectroscopy (FT-IR) and Thermogravimetric analysis (TGA).

## 2.7 Chromatographic Conditions

High Performance Liquid Chromatography (HPLC) instrument in which LC solutions data handling system (Waters 1525 Binary HPLC Pump, Waters)

with Photodiode Array Detector PAD (Waters 2998), was used for the analysis. The data was recorded using Breeze QS software program. The purity determination performed on a column 250 mm cartridge long, 4.6 mm internal diameter (X TERRA C18, 5µm, 250 mm x 4.6 mm). The mobile phase consisted of 36% water and 64% acetonitrile. The flow rate was kept at 1 mL/min. The wavelength of the UV detector was 229 nm in case of determining difenoconazole, and 220 nm in case of tetraconazole measurement.

## 2.8 Pesticides Detection in Real Water Samples

Two real samples of Groundwater from Burqin in Jenin city, and Rafidia in Nablus city were taken in order to measure the amount of Difenoconazole and Tetraconazole pesticides. The results for samples analysis using UV-Visible spectrophotometry and HPLC instruments showed absence of these two pesticides in the two real groundwater samples in Palestine.

## 2.9 Calibration Curves

### 2.9.1 Calibration Curves of Difenoconazole

Depending on dilution calculations, several standard solutions with (2.0, 4.0, 6.0, 8.0 ppm) concentrations of difenoconazole pesticide were prepared from a solution of 10.0 ppm Difenoconazole (10.0 mg of Difenoconazole pesticides in 1 L solution). The stock solution has then been sonicated for 10 minutes before dilution. The standard solutions were analyzed using UV-Visible Spectrophotometer (Figure 2.5 A) and HPLC instrument (Figure 2.5

B) at wavelength 229 nm. Calibration curves of Difenoconazole pesticide are shown in (Figure 2.5).

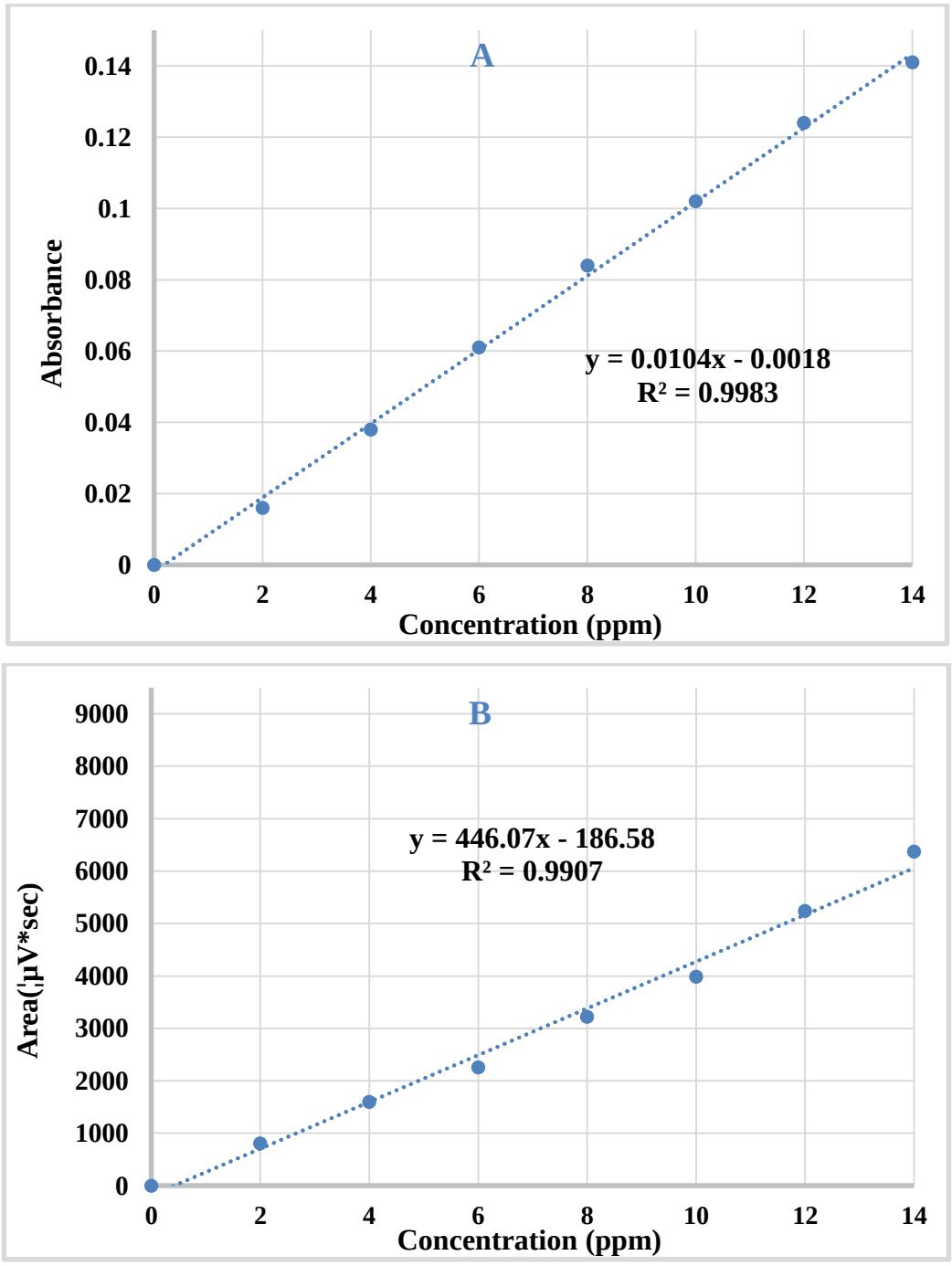


**Figure 2.5:** Calibration curves of Difenoconazole. (A) Using UV-Visible Spectrophotometer, (B) using HPLC.

### 2.9.2 Calibration Curves of Tetraconazole

Several standard solutions with (1.0, 5.0, 10.0, 15.0 and 20.0 mg/L) concentrations of Tetraconazole pesticide were prepared from stock solution of 100.0 ppm that was prepared by dissolving 100 mg tetraconazole in 1 L solution, and then analyzed using UV-Visible Spectrophotometer (Figure 2.6 A) and HPLC instrument (Figure 2.6 B) at wavelength 220 nm. Calibration curves of Tetraconazole are shown in (Figure 2.6).

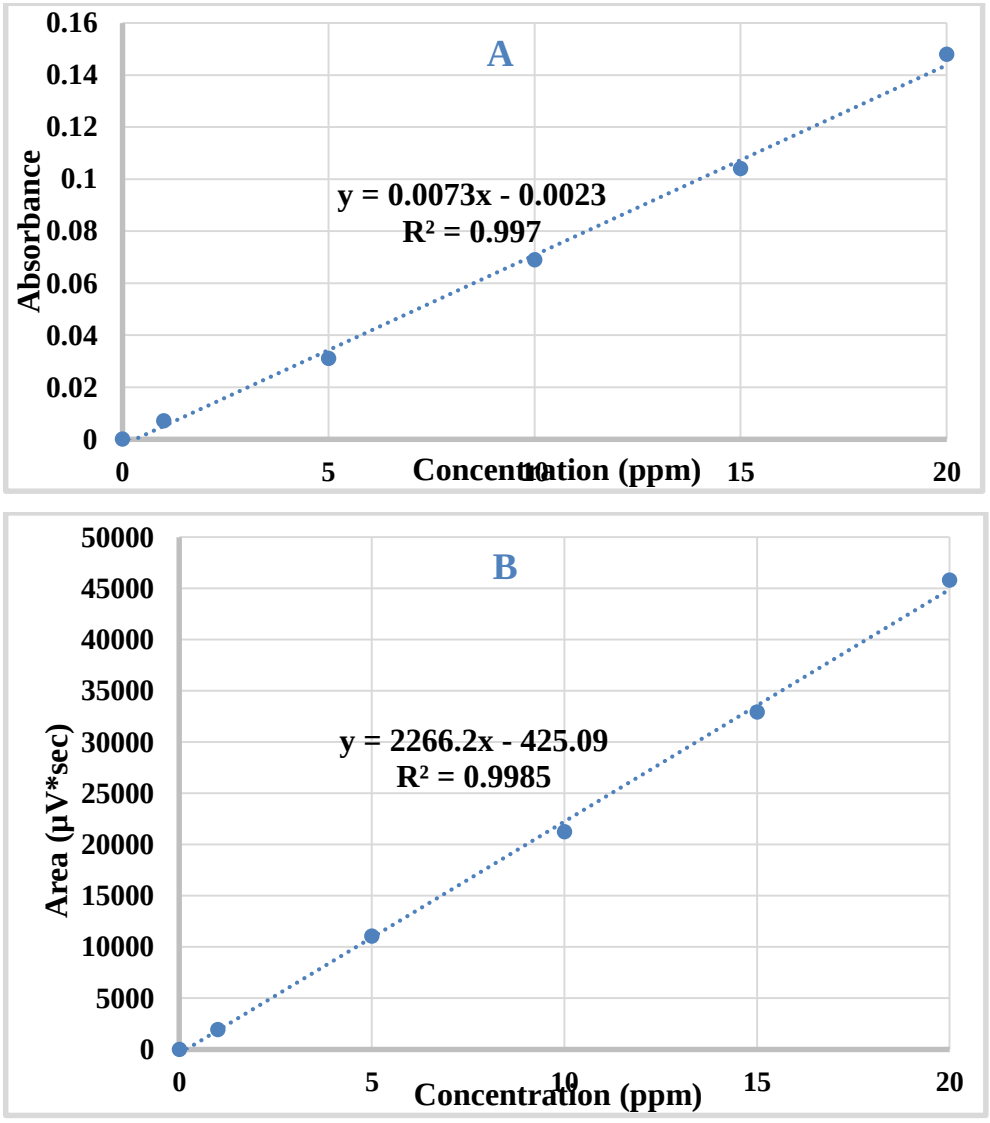


**Figure 2.6:** Calibration curves of Tetraconazole. (A) Using UV-Visible Spectrophotometer, (B) using HPLC.

## 2.10 Batch Experiments

Solution conditions effects were discussed. Such that, 10 mg of each adsorbent with 10.0 mL water containing known concentration of each pesticide was shaken for studying the effects of Difenoconazole or Tetraconazole concentrations, contact time, pH value and temperature. For studying the adsorbent dose effect, the adsorbent mass was ranged from 1 mg to 20 mg.

Each experiment was done in triplicate and the average was calculated. HPLC and UV-Visible Spectrophotometer were used for the filtrate in order to detect the remained amount of Difenoconazole or Tetraconazole pesticide and hence to determine the extent of the adsorption efficiency. As well as, HPLC instrument was used to measure the remained pesticides concentrations for samples containing a mixture of equal amounts of both difenoconazole and Tetraconazole.

### 2.10.1 Effect of Contact Time

10.0 ppm concentration and 10.0 mL volume of standard pesticide solution at pH value equals 7 was taken in a volumetric flask and shaken with 10 mg of each adsorbent. In order to investigate the contact time effect on each adsorption process, all of the solution conditions should be fixed except the time of shaking that will range from 1 minute to 120 minutes. For each adsorption process, temperature was kept at 20 $^{o}$C. At the end of time intervals, each mixture was filtered off and the remained pesticide amount was detected.

### 2.10.2 Effect of pH

For investigating the optimum pH value, mixture of 10.0 ppm concentration and 10.0 mL volume of standard pesticide solution was shaken with 10.0 mg of each adsorbent at temperature equals 20 $^{o}$C, and at the optimum time for each process.

pH value is varied from 2.0 to 10.0 and it was adjusted using concentrations from 0.1 M NaOH solution and 0.1 M HCl solution. At the end of each adsorption, each sample was filtered off and the remained pesticide concentration was detected.

### 2.10.3 Effect of Pesticide Concentration

To find out the optimum pesticide concentration, sample of 10.0 mg of the adsorbent was mixed with 10.0 mL of the prepared Difenoconazole or Tetraconazole standard solutions with different concentrations (1.0, 2.0, 4.0, 6.0, 8.0, 10.0, 12.0 and 14.0 ppm) at 20 °C, with taking into account the optimum conditions of pH and contact time for each adsorption. Then, the remained concentration of difenoconazole or tetraconazole pesticide is measured for each filtrate at the end of each adsorption process.

### 2.10.4 Effect of Temperature

10.0 mL of standard pesticide solution was mixed with 10.0 mg of each adsorbent. In order to investigate the temperature effect on each adsorption process, all of the optimum conditions of time, pH and pesticide concentration should be applied at this stage. The temperature value was

ranging from 10.0 °C to 70.0 °C. At the end of time intervals, each mixture was filtered off, and the remained pesticide amount was detected.

### 2.10.5 Effect of Adsorbent Dose

For detecting the optimum mass for each of the three adsorbents, different vials containing 10 mL of pesticide solution with the optimum concentration at different adsorbent doses (1.0, 5.0, 10.0, 15.0 and 20.0 mg). Each sample was placed in water bath for a time period equals the optimum contact time for each process. The other optimum conditions of temperature, pesticide concentration, and pH value for each adsorption process are taken into consideration. After that, pesticide remained concentration in the filtrate is investigated.

## 2.11 Adsorbents Regeneration

10.0 mg sample of cellulose modified with 2-furan carbonyl chloride or cellulose modified with 2,6-pyridine dicarbonyl dichloride adsorbent with 10.0 mL of distilled water containing 10.0 ppm concentration of difenoconazole or tetraconazole was shaken; taking into consideration the optimum solution conditions. After that, the pesticide residue in the filtrate was determined, and the adsorbent after each adsorption process is washed with diluted sulfuric acid (0.1 N), then with ethanol, and then using distilled water for three times. After that, each regenerated adsorbent was left to dry for one night before reusing. Then, the same technique of recovery is used for each regenerated adsorbent in order to prove that the new synthesized

cellulose based derivatives can be used for several times with small effect on the percentage removal of pesticides in water.

# CHAPTER THREE

# RESULTS AND DISCUSSION

## 3.1 Polymers Synthesis

Grafting of cellulose with 2-furan carbonyl group (Cel-F) and crosslinking of cellulose polymer with the chemical reagent 2,6-pyridine dicarbonyl dichloride (Cel-P) was carried in the solvent mixture DMAc/LiCl, as appeared in Figures 3.1 and 3.2. The reagents were chosen because of the functional groups they have, such that; the existence of the aromatic heterocyclic, the carbonyl group, chloride, and hydroxyl groups ,makes them perfect adsorbents for removing pesticides from water. Such that; these functional groups bind tetraconazole and difenoconazole through various physical interactions including, Hydrogen bonding, dipole-dipole interaction and π-π stacking.

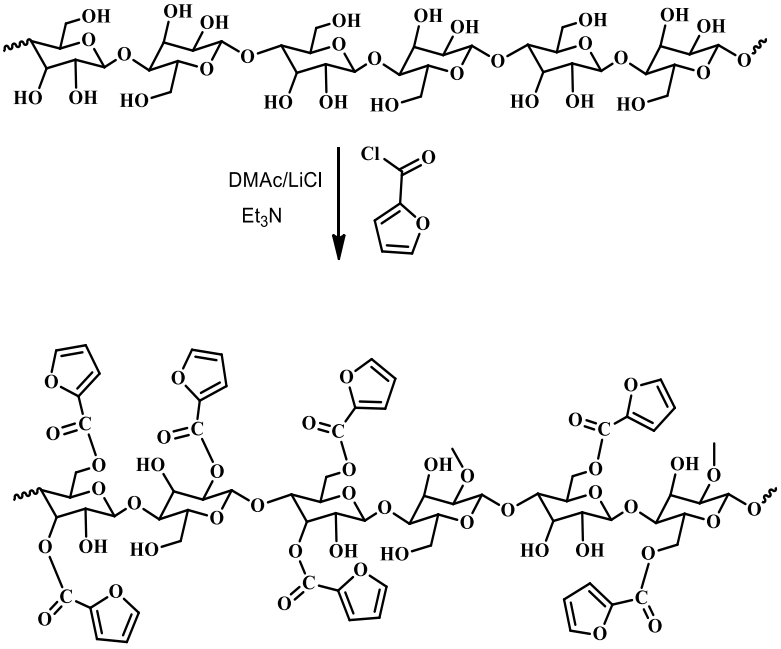


**Figure 3.1:** Acylation of cellulose with 2-furan carbonyl chloride (Cel-F).

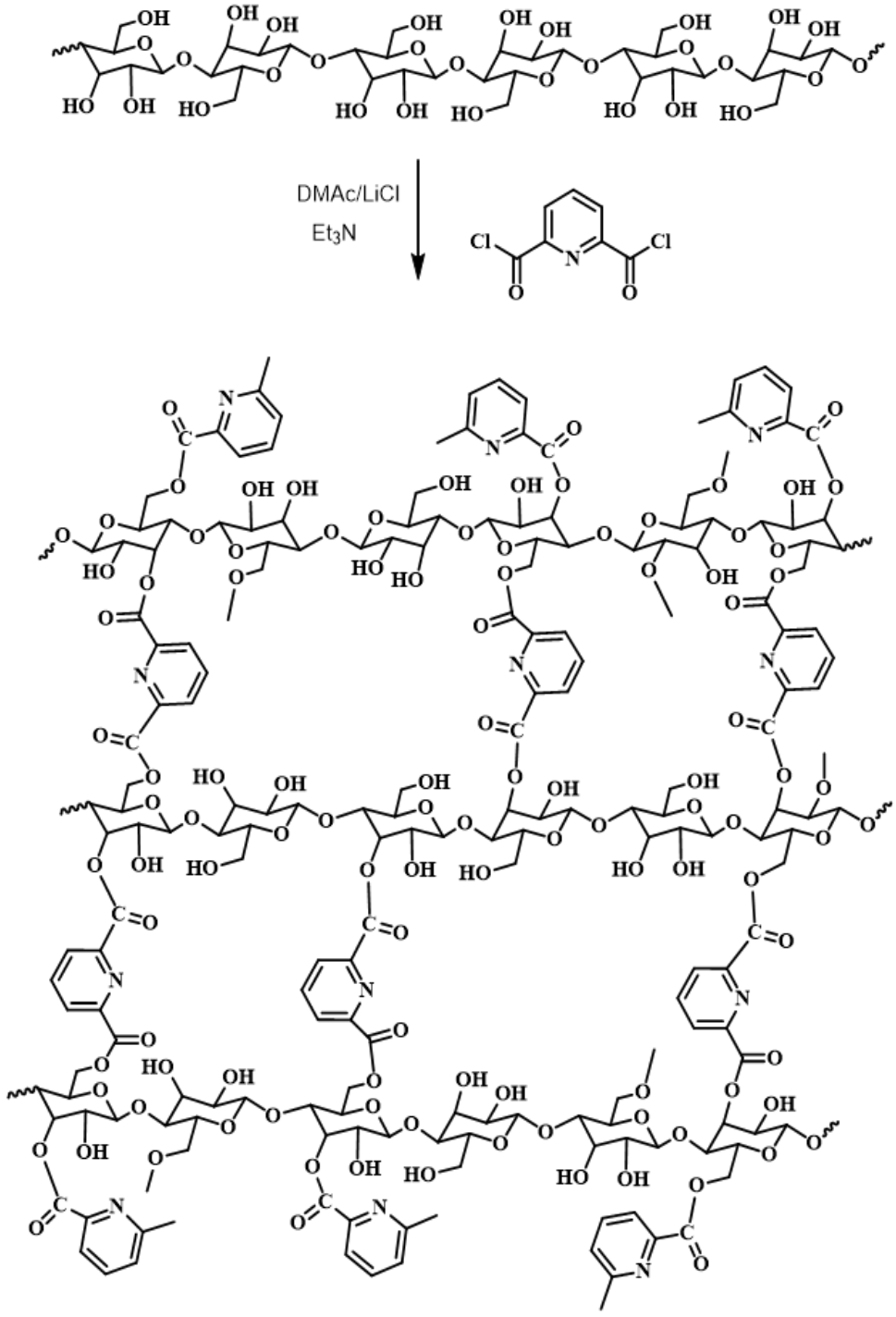


**Figure 3.2:** Crosslinking of cellulose with 2,6-pyridine dicarbonyl dichloride (Cel-P).

## 3.2 Polymers Characterization

### 3.2.1 Proton Nuclear Magnetic Resonance

$^{1}$H NMR spectra was carried at the Research Center Juelich in Germany, using a Bruker 600 MHz spectrometer, equipped with a 5 mm broadband CryoProbe Prodigy. The acquisition parameters include: 90° pulse calibrated at 12 μs, 2 s relaxation time, 1.3 s acquisition time, 2048 scans, 300 K temperature and no spinning.

The three nanopolymers, including cellulose nanocrystaline (CNC), cellulose functionalized with 2-furan carbonyl chloride, cellulose functionalized with 2,6-pyridine dicarbonyl dichloride, were all characterized using proton Nuclear Magnetic Resonance analysis. The $^{1}$H NMR of CNC is shown in Figure 3.3.

Cellulose solution in DMAc-d6/LiCl, was obtained by solvent exchanged as shown in chapter two (section 2.5.1). The proton NMR spectrum shows downfield peaks at value of 4.35 δ that could be assigned to the proton $H^{1}$ at the anomeric carbon [118]. The two multiple peaks at the values 3.92 δ and 3.85 δ could be attributed to the two protons at C-6. The results are consistent with the previous reported [119]. The four peaks that have been showed between 3.1 δ and 3.60 δ are from the four protons at the carbons C2, C3, C4 and C5, the peak at 3.1 δ is consistent with H2 chemical shift [118].

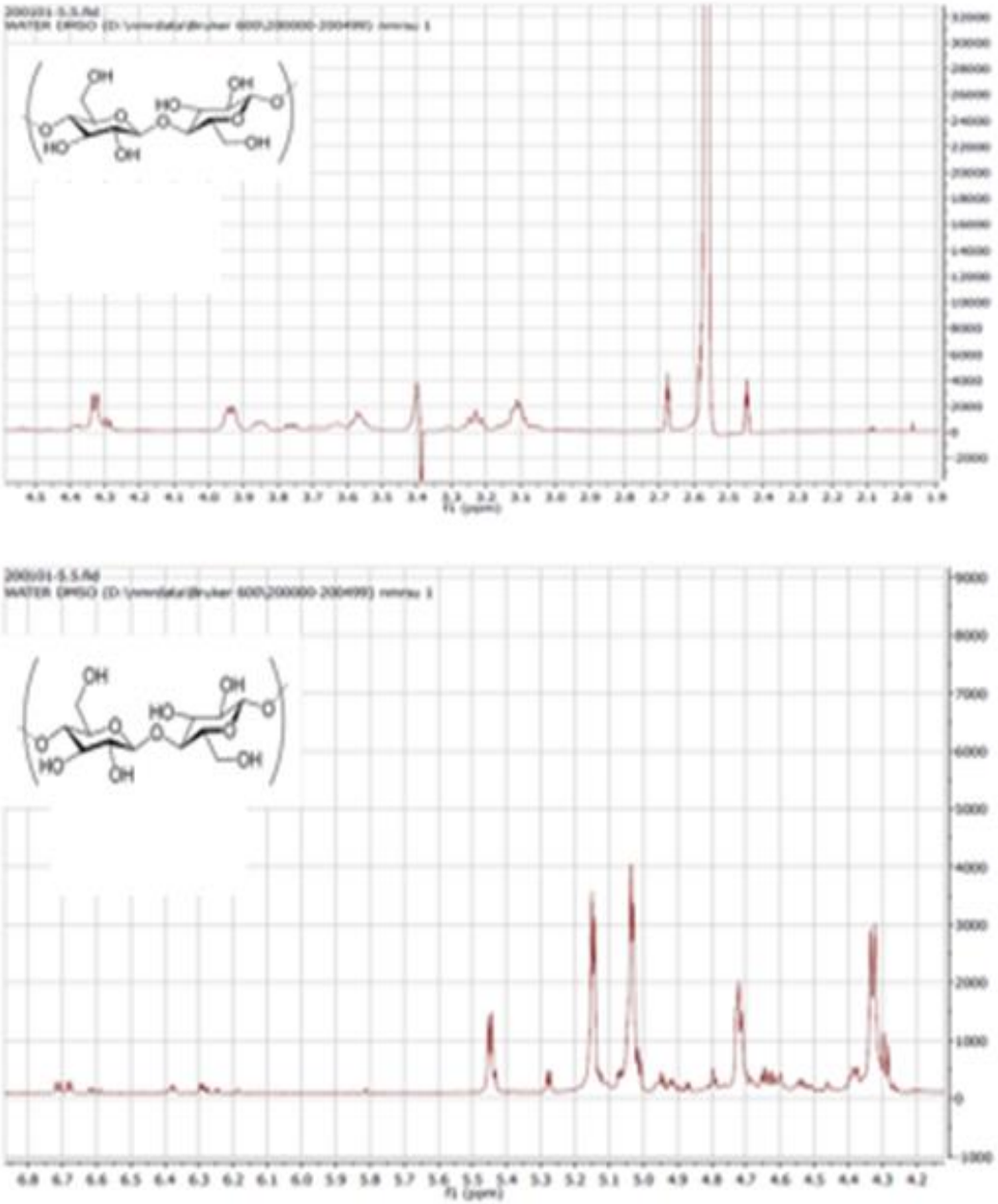

**Figure 3.3:** $H^1$ NMR Spectra for Cellulose Nanocrystalline.

The proton NMR analysis for Cel-F nanopolymer is shown in Figure 3.4, the spectrum detects the presence of three peaks in the range from 6.71 ppm to 8.12 ppm, which could be assigned to the protons for the aromatic furan, the cellulose peaks appear between 2.7 ppm and 5.0 ppm.

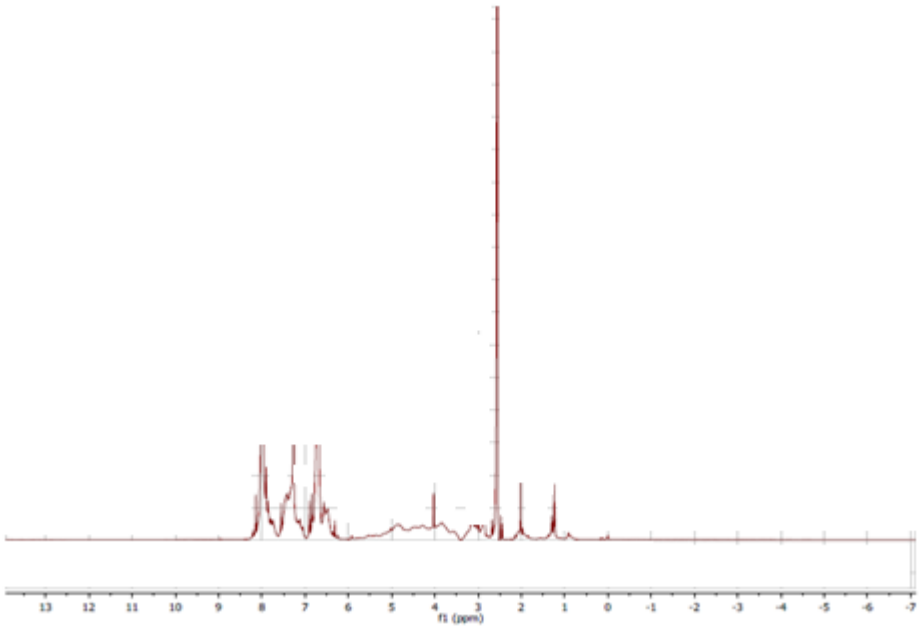

**Figure 3.4:** $H^1$ NMR Spectra of Cellulose modified with 2-furan carbonyl chloride.

$H^1$ NMR Spectra of Cellulose modified with 2,6-pyridine dicarbonyl dichloride is shown in Figure 3.5. As shown in the spectra, the peaks in the region between 2.0 – 5.49 ppm are due to cellulose backbones. As well as, the peaks between 7.9 – 8.5 ppm could be corresponding to the aromatic rings of pyridine in the synthesized nanopolymer.

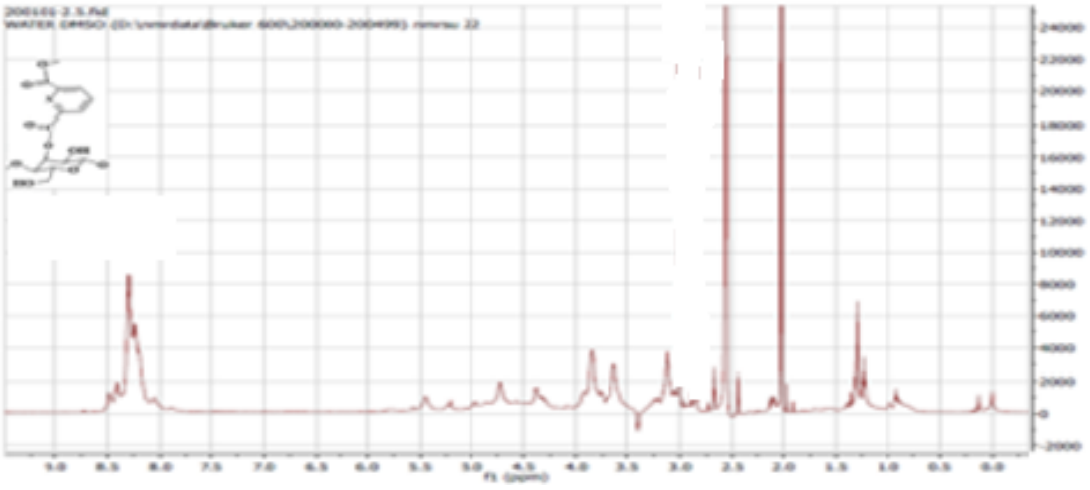

**Figure 3.5:** $H^1$ NMR Spectra of cellulose modified with 2,6-pyridine dicarbonyl dichloride.

### 3.2.2 Scanning Electron Microscopy

To study the the adsorbents surface morphology, we used scanning electron microscopy (SEM) at Research center Juelich in Germany. For this, the adsorbents were fixed onto a double-sided C tape and mounted onto the sample holder. All adsorbents were subjected to a sputter coating of a 10 nm-thick gold film onto the sample for minimizing charging effects and hence taking high magnification images. The nanopolymers have been placed into the vacuum sample chamber and surface micrographs were detected using Emission Scanning Electron Microscope instrument (JEOL 7400F Oxford Instruments Inca, Tubney Woods, Abingdon, Oxon OX13 5QX, UK).

#### 3.2.2.1 SEM of Olive Industry Solid Waste

SEM characterization for Olive Solid Waste (OSW) was performed, and images at two different magnifications (5 µm and 10 µm) were collected. The analysis pictures for OSW expose the existence of two morphology structures, one of them is the spongy which is the main morphology that is related to the olive pith, while the other one is related to the seeds which is the hard part of OSW. This illustrates that the steps of pulping and bleaching used for cellulose extraction in our work are a moderate version to those used in the timber industry. In addition, we can notice that OSW has conductive properties as shown in the white regions of its SEM analysis (Figure 3.6).

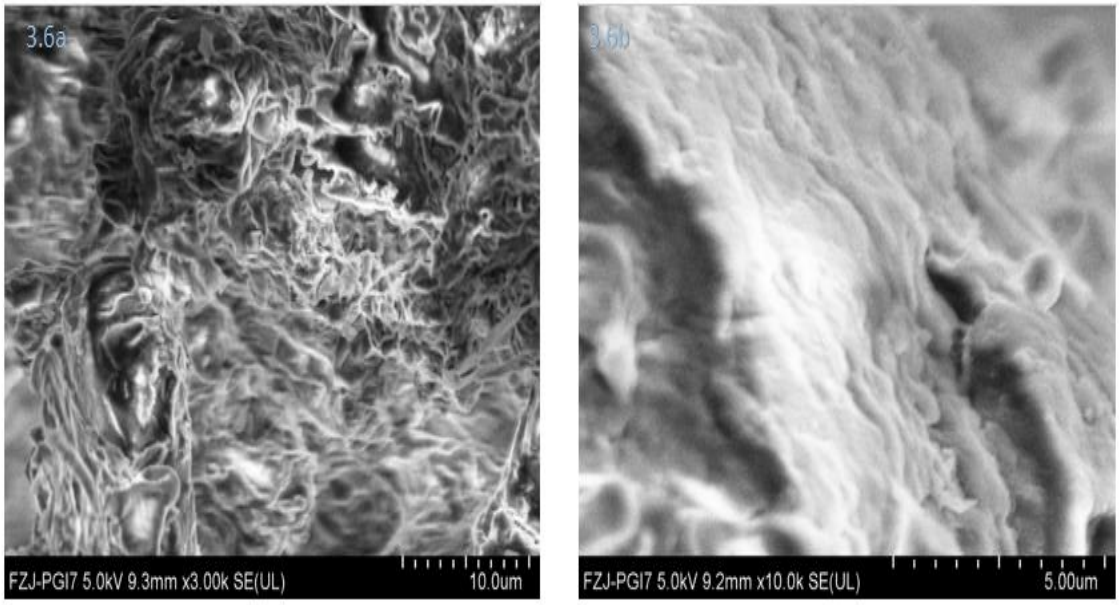


**Figure 3.6:** SEM Analysis of OSW at two different magnifications 3.6a) 10 µm, 3.6b) 5 µm.

### 3.2.2.2 SEM of Cellulose Microcrystalline

(Figure 3.7) illustrates the Scanning Electron Microscope analysis (SEM) for cellulose Microcrystalline that was extracted from olive solid waste. SEM images of the extracted cellulose microcrystalline (MCC) were collected at two different magnifications (5 µm and 20 µm). As shown below, cellulose microcrystalline (MCC) particles have a regular flat shape with semi porous surface morphology.

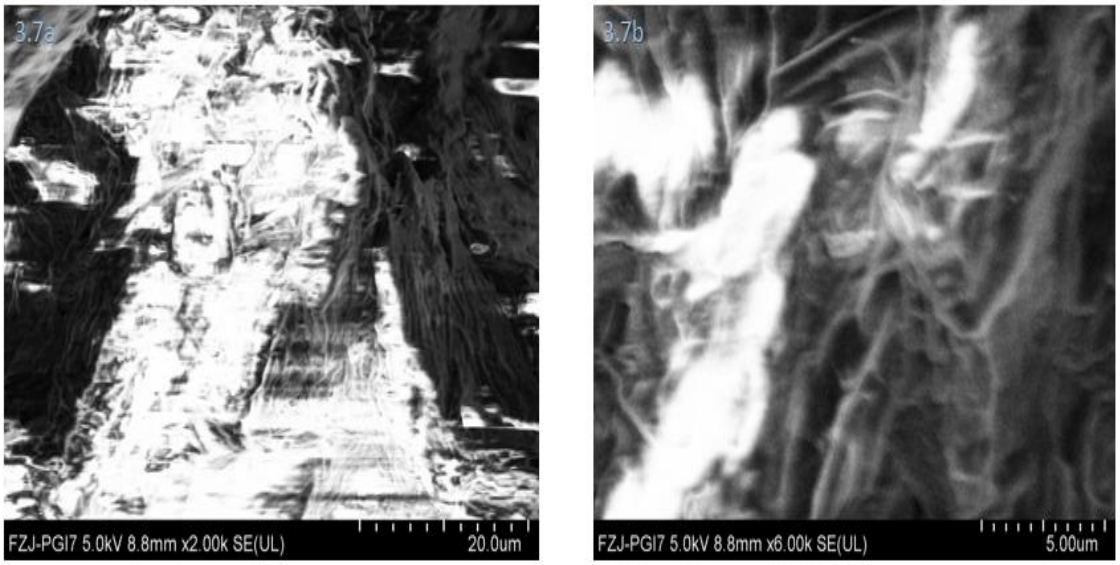


**Figure 3.7:** SEM Characterization of Cellulose Microcrystalline at two different magnifications 3.7a) 20 µm, 3.7b) 5 µm.

### 3.2.2.3 SEM of NanoCellulose

Scanning Electron Microscope analysis (SEM) images for NanoCellulose at the three different magnifications (1 µm, 10 µm and 100 µm) are shown in Figure 3.8. As shown below, Cellulose Nanocrystalline (CNC) particles have high surface area to volume ratio, hence the surface morphology of CNC suggests its high ability of adsorption and removal for different pollutants from water.

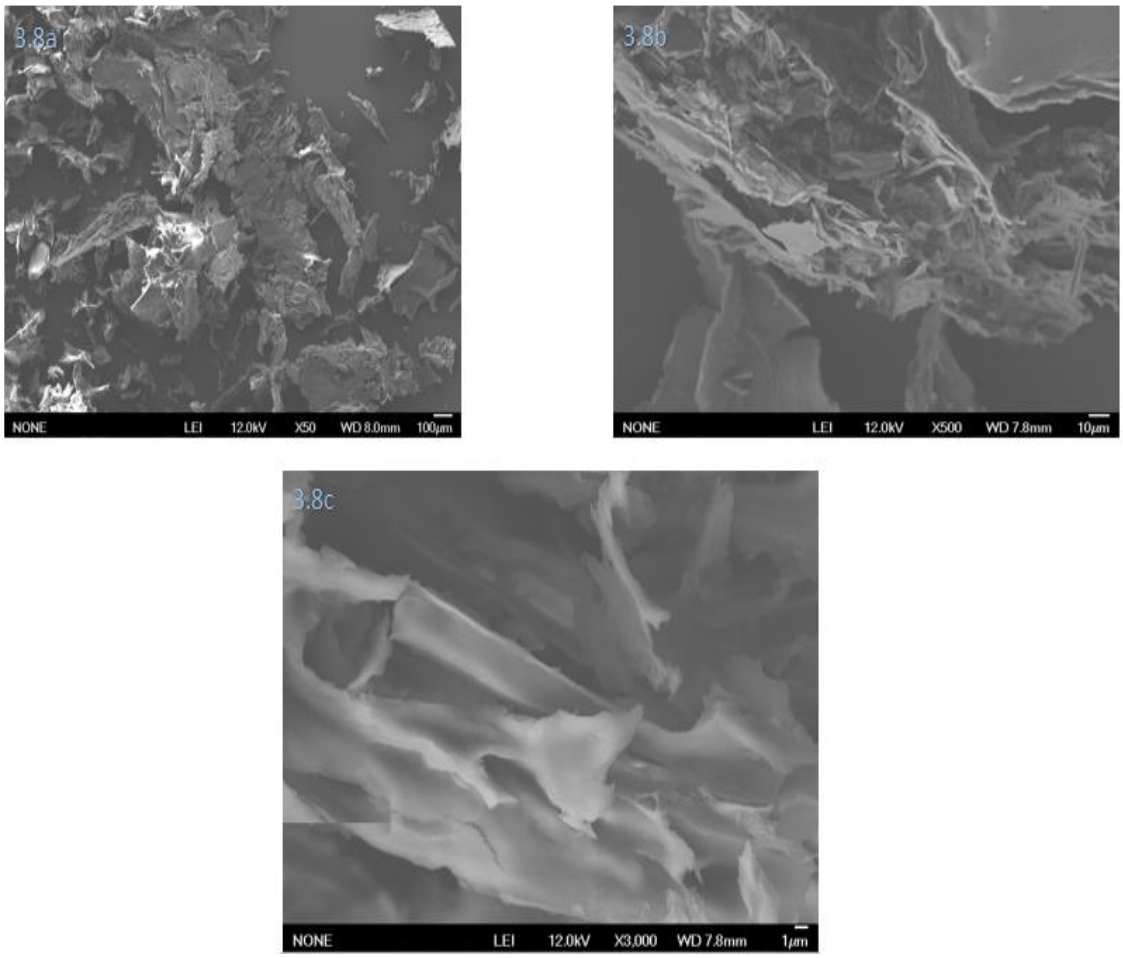


**Figure 3.8:** Three magnifications SEM analysis morphology of Cellulose Nanocrystalline at: 3.8a) 100 µm, 3.8b) 10 µm and 3.8c) 1 µm.

### 3.2.2.4 SEM of Cellulose functionalized with 2-furan carbonyl chloride (Cel-F)

SEM images of Cel-F at the three different magnifications (1 µm, 10 µm and 100 µm) are shown in Figure 3.9. As shown below, the morphology for this adsorbent shows a relatively high surface-to-volume ratio; which enhance its adsorption efficiency for pesticides removal from water, through the adhesion and $\Pi$-$\Pi$ interaction between this cellulose derivative and adsorbate particles.

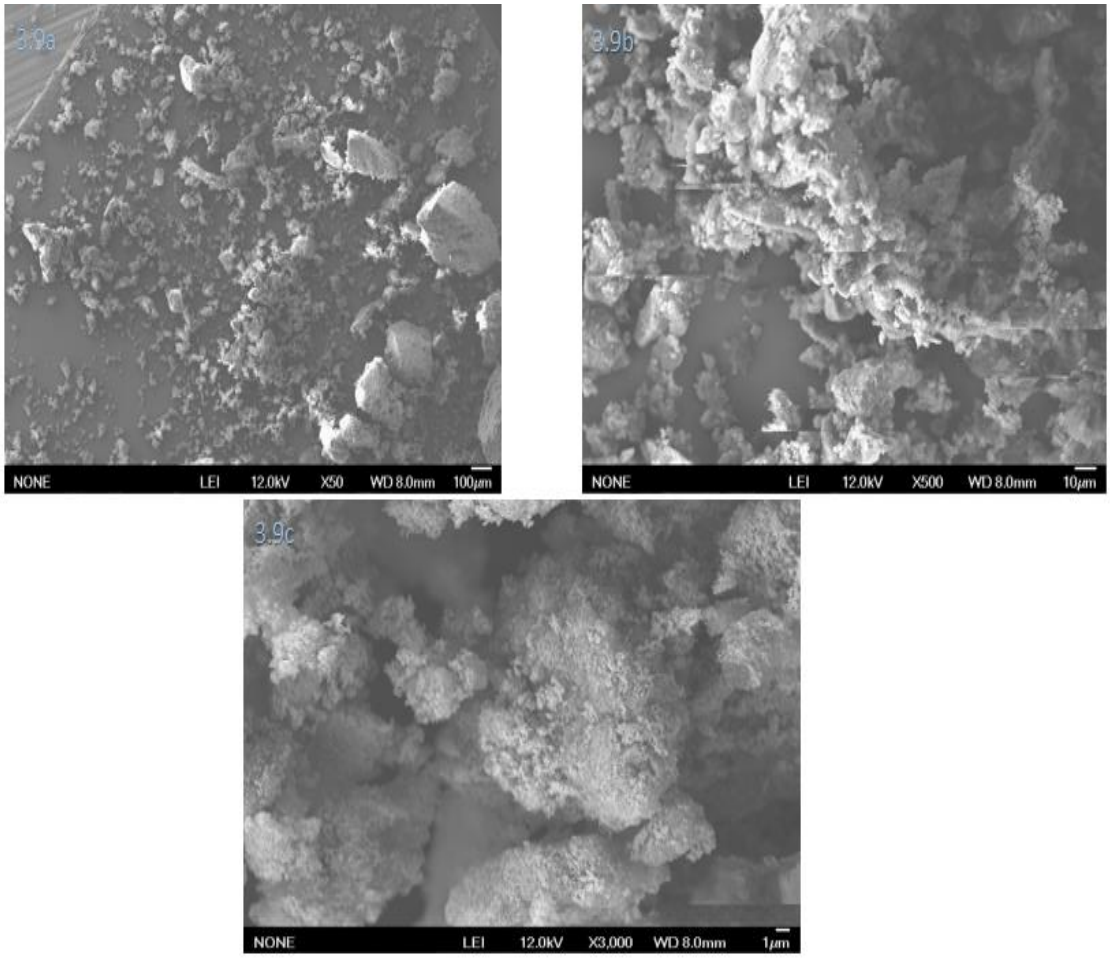


**Figure 3.9:** Three magnifications SEM analysis morphology of Cellulose functionalized with 2-furan carbonyl chloride at: 3.9a) 100 µm, 3.9b) 10 µm and 3.9c) 1 µm.

### 3.2.2.5 SEM of Cellulose Functionalized with 2,6-pyridine dicarbonyl dichloride (Cel-P)

SEM images for Cel-P at three different magnifications (1 µm, 10 µm and 100 µm) are shown in Figure 3.10. As shown below, the surface morphology for this cellulose derivative shows a high surface to volume ratio, hence suggesting a good adsorption efficiency for pesticides removal through

adhesion and 𝜋-𝜋 interaction between this adsorbent and the pesticide particles.

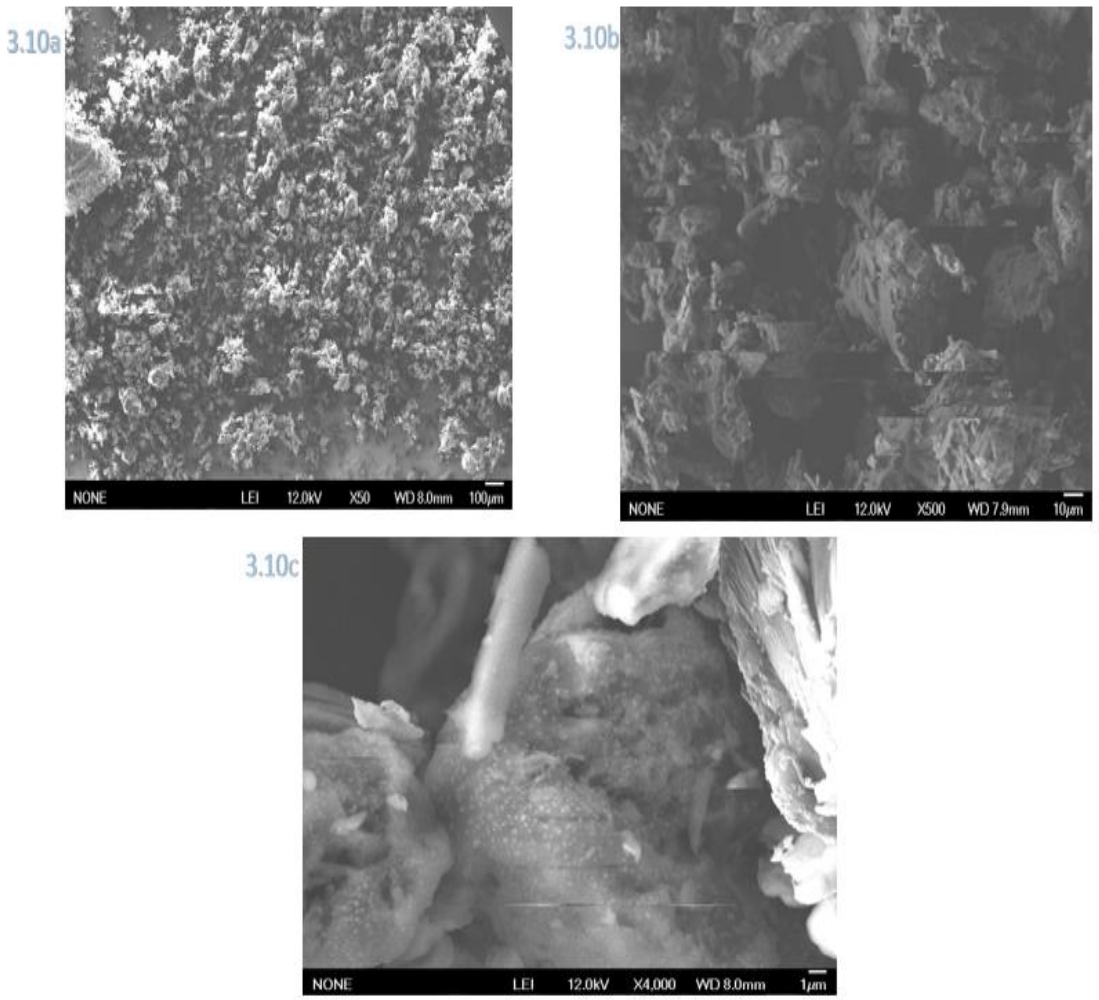


**Figure 3.10:** Three magnifications SEM analysis morphology of Cellulose functionalized with 2,6-pyridine dicarbonyl dichloride at: 3.10a) 100 µm, 3.10b) 10 µm and 3.10c) 1 µm.

### 3.2.3 Fourier Transform Infrared spectroscopy (FT-IR)

#### 3.2.3.1 FT-IR Spectra of Cellulose Nanocrystalline

As shown in the FT-IR spectra of CNC (Figure 3.11). The band at the wave number 1160.35 $cm^{-1}$ corresponds to C-O-C stretching of β-glycosidic linkage. The bands at 1378.36 and 1316.15 $cm^{-1}$ correspond to the C-O stretching of ether and alcohol groups. The band at 1495.15 $cm^{-1}$ could be attributed to $CH_2$ asymmetric bending. The band at the wavenumber 2902.54 $cm^{-1}$ corresponds to the CH stretching vibration in $CH_2$ and CH anhydroglucose units of cellulose nanocrystalline. The band at 3339.67 $cm^{-1}$ could be assigned to the hydrogen bonded hydroxyl group (OH) stretching vibration.

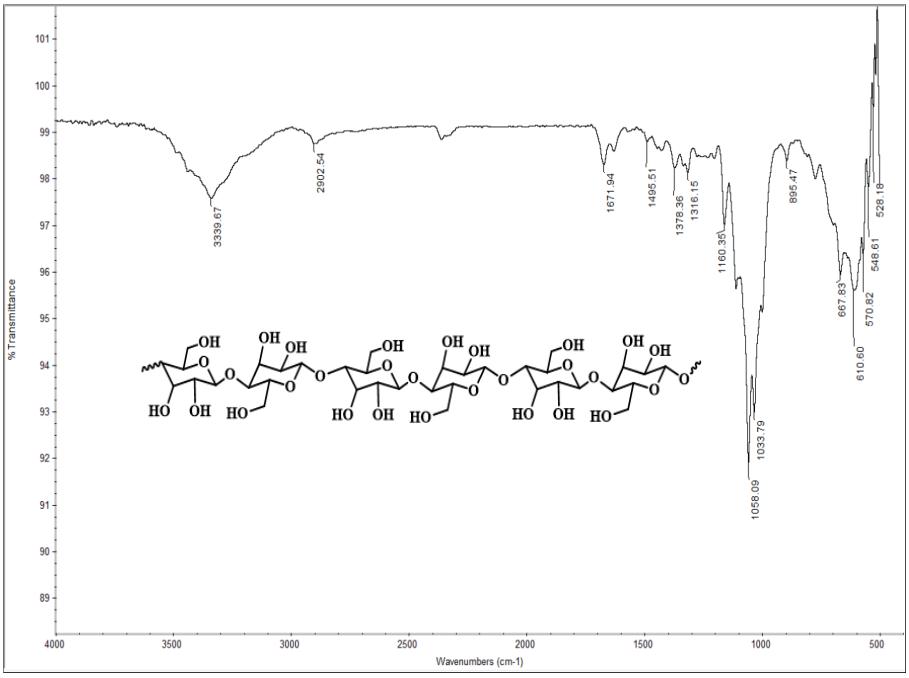


**Figure 3.11:** FT-IR Spectra for Cellulose Nanocrystalline.

### 3.2.3.2 FT-IR of Cel-F and Cel-P

The prepared cellulose derivatives Cel-F and Cel-P were also characterized by FT-IR. Cel-F as shown in Figure. 3.12. The FT-IR spectrum detects the presence of a band at 1717.61 $cm^{-1}$ wavenumber that could be attributed to the ester carbonyl, the low frequency of the carbonyl groups could be due to the conjugation with heterocyclic double bond. The C=C double bond of the aromatic furan ring showed a small peak at 1536 $cm^{-1}$ wavenumber. The band at 1179.74 $cm^{-1}$ could be assigned to β-glycosidic linkage (C-O-C) of cellulose. The FT-IR analysis spectrum of Cel-P nanopolymer showed approximately similar peaks as Cel-F adsorbent, with slight shift in the values of frequency.

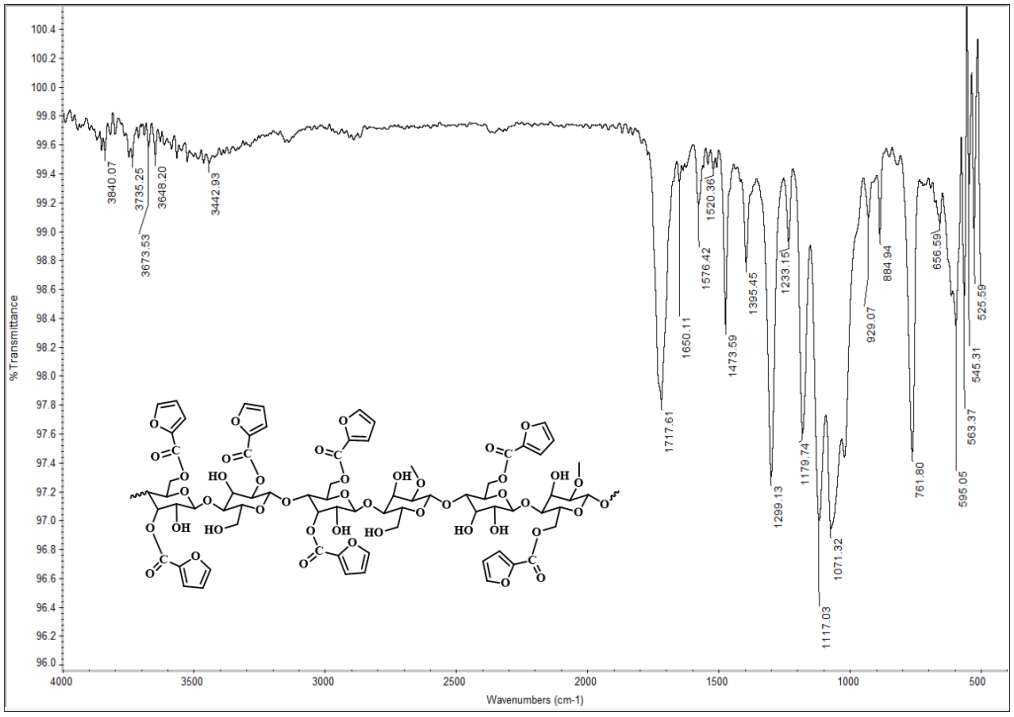


**Figure 3.12:** FT-IR Spectra for Cel-F and Cel-P nanopolymers.

### 3.2.4 Thermal Gravimetric Analysis (TGA)

The mass of each sample is measured over time as a function of temperature, in order to determine the thermal stability and hence knowing the decomposition behavior for each compound as the temperature increases. Since the higher temperature at which a material is thermally decomposed is directly related to its thermal stability.

The TGA analysis was performed for CNC, Cel-F and Cel-P nanopolymers, and results are represented in Figure 3.13. TGA graphs detect the loss of weight with increasing temperature. The three nanopolymers showed good stability at temperature over 200 $^{o}$C, since the major mass loss appears at about 250 $^{o}$C.

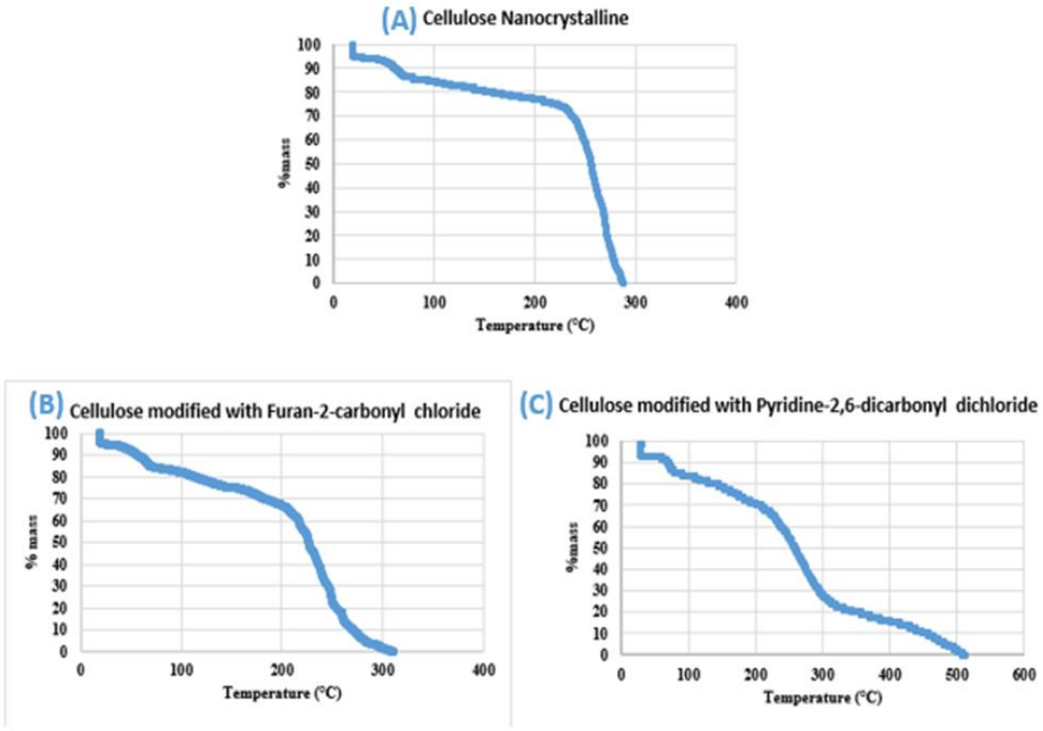


**Figure 3.13:** TGA analysis of the nanopolymers: (A) Cellulose Nanocrystalline, (B) Cellulose functionalized with 2-furan carbonyl chloride and (C) Cellulose functionalized with 2,6-pyridine dicarbonyl dichloride.

### 3.3 Adsorption of Difenoconazole and Tetraconazole pesticides

One of the objectives of this work is using the newly synthesized cellulose-based derivatives Cel-F and Cel-P, as well as, the underivatized cellulose nanocrystalline, for removing difenoconazole and tetraconazole pesticides from water and comparing the adsorption efficiency of different adsorbents. This was done by investigating the adsorption capacities of these cellulose based derivatives towards difenoconazole and tetraconazole.

All experiments were performed in plastic vials that were placed in a shaker immersed in a water bath equipped with a shaker and a thermostat. The effect of various solution variables on the nanopolymer efficiency, for instance; pH value effect, initial concentration ($C_o$), dosage of adsorbent, shaking time, and temperature were all investigated. After each run, sample was collected from the mixture using a 10.0 mL plastic syringe, filtered through a 0.45-µm filter paper and subjected to analysis by a HPLC analysis at 220 nm and 229 nm wavelengths respectively; to determine residual concentration of tetraconazole and difenoconazole respectively. All adsorption batch experiments were performed in triplicate, and the average value of the three runs was reported. The amount of each of tetraconazole and difenoconazole adsorbed by CNC, Cel-F and Cel-P nanopolymers was determined according to Eq. 3.1

$$\%\ of\ Removal = \frac{C_I - C_F}{C_I} * 100\% \qquad (3.1)$$

Where;

$C_I$ and $C_F$ represent the initial and the final pesticide concentrations in water, respectively with a unit of (mg/L) or (ppm).

Comparison of the differences in adsorption efficiency was done by comparing the adsorption behavior using the same adsorbent with difenoconazole or tetraconazole, or by using the same pesticide with different adsorbents including Cellulose nanocrystalline (CNC), Cellulose functionalized with 2-furan carbonyl chloride (Cel-F) or Cellulose functionalized with 2,6-pyridine dicarbonyl dichloride (Cel-P).

### 3.3.1 Using the same Pesticide with Different Adsorbents

#### 3.3.1.1 Adsorption of Difenoconazole

Changing in solution conditions will result in changing in the adsorption efficiency. Here, the adsorption of Difenoconazole pesticide on Nanocellulose, Cellulose functionalized with 2-furan carbonyl chloride (Cel-F) or Cellulose functionalized with 2,6-pyridine dicarbonyl dichloride (Cel-P) is measured. Such that, the adsorption dependence on the adsorbent nature is detected.

##### 3.3.1.1.1 Contact Time Effect

In order to choose the most appropriate shaking time between difenoconazole and each adsorbent, the percent's of difenoconazole removal were detected versus the contact time, as appears in (Figure 3.14).

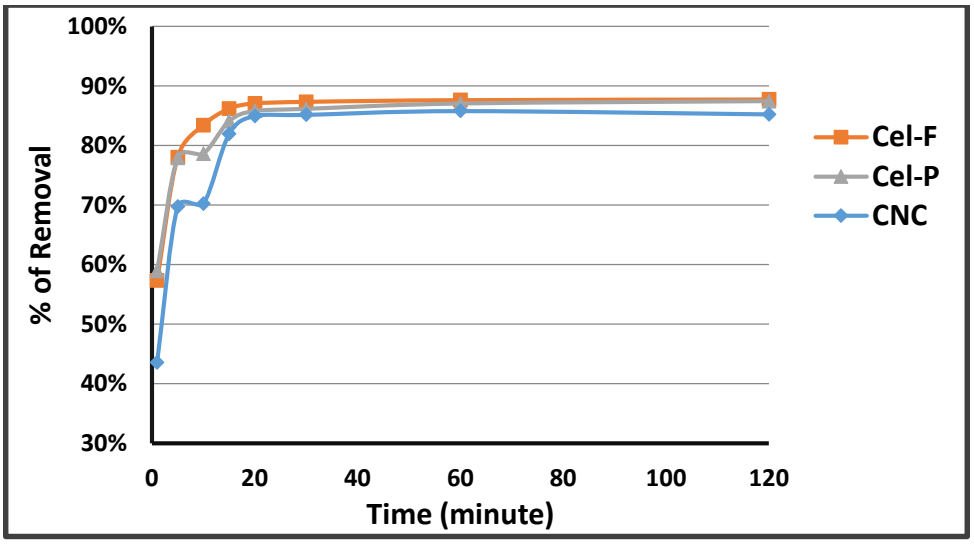


**Figure 3.14:** Contact time effect for Difenoconazole removal by CNC, Cel-F and Cel-P, (nanopolymer dosage = 10 mg, reaction mixture volume = 10 mL, initial concentration = 10 mg/L, pH = 7, temperature = 20 °C).

(Figure 3.14) detects that the highest percentage of difenoconazole removal was for cellulose functionalized with 2-furan carbonyl chloride after 20 minutes that represents the optimum or equilibrium contact time between the pesticide and Cel-F, this percentage was 87.07%. While when Cellulose functionalized with 2,6-pyridine dicarbonyl dichloride (Cel-P) is used for difenoconazole pesticide adsorption, the percent of removal was 87.05% and the equilibrium time was 60 minutes. In case of using Nanocellulose, the optimum contact time was 20 minutes, with 84.97% as percentage removal. For Nanocellulose, Cel-F and Cel-P; the remaining amount of the difenoconazole pesticide at equilibrium becomes approximately steady. The high percentages of difenoconazole removal are due the functional groups in the synthesized adsorbents that result in strong chemical bonding between the polymers and difenoconazole, as well as, making a cyclic cavity which is packed with the various binding sites, which makes an unique and perfect

adsorbent with its ability in trapping difenoconazole through several intermolecular forces, for instance; π-π stacking and Hydrogen bonding; such that, the presence of many vacant sites on the adsorbent surface and the strong intermolecular bonding that could occur between the two components represented by H-bonding and π-π interaction. Such that, the adsorption capacity increases as the shaking time of adsorbent and adsorbate interaction increases, this enables difenoconazole to adsorb efficiently with the newly synthesized adsorbents until reaching constant adsorption value at equilibrium time ($t_e$).

After $t_e$, the adsorption capacity $q_e$ remains steady. The constant value of the adsorption capacity ($q_t$) may happened due to filling off most of the surface sites of adsorbents by adsorbate which named by “fill-pores mechanism”, the remaining adsorbate molecules may compete with the adsorbed difenoconazole in the adsorbent sites, and cause a random movement of molecules with the passage of time which lead to steady value of the amount of adsorption capacity with increasing of contact time.

#### 3.3.1.1.2 pH Effect

pH value effect on adsorption considers a vital parameter for controlling the removal for pesticides from water. (Figure 3.15) detects pH effect for difenoconazole uptake in each adsorption. These experiments were detected at the equilibrium times for Nanocellulose, Cellulose functionalized with 2-furan carbonyl chloride (Cel-F) or Cellulose functionalized with 2,6-pyridine

dicarbonyl dichloride (Cel-P), with varying the pH of the mixture that ranges from 2.0 to 10.0.

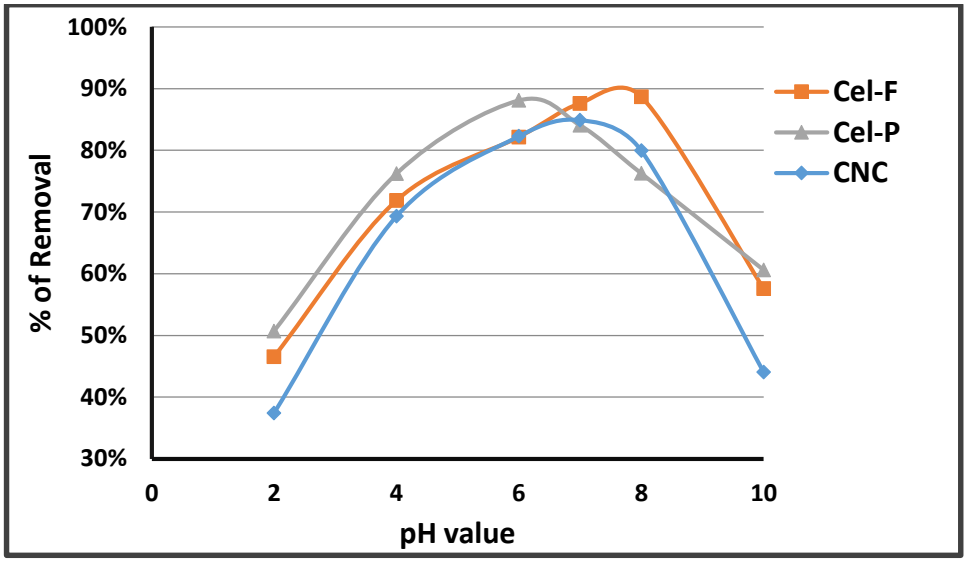


**Figure 3.15:** pH Effect for Difenoconazole removal by CNC, Cel-F and Cel-P, (nanopolymer dosage = 10 mg, reaction mixture volume = 10 mL, initial concentration = 10 mg/L, temperature = 20 °C).

The pH value considers a critical and vital element in adsorption process because that pH value could control the surface charge of the adsorbent and adsorbate. At pH lower than 3.0, all difenoconazole amines are is in the ammonium form ($-NR_3H^+$). Because of this the adsorption efficiency was the lowest (less than 40%). However, at pH values higher than 6.0, the amines are in the basic form, each pair of electrons is available for binding, the highest difenoconazole removal efficiency was observed at pH value in the range 4.0 to 7.0. In the case of using cellulose modified with 2-furan carbonyl chloride (Cel-F), the removal percentage is directly proportional with pH until attain a maximum at pH value of 8, after that; it decays with further increasing in the value of pH. Cel-F has the maximum percentage of difenoconazole removal that was 88.70%, the percent for cellulose modified

with 2,6-pyridine dicarbonyl dichloride (Cel-P) was 88.10%, and for cellulose nanocrystalline bio-adsorbent, the removal percent was 84.89%.

In addition, pH effect on adsorption efficiency of Nanocellulose and Cellulose functionalized with 2,6-pyridine dicarbonyl dichloride (Cel-P) increases with pH for the range from pH of 2 and until reaching a pH value of 7 (for Cel-F) and pH 6 (for Cel-P), then; the percent of difenoconazole removal decreases as pH increases. Low uptake capacity occurs at lower pH, this is probably due to protonation of alcohol oxygen atoms of the adsorbent. The binding of pesticide on each adsorbent is properly controlled by H-bond interaction between hydrogen bonding donor group and O-donor group, here H-bonding between OH group in cellulose derivatives and carbonyl group (-C=O) in difenoconazole may be likely dominated. Difenoconazole pesticide has low solubility in water (15 mg/L), the results demonstrated that difenoconazole adsorption decreased as pH increased, suggesting that the negative surface of adsorbent and the anionic difenoconazole may generate an electrostatic repulsion.

The increase in pesticide removal at the medium pH values for the three adsorbents can be explained by increasing dipole-dipole interaction between difenoconazole and the new synthesized cellulose derivatives comparing with too low (pH = 2) or too high (pH =10).

#### 3.3.1.1.3 Pesticide Concentration Effect

The initial concentration of difenoconazole will effect on the value of percentage removal. Percent’s of pesticide removal using the three prepared

adsorbents are investigated at the optimum values of shaking time and pH for each adsorption process. Difenoconazole maximum percentage removal was 88.90% for Cellulose modified with 2-furan carbonyl chloride (Cel-F) by using a concentration of 10 ppm from Difenoconazole solution. However, the detected initial difenoconazole concentrations on Nanocellulose and Cellulose functionalized with 2,6-pyridine dicarbonyl dichloride (Cel-P) compounds are 12.0 ppm and 8.0 ppm respectively, in which the pesticide percentage removal was 87.70% for Nanocellulose, and 88.31% for Cellulose functionalized with 2,6-pyridine dicarbonyl dichloride (Cel-P) (Figure 3.16).

As the initial concentration of pesticide increases, the mass transfer driving force will facilitate difenoconazole diffusion from the bulk solution to cellulose derivatives surfaces, and this will enhance the equilibrium adsorption capacity.

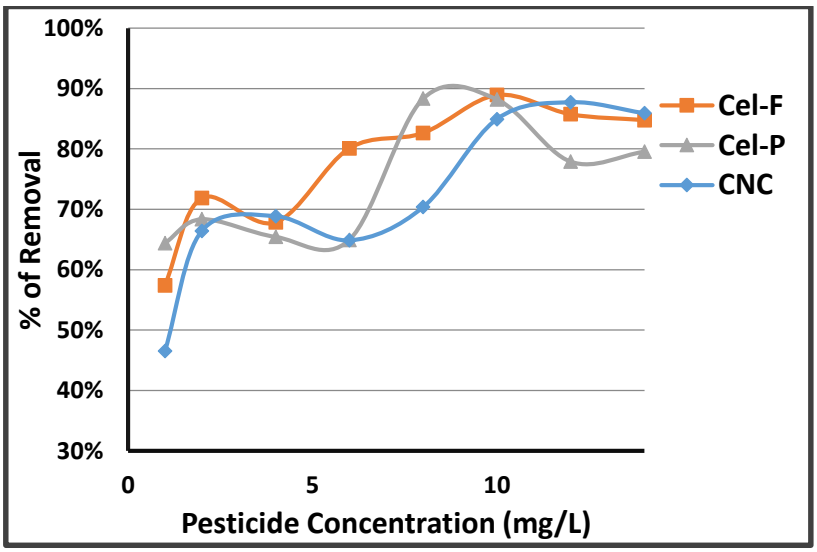


**Figure 3.16:** Pesticide concentration effect for Difenoconazole removal by CNC, Cel-F and Cel-P, (nanopolymer dosage = 10 mg, reaction mixture volume = 10 mL, temperature = 20 °C).

### 3.3.1.1.4 Temperature Effect

To investigate the temperature effect for Difenoconazole adsorption on Nanocellulose, Cellulose functionalized with 2-furan carbonyl chloride (Cel-F) or Cellulose functionalized with 2,6-pyridine dicarbonyl dichloride (Cel-P). All optimum values of pH, time and pesticide concentration values were taken into account. Generally, difenoconazole adsorption efficiency decreases at high values of temperature.

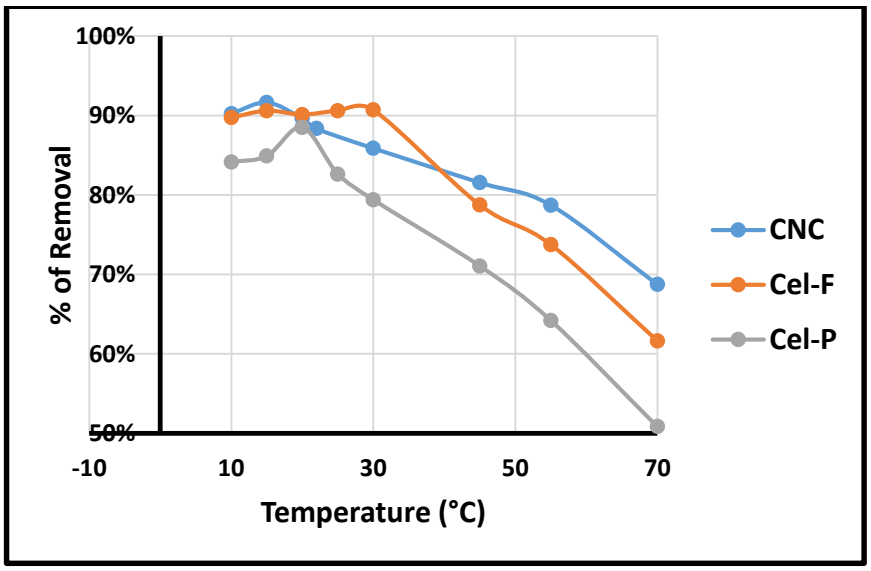


**Figure 3.17:** Temperature effect for Difenoconazole removal by CNC, Cel-F and Cel-P, (nanopolymer dosage = 10 mg, reaction mixture volume = 10 mL pesticide concentration = 12, 10, 8 ppm for CNC, Cel-F and Cel-P respectively).

(Figure 3.17) detects adsorption of Difenoconazole pesticide on the three synthesized adsorbents including Nanocellulose, Cellulose functionalized with 2-furan carbonyl chloride (Cel-F) or Cellulose functionalized with 2,6-pyridine dicarbonyl dichloride (Cel-P) has been found to increase with increasing in temperature until reaching the optimum removal percent at 15 °C, 30 °C and 20 °C respectively. Then, difenoconazole percentage removal

decays with further heating, the percentages of removing at each optimum temperature was 91.65% of Nanocellulose, 90.70% for Cellulose functionalized with 2-furan carbonyl chloride (Cel-F) and 88.49% for Cellulose functionalized with 2,6-pyridine dicarbonyl dichloride (Cel-P). At these optimum temperatures of the solution, the interaction ability between difenoconazole and the synthesized compounds was enhanced, and this resulted in increasing the adsorption efficiency. While, at high temperature values, the adsorption capacity between the adsorbate and the adsorbent was low.

Increasing the temperature above room temperature has slight influence on the adsorption capacity of the new modified adsorbent surface. During the temperature range from 10°C to 30 °C, increasing of the amount of the pesticide adsorbed with increasing in temperature (between 10 °C and 30 °C) may result from increasing in the diffusion rate of difenoconazole molecules neighboring the external surface and internal pores of the adsorbent. Increase in temperature may have also been responsible for increase in porosity and total pore volume of the adsorbent. As well as, the chemical structure and the functional groups in each adsorbent make them perfect for removing difenoconazole pesticide at the optimum temperature values.

#### 3.3.1.1.5 Adsorbent Dose Effect

The adsorptions experimental results for Difenoconazole removal using Nanocellulose, Cellulose functionalized with 2-furan carbonyl chloride (Cel-F) or Cellulose functionalized with 2,6-pyridine dicarbonyl dichloride (Cel-

P) are appeared in (Figure 3.18). The adsorbent dose was ranged from 1.0 mg to 20.0 mg, and all optimum conditions of time, pH, adsorbate concentration and temperature were applied for each experiment.

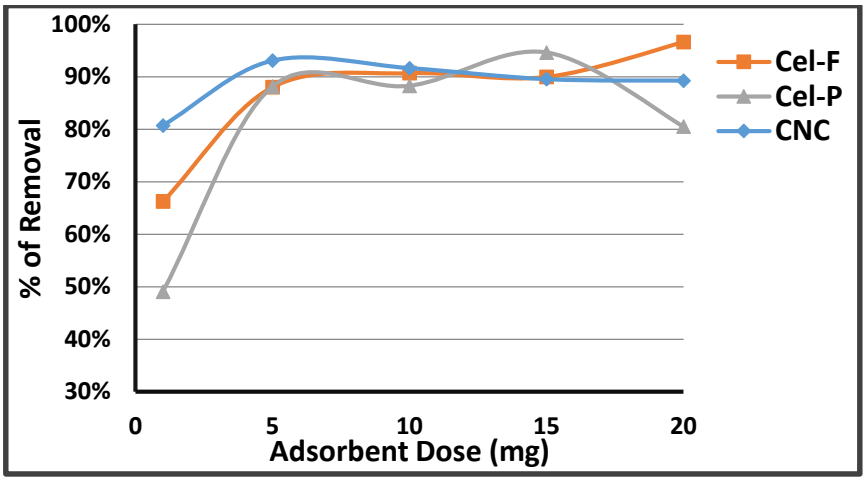


**Figure 3.18:** Adsorbent dose effect for Difenoconazole removal by CNC, Cel-F and Cel-P, (reaction volume solution = 10 mL).

The highest percent of Difenoconazole removal was 96.63% using 20.0 mg of Cellulose functionalized with 2-furan carbonyl chloride (Cel-F). Such that, the mass of this new synthesized adsorbent is directly proportional with the Difenoconazole percentage removal. Also, the same relation between percent of pesticide removal and the adsorbent mass between dosage (1.0 to 15.0 mg) was also observed for Cellulose functionalized with 2,6-pyridine dicarbonyl dichloride (Cel-P) with 15 mg of adsorbent and 94.65% as percentage of difenoconazole removal. However, Nanocellulose gave a different adsorbent dose effect in which the maximum percent that was detected of Difenoconazole removal was 93.08% with only 5.0 mg dose that can be explained by the promising porosity and the high surface area to volume ratio for Cellulose nanocrystalline

The results indicated that, the adsorption process on the synthesized nanopolymers could be taking place through diffusion process and surface coordination mechanisms. An increasing in the nanopolymer dosage was resulted in an increase in the number of available adsorption sites, as a results of the rare of difenoconazole adsorption increased. When all the adsorption sites on the adsorbent get occupied, then, diffusion process will begin to occur, which can be controlled by osmosis, so as the concentration of the adsorbate in the nanopolymer body is equal to that in the solution, the adsorption reaches the plateau.

The rapidly increasing in pesticides percentage removal with increasing in adsorbent mass for Cellulose functionalized with 2-furan carbonyl chloride (Cel-F) or Cellulose functionalized with 2,6-pyridine dicarbonyl dichloride (Cel-P), is because of the presence of greater availability of exchangeable sites on the adsorbent surface area, as well as increasing Hydrogen Bonding with increasing adsorbent mass. However, when Nanocellulose was used, it has been detected that just only (5.0 mg) of this adsorbent resulting in high ability for removing difenoconazole from water, because of the functional groups (hydroxyl groups) in its chemical structure and its unique porosity which make it perfect adsorbent.

**Table 3.1: The results for Difenoconazole removal by Cellulose Nanocrystalline, Cellulose functionalized with 2-furan carbonyl chloride (Cel-F) or Cellulose functionalized with 2,6-pyridine dicarbonyl dichloride (Cel-P).**

| Adsorption of Difenoconazole | | | |
|---|---|---|---|
| Optimum Condition and % of Difenoconazole Removal | CNC | Cel-F | Cel-P |
| Contact Time (minute)<br>% of Removal | 20<br>84.97% | 20<br>87.07% | 60<br>87.05% |
| pH value<br>% of Removal | 7<br>84.89% | 8<br>88.70% | 6<br>88.10% |
| Adsorbate Concentration(ppm)<br>% of Removal | 12<br>87.70% | 10<br>88.90% | 8<br>88.31% |
| Temperature (°C)<br>% of Removal | 15<br>91.65% | 30<br>90.70% | 20<br>88.49% |
| Adsorbent Dose (mg)<br>% of Removal | 5<br>93.08% | 20<br>96.63% | 15<br>94.65% |

### 3.3.1.2 Adsorption of Tetraconazole

Solution conditions effects for Tetraconazole pesticide adsorption on Nanocellulose, Cellulose functionalized with 2-furan carbonyl chloride (Cel-F) or Cellulose functionalized with 2,6-pyridine dicarbonyl dichloride (Cel-P) are investigated.

#### 3.3.1.2.1 Contact Time Effect

For determining the optimum time of each adsorption process between tetraconazole adsorbate and each of the used adsorbents, percent's of removal for this pesticide were calculated at different values of shaking time ranging from 1 minute to 2.0 hours, as appears in (Figure 3.19).

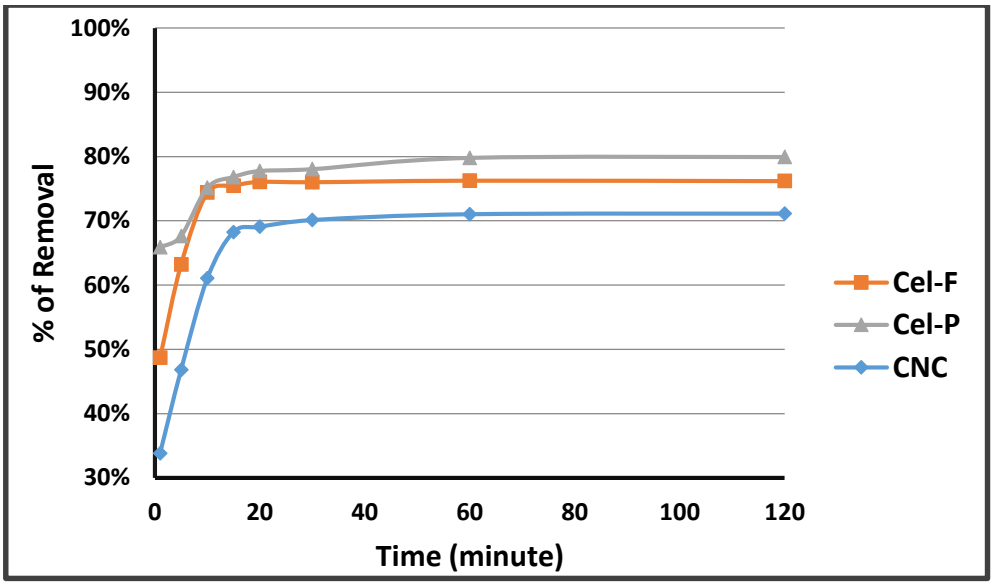


**Figure 3.19:** Contact time Effect for Tetraconazole removal by CNC, Cel-F and Cel-P, (nanopolymer dosage = 10 mg, reaction mixture volume = 10 mL, initial concentration = 10 mg/L, pH = 7, temperature = 20 °C).

This Figure clarifies that Tetraconazole adsorption was at maximum value for Cellulose functionalized with 2,6-pyridine dicarbonyl dichloride (Cel-P) after 20 minutes of shaking, this time represents the optimum contact time between Tetraconazole and Cel-P, this percentage was 77.75%. However, when Cellulose functionalized with 2-furan carbonyl chloride (Cel-F) is used for tetraconazole adsorption, the percent of removal was 75.47%, with optimum time of 15 minutes. In case of using Nanocellulose, the optimum contact time was 30 minutes with 70.12% as percentage removal. For Nanocellulose, Cel-F and Cel-P; the adsorbed amount of tetraconazole pesticide at the equilibrium time remains approximately without changing. These large removal percentages of pesticide are due the high percentages of tetraconazole removal are due to the unique chemical structure of the adsorbents, as well as, making a cyclic cavity which is packed with the various binding sites, which makes an unique and perfect adsorbent with its

ability in trapping the adsorbate tetraconazole through several intermolecular bonding forces, for instance; π-π stacking and H-bonding, such that the presence of high availability of empty sites on the adsorbent surface and the strong intermolecular bonding that occur between the two components represented by π-π interaction and H-bonding forces. Such that, the adsorption capacity increases as the shaking time of the adsorbent and adsorbate interaction increases, this enables Tetraconazole to interact efficiently with the newly synthesized adsorbents after reaching equilibrium time ($t_e$).

After $t_e$, the adsorption capacity $q_e$ remains steady. The constant value of the adsorption capacity ($q_t$) may occur because of filling of most of the surface sites of adsorbents by adsorbate that named by “fill-pores mechanism”, the remaining adsorbate molecules may compete with the adsorbed Tetraconazole in the adsorbent sites and cause a random movement of molecules with the passage of time, which leading into a steady value of the amount of adsorption capacity with increasing of contact time.

**3.3.1.2.2 pH Effect**

(Figure 3.20) clarifies the pH value effect for tetraconazole uptake on each adsorbent. These experiments were done at the optimum time of adsorption for Nanocellulose, Cellulose functionalized with 2-furan carbonyl chloride (Cel-F) or Cellulose functionalized with 2,6-pyridine dicarbonyl dichloride (Cel-P) with changing the pH of solution that ranges from 2.0 to 10.0.

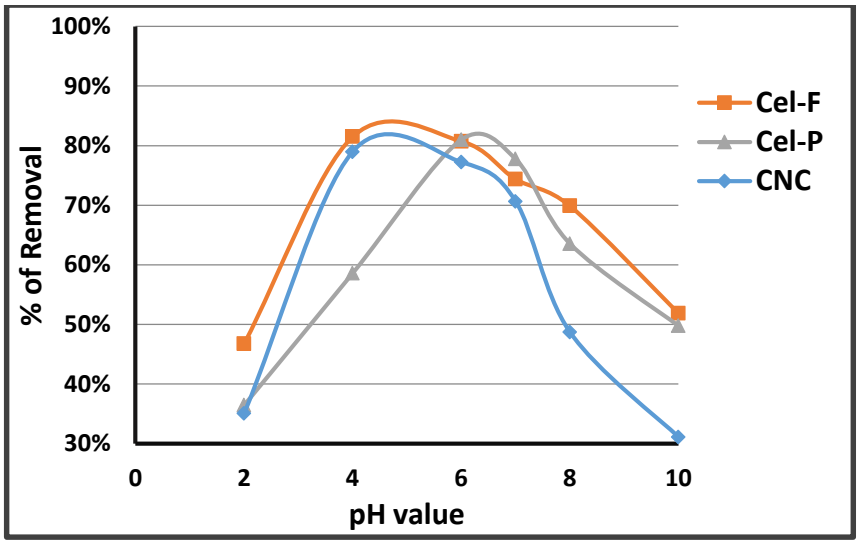


**Figure 3.20:** pH Effect for Tetraconazole removal by CNC, Cel-F and Cel-P, (nanopolymer dosage = 10 mg, reaction mixture volume =10 mL, initial concentration = 10 mg/L, temperature = 20 °C).

The pH value is a critical and vital factor in controlling the adsorption process, such that, pH value could control the surface charge of the nanopolymer adsorbent and tetraconazole pesticide. At pH lower than 3.0, all tetraconazole amines are is in the ammonium form ($-NR_3H^+$). Because of this, the adsorption efficiency was very low (less than 40%). However, at pH values higher than 6.0, the amines are all in the basic form, in which each pair of electrons available for binding. The highest tetraconazole removal efficiency was observed at pH value in the range 4.0 to 7.0. In the case of using Cellulose modified with 2-furan carbonyl chloride (Cel-F), % removal of adsorption increases from a range of pH from 2.0 to 4.0, and thereafter, the removing percent decreases with higher values of pH values. From the graph, it appears that (Cel-F) has the maximum removing percent of Tetraconazole that is 81.51%. However, Cellulose modified with 2,6-

pyridine dicarbonyl dichloride (Cel-P) has percentage removal equals 81.00% and for Nanocellulose Bio-adsorbent, it equals 78.97%.

Additionally, it was detected that the influence of pH value on the percent of Tetraconazole removal for Nanocellulose and Cellulose functionalized with 2,6-pyridine dicarbonyl dichloride (Cel-P) increases for the pH range from 2.0 and until reaching a maximum percent at pH 4.0 (for Nanocellulose) and pH 6.0 ( for Cel-P), and thereafter, the percent of tetraconazole removal decreases with higher pH values.

Low uptake capacity occurs at lower pH, this is probably due to protonation of alcohol oxygen atoms on the adsorbent. The binding of pesticide on each adsorbent is properly controlled by H-bond interaction between hydrogen bonding donor group and O-donor group, here H-bonding between OH group in cellulose derivatives in and carbonyl group (-C=O) in Tetraconazole may be likely dominated. The results demonstrated that Tetraconazole adsorption decreased as pH increased, suggesting that the negative surface of adsorbent and the anionic Tetraconazole may generate an electrostatic repulsion.

The increase in pesticide removal at the medium pH values for the three adsorbents can be explained by increasing dipole-dipole interaction between tetraconazole pesticide and the new synthesized cellulose derivatives comparing with too low (pH = 2) or too high (pH =10).

### 3.3.1.2.3 Pesticide Concentration Effect

Tetraconazole initial concentration effect on the percentage removal using cellulose nanocrystalline, Cel-F and Cel-P is detected at the previous optimum conditions, including optimum shaking time and pH for each adsorption process. The maximum percent for Tetraconazole removal was 92.93% for Cellulose modified with 2,6-pyridine dicarbonyl dichloride (Cel-P) by using 6.0 ppm concentration of Tetraconazole. However, the observed concentrations for having the highest percent of Tetraconazole removal on Nanocellulose and Cellulose modified with 2-furan carbonyl chloride (Cel-F) compounds, are 4.0 ppm with removal percent equals 91.63% for Nanocellulose, and 8.0 ppm with 90.09% percentage removal for Cellulose modified with 2-furan carbonyl chloride, as appears in (Figure 3.21).

As the initial concentration of pesticide increases, the mass transfer driving force will facilitate Tetraconazole diffusion from the bulk solution to cellulose derivatives surfaces, and this will enhance the equilibrium adsorption capacity.

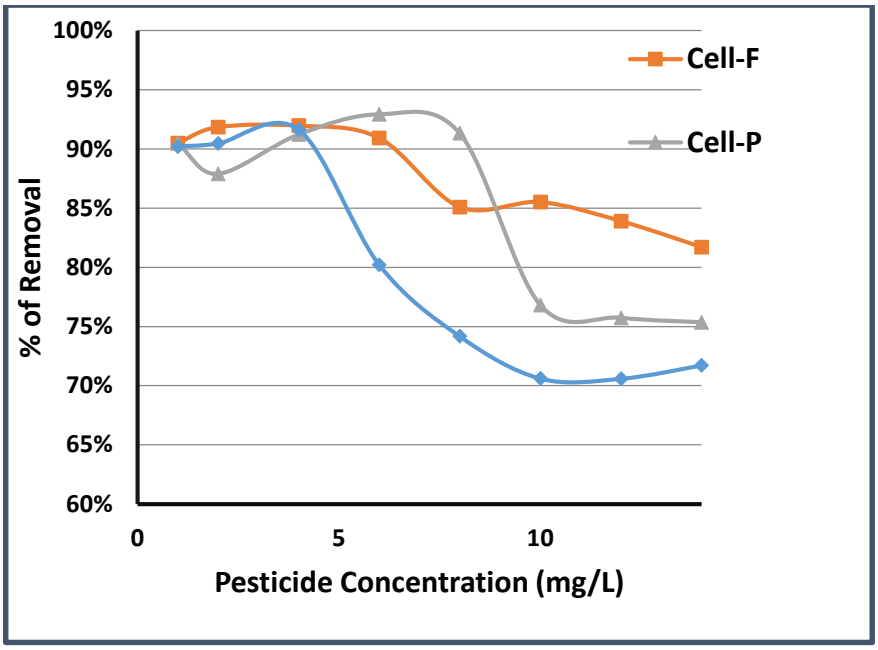


**Figure 3.21:** Pesticide concentration Effect for Tetraconazole removal by CNC, Cel-F and Cel-P, (nanopolymer dosage = 10 mg, reaction mixture volume = 10 mL, temperature = 20 °C).

### 3.3.1.2.4 Temperature Effect

In order to find out the effect of temperature for the adsorption of Tetraconazole on Nanocellulose, Cellulose functionalized with 2-furan carbonyl chloride (Cel-F) or Cellulose functionalized with 2,6-pyridine dicarbonyl dichloride (Cel-P). The best solution conditions, including contact time, pH and pesticide concentration values must be taken into account. In general, percent's of Tetraconazole removal drop with high temperatures.

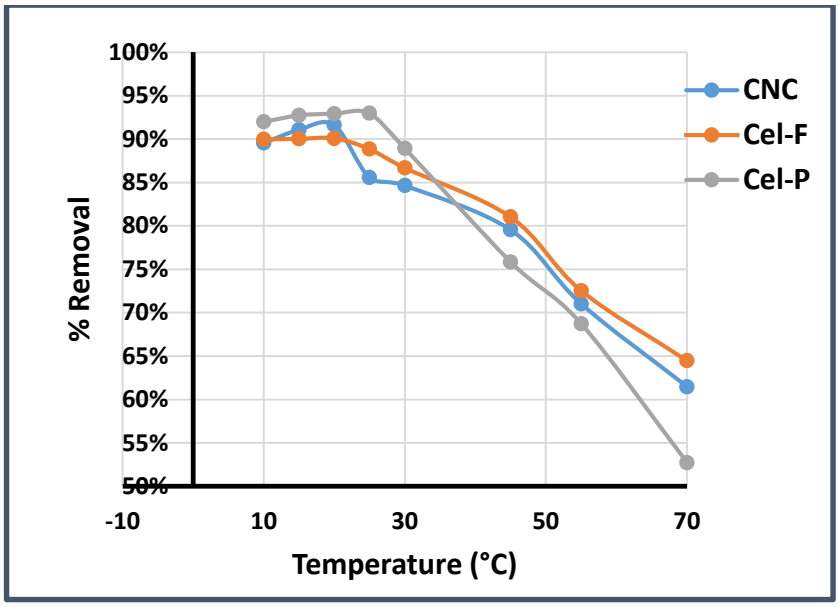


**Figure 3.22:** Temperature Effect for Tetraconazole removal by CNC, Cel-F and Cel-P, (nanopolymer dosage = 10 mg, reaction mixture volume = 10 mL, pesticide concentration = 4, 8, 6 ppm for CNC, Cel-F and Cel-P respectively).

(Figure 3.22) shows that the adsorption of Tetraconazole pesticide on the three adsorbents, including Nanocellulose, Cellulose functionalized with 2-furan carbonyl chloride (Cel-F) or Cellulose functionalized with 2,6-pyridine dicarbonyl dichloride (Cel-P) has been found to increase with increasing in temperature until reaching a maximum amount at 20 °C, 20 °C and 25 °C respectively, and thereafter more heating resulted in decreasing the percentage of Tetraconazole removal. Pesticide percentages removal at the optimum temperature value were 91.63% for Nanocellulose, 90.09% for (Cel-F) and 92.98% for (Cel-P). These temperatures of the solution enhanced the interaction ability between Tetraconazole and each of synthesized compounds and hence increasing the efficiency of the adsorption process. While, at high temperature values, the adsorption capacity between the pesticide and the adsorbent was low. During the temperature range from 10°C to 25 °C, increasing of the amount of pesticide adsorbed with

increasing in temperature may resulted from the increasing in the rate of diffusion of tetraconazole molecules neighboring the external surface and internal pores of the adsorbent. Increase in temperature may also have be responsible for increasing in porosity and the total pore volume of the adsorbent. Additionally, the unique chemical structure and the suitable functional groups in each adsorbent make them perfect for removing tetraconazole at the optimum temperatures.

### 3.3.1.2.5 Adsorbent Dose Effect

The experimental results for Tetraconazole adsorption on Nanocellulose, Cellulose functionalized with 2-furan carbonyl chloride (Cel-F) or Cellulose functionalized with 2,6-pyridine dicarbonyl dichloride (Cel-P) are appeared in (Figure 3.23) with adsorbent dose ranging from 1.0 mg to 20.0 mg, at the most favorable conditions of shaking time, pH value, pesticide concentration and temperature.

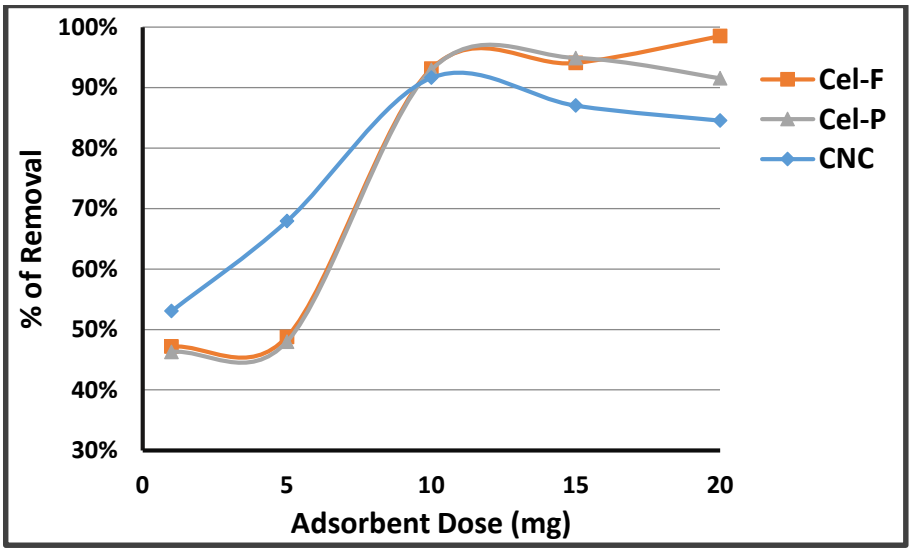


**Figure 3.23:** Adsorbent dose Effect for Tetraconazole removal by CNC, Cel-F and Cel-P, (reaction mixture volume = 10 mL).

Tetraconazole maximum adsorption was 98.73% using 20.0 mg of Cellulose functionalized with 2-furan carbonyl chloride (Cel-F). Such that, this new synthesized adsorbent appears increasing in the percentage removal with increasing the mass of Cel-F. In addition, the same relation between percentage removal and adsorbent mass between dosage (1.0 to 15.0 mg) is observed for Cellulose modified with 2,6-pyridine dicarbonyl dichloride (Cel-P) with 15.0 mg of adsorbent dose and 94.51% as percentage removal. Tetraconazole maximum percentage removal in case of using Nanocellulose Adsorbent was 91.73% with 10.0 mg adsorbent dose, which can be explained by vacant sites availability and the unsaturation of adsorption sites. The results indicate that, the adsorption process could be controlled through the diffusion process and surface coordination mechanisms. An increasing in the nanopolymer dosage resulted in an increase in the number of the available adsorption sites on the adsorbent. When all adsorption sites on the nanopolymers get occupied, then the diffusion process begins to occur, which is controlled by osmosis, so as the concentration of the adsorbate in the polymer body is equal to that in the solution, the adsorption reaches the plateau.

The rapidly increased percentage removal of Tetraconazole with increasing the dose for (Cel-F) or (Cel-P), is due to the high availability of the exchangeable sites on the adsorbent surface area and increasing H-Bonding with increasing adsorbent mass.

**Table 3.2: The results for Tetraconazole removal by Cellulose Nanocrystalline, Cellulose Functionalized with 2-furan carbonyl chloride (Cel-F) or Cellulose Functionalized with 2,6-pyridine dicarbonyl dichloride (Cel-P).**

| Adsorption of Tetraconazole | | | |
|---|---|---|---|
| Optimum Condition and % of Tetraconazole Removal | CNC | Cel-F | Cel-P |
| Contact Time (minute)<br>% of Removal | 30<br>70.12% | 15<br>75.47% | 20<br>77.75% |
| pH value<br>% of Removal | 4<br>78.97% | 4<br>81.51% | 6<br>81.00% |
| Adsorbate Concentration(ppm)<br>% of Removal | 4<br>91.63% | 8<br>90.09% | 6<br>92.93% |
| Temperature (°C)<br>% of Removal | 20<br>91.63% | 20<br>90.09% | 25<br>92.98% |
| Adsorbent Dose (mg)<br>% of Removal | 10<br>91.73% | 20<br>98.51% | 15<br>94.88% |

### 3.3.2 Using The Same Adsorbent with Different Pesticides

#### 3.3.2.1 Adsorption by Cellulose Nanocrystalline

Solution conditions Effects for the same adsorbent and different pesticides are measured for the adsorption on Cellulose Nanocrystalline for the removal of Difenoconazole and Tetraconazole pesticides, as shown in the following Figures from (Figures 3.24) to (Figure 3.28).

### 3.3.2.1.1 Contact Time Effect

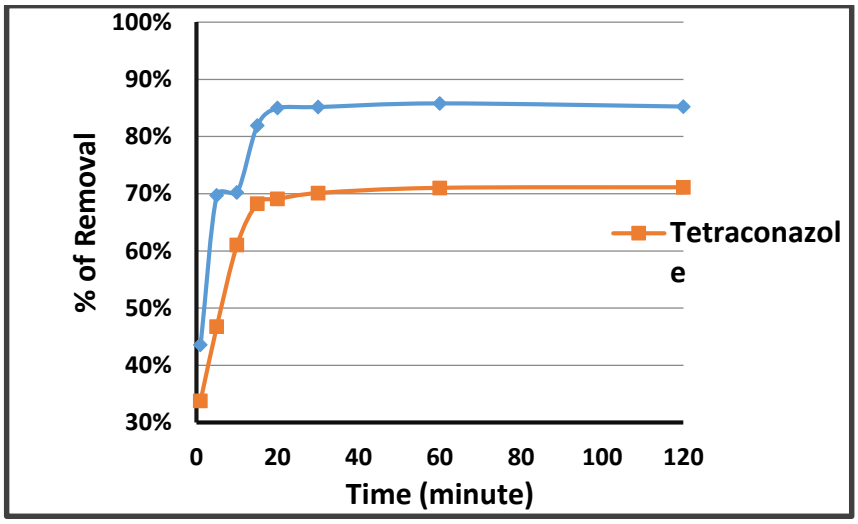


**Figure 3.24:** Contact time Effect for Difenoconazole and Tetraconazole removal by Cellulose Nanocrystalline, (nanopolymer dosage = 10 mg, reaction mixture volume = 10 mL, initial concentration = 10 mg/L, pH = 7, temperature = 20 °C).

### 3.3.2.1.2 pH Effect

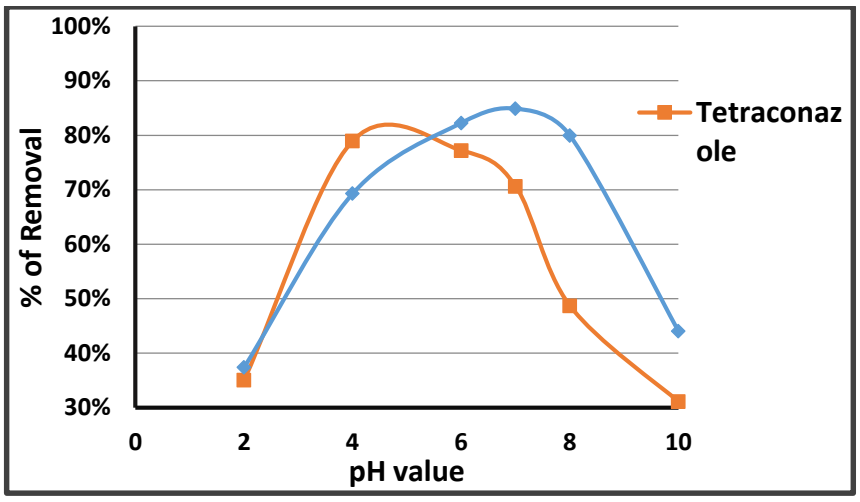


**Figure 3.25:** pH Effect for Difenoconazole and Tetraconazole removal by Cellulose Nanocrystalline, (nanopolymer dosage = 10 mg, reaction mixture volume = 10 mL, initial concentration =10 mg/L, temperature = 20 °C).

### 3.3.2.1.3 Pesticide Concentration Effect

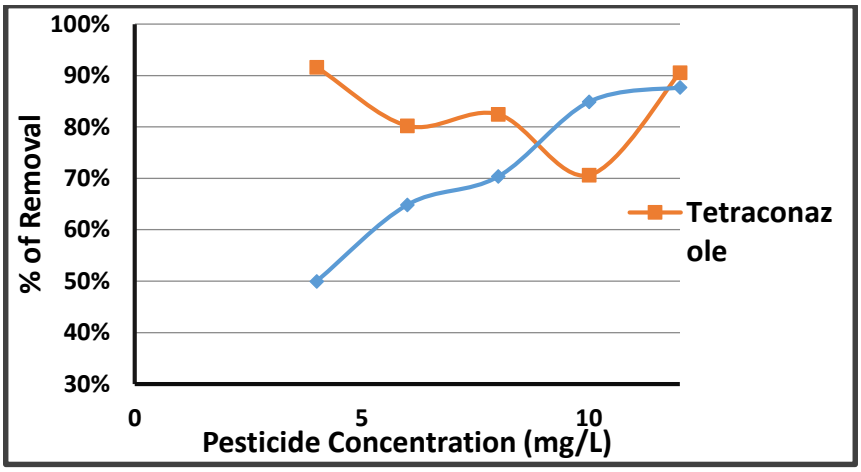


**Figure 3.26:** Pesticide concentration Effect for Difenoconazole and Tetraconazole removal by Cellulose Nanocrystalline, (nanopolymer dosage = 10 mg, reaction mixture volume = 10 mL, temperature = 20 °C).

### 3.3.2.1.4 Temperature Effect

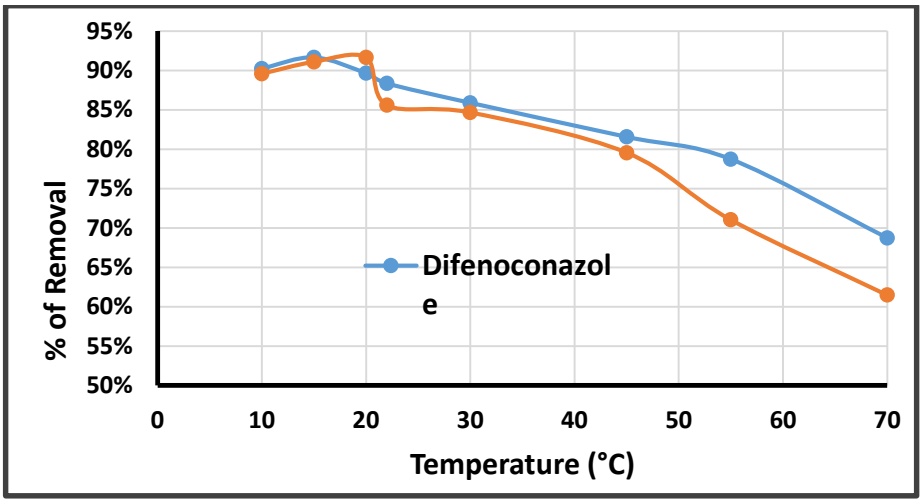


**Figure 3.27:** Temperature Effect for Difenoconazole and Tetraconazole removal by Cellulose Nanocrystalline, (nanopolymer dosage = 10 mg, reaction mixture volume = 10 mL).

### 3.3.2.1.5 Adsorbent Dose Effect

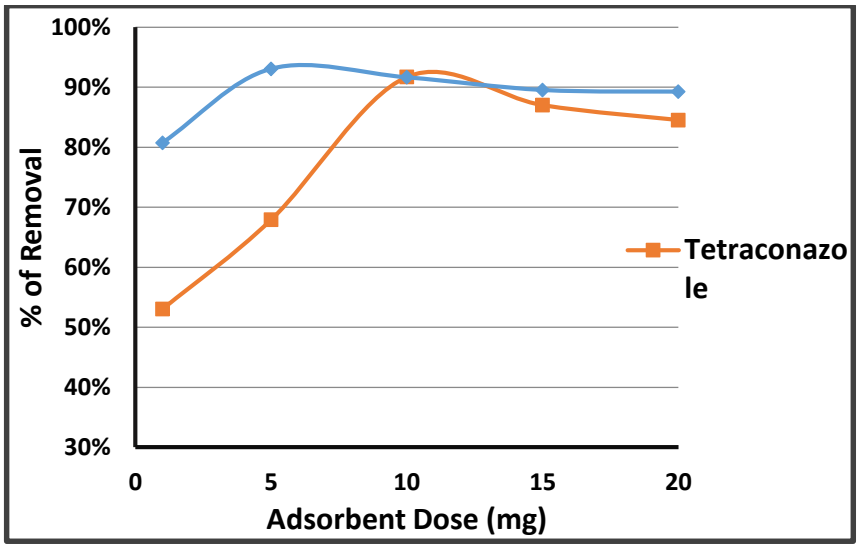


**Figure 3.28:** Adsorbent dose Effect for Difenoconazole and Tetraconazole removal by Cellulose Nanocrystalline, (reaction mixture volume = 10 mL).

**Table 3.3: The adsorption results for Difenoconazole and Tetraconazole removal from water using Cellulose Nanocrystalline.**

| Adsorption on Cellulose Nanocrystalline | | |
|---|---|---|
| Optimum Condition and % of Removal | Difenoconazole | Tetraconazole |
| Contact Time (minute)<br>% of Removal | 20<br>84.97% | 30<br>70.12% |
| pH value<br>% of Removal | 7<br>84.89% | 4<br>78.97% |
| Adsorbate Concentration(ppm)<br>% of Removal | 12<br>87.70% | 4<br>91.63% |
| Temperature (°C)<br>% of Removal | 15<br>91.65% | 20<br>91.63% |
| Adsorbent Dose (mg)<br>% of Removal | 5<br>93.08% | 10<br>91.73% |

### 3.3.1.2 Adsorption by Cellulose Functionalized with 2-furan carbonyl chloride

The effect of solution conditions for the adsorption on Cellulose functionalized with 2-furan carbonyl chloride for the removal of Difenoconazole and Tetraconazole pesticides was determined, as shown in the following Figures from (Figures 3.29) to (Figure 3.33).

### 3.3.2.2.1 Contact Time Effect

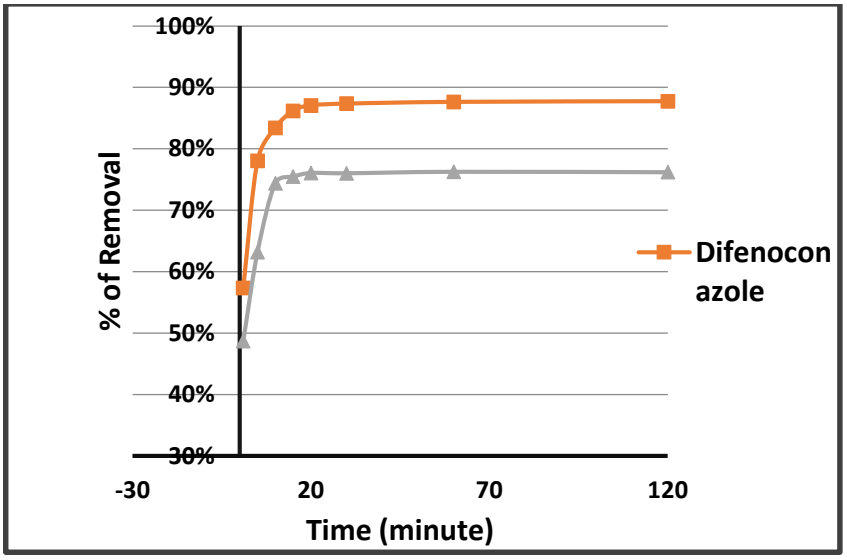


**Figure 3.29:** Contact time Effect for Difenoconazole and Tetraconazole removal by Cellulose functionalized with 2-furan carbonyl chloride, (nanopolymer dosage = 10 mg, reaction mixture volume = 10 mL, initial concentration = 10 mg/L, pH = 7, temperature = 20 °C).

### 3.3.2.2.2 pH Effect

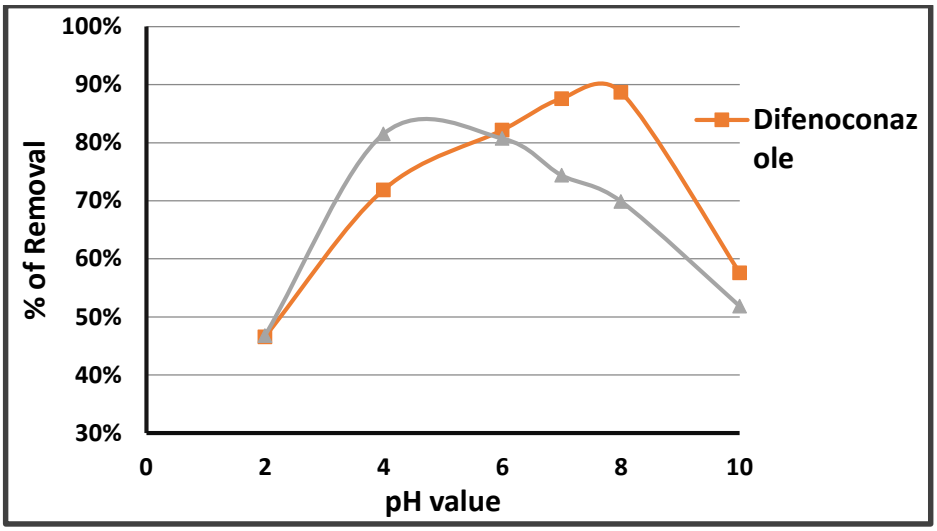


**Figure 3.30:** pH Effect for Difenoconazole and Tetraconazole removal by Cellulose functionalized with 2-furan carbonyl chloride, (nanopolymer dosage = 10 mg, reaction mixture volume = 10 mL, initial concentration = 10 mg/L, temperature = 20 °C).

### 3.3.2.2.3 Pesticide Concentration Effect

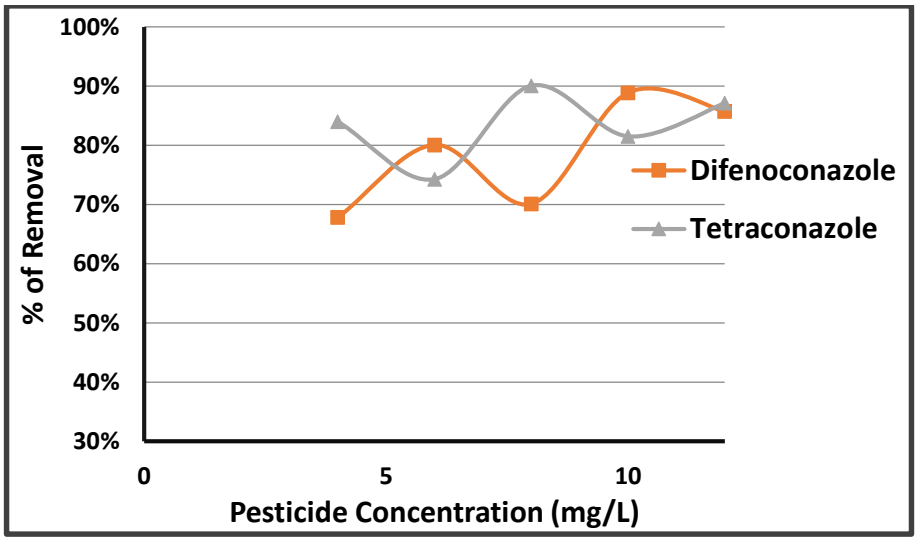


**Figure 3.31:** Pesticide concentration Effect for Difenoconazole and Tetraconazole removal by Cellulose functionalized with 2-furan carbonyl chloride, (nanopolymer dosage = 10 mg, reaction mixture volume = 10 mL, temperature = 20 °C).

### 3.3.2.2.4 Temperature Effect

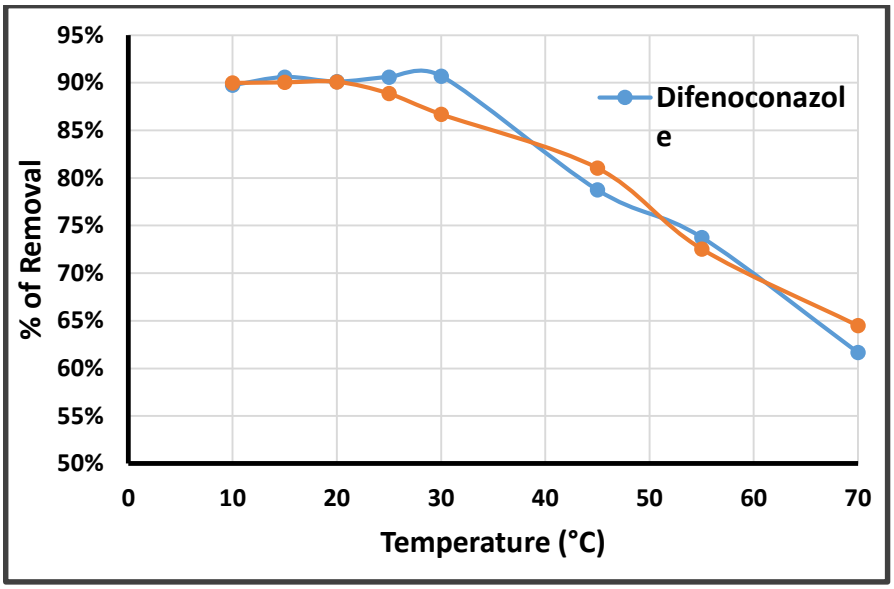


**Figure 3.32:** Temperature Effect for Difenoconazole and Tetraconazole removal by Cellulose functionalized with 2-furan carbonyl chloride, (nanopolymer dosage = 10 mg, reaction mixture volume = 10 mL).

### 3.3.2.2.5 Adsorbent Dose Effect

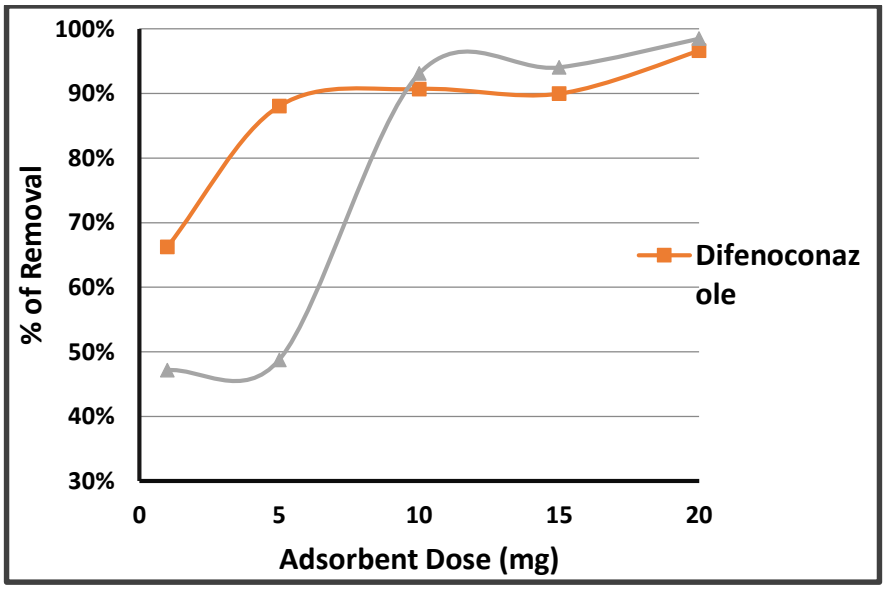


**Figure 3.33:** Adsorbent dose Effect for Difenoconazole and Tetraconazole removal by Cellulose functionalized with 2-furan carbonyl chloride, (reaction mixture volume = 10 mL).

**Table 3.4: The adsorption results for Difenoconazole and Tetraconazole removal from water using Cellulose Functionalized with 2-furan carbonyl chloride.**

| Adsorption on Cellulose Modified with 2-furan carbonyl chloride | | |
|---|---|---|
| Optimum Condition and % of Removal | Difenoconazole | Tetraconazole |
| Contact Time (minute)<br>% of Removal | 20<br>87.07% | 15<br>75.47% |
| pH value<br>% of Removal | 8<br>88.70% | 4<br>81.51% |
| Adsorbate Concentration(ppm)<br>% of Removal | 10<br>88.90% | 8<br>90.09% |
| Temperature (°C)<br>% of Removal | 30<br>90.70% | 20<br>90.09% |
| Adsorbent Dose (mg)<br>% of Removal | 20<br>96.63% | 20<br>98.51% |

### 3.3.2.3 Adsorption by Cellulose Functionalized with 2,6-Pyridine dicarbonyl dichloride

Solution conditions effects are investigated for the adsorption process on Cellulose functionalized with 2,6-pyridine dicarbonyl dichloride that was used for the removal of Difenoconazole and Tetraconazole pesticides, as shown in the following Figures from (Figures 3.34) to (Figure 3.38).

### 3.3.2.3.1 Contact Time Effect

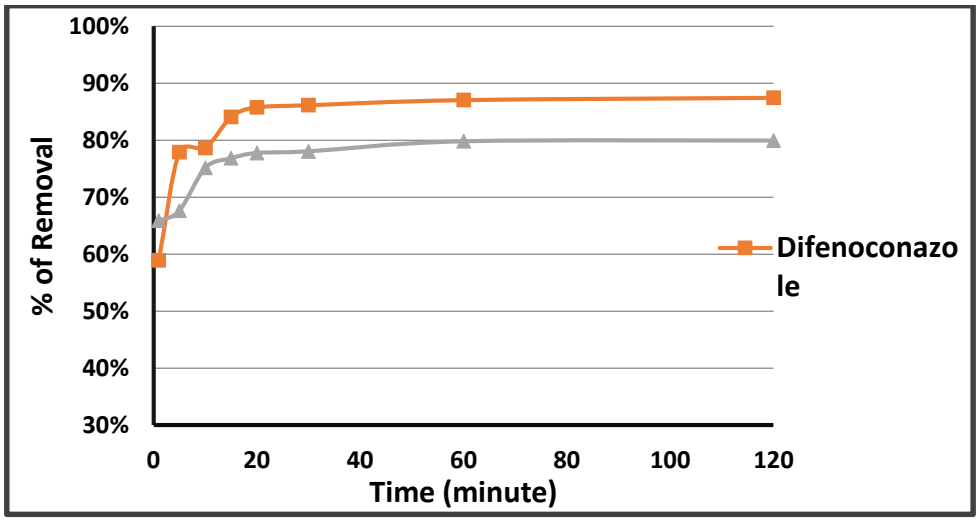


**Figure 3.34:** Contact time Effect for Difenoconazole and Tetraconazole removal by Cellulose functionalized with 2,6-pyridine dicarbonyl dichloride, (nanopolymer dosage = 10 mg, reaction mixture volume = 10 mL, initial concentration = 10 mg/L, pH = 7, temperature = 20 °C).

### 3.3.2.3.2 pH Effect

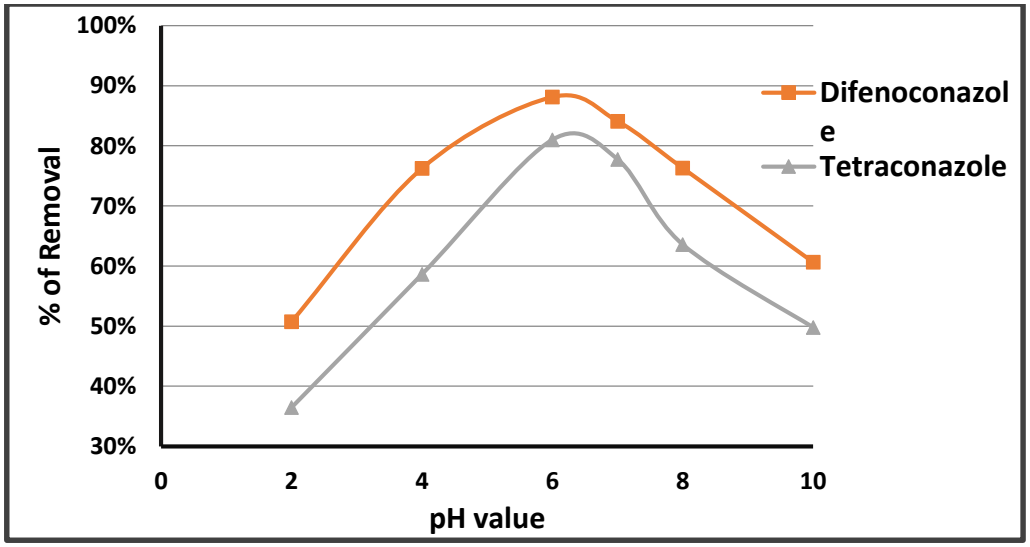


**Figure 3.35:** pH Effect for Difenoconazole and Tetraconazole removal by Cellulose functionalized with 2,6-pyridine dicarbonyl dichloride, (nanopolymer dosage = 10 mg, reaction mixture volume = 10 mL, initial concentration = 10 mg/L, temperature = 20 °C).

### 3.3.2.3.3 Pesticide Concentration Effect

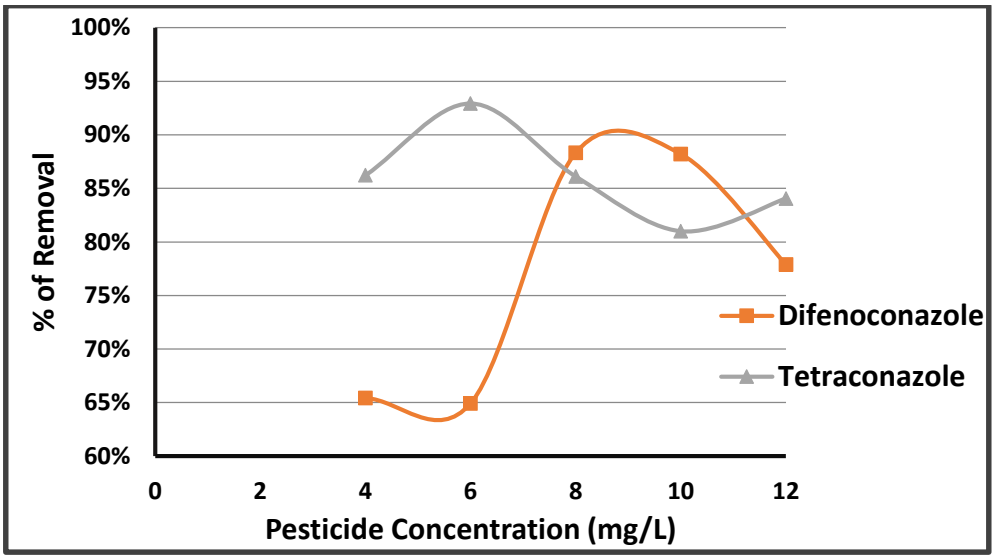


**Figure 3.36:** Pesticide concentration Effect for Difenoconazole and Tetraconazole removal by Cellulose functionalized with 2,6-pyridine dicarbonyl dichloride, (nanopolymer dosage = 10 mg, reaction mixture volume = 10 mL, temperature = 20 °C).

### 3.3.2.3.4 Temperature Effect

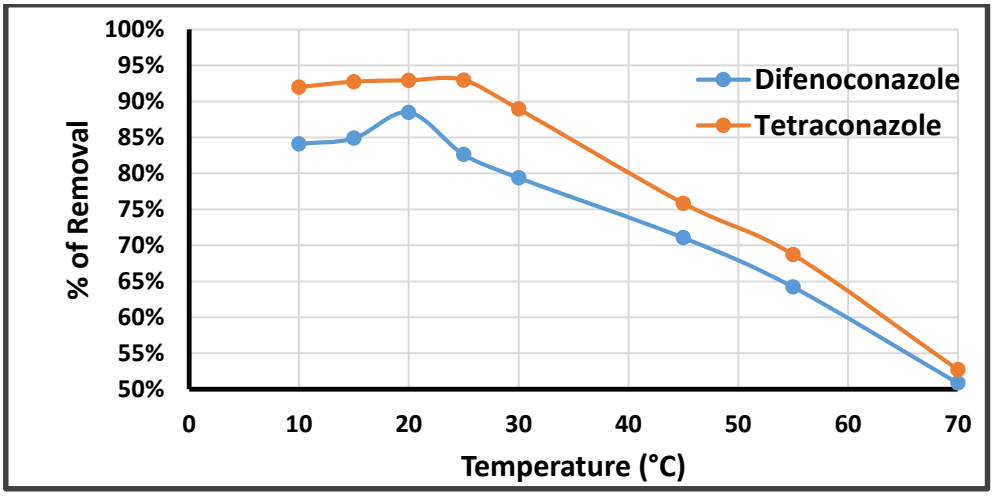


**Figure 3.37:** Temperature Effect for Difenoconazole and Tetraconazole removal by Cellulose functionalized with 2,6-pyridine dicarbonyl dichloride, (nanopolymer dosage = 10 mg, reaction mixture volume = 10 mL).

### 3.3.2.3.5 Adsorbent Dose Effect

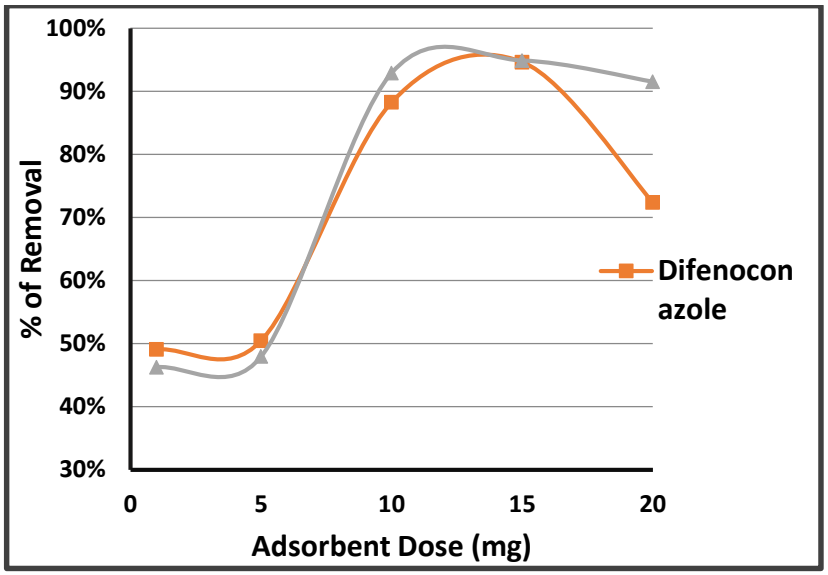


**Figure 3.38:** Adsorbent dose Effect for Difenoconazole and Tetraconazole removal by Cellulose functionalized with 2,6-pyridine dicarbonyl dichloride, (reaction mixture volume = 10 mL).

**Table 3.5: The adsorption results for Difenoconazole and Tetraconazole removal from water using Cellulose Functionalized with 2,6-pyridine dicarbonyl dichloride.**

| Adsorption on Cellulose Modified with 2,6-pyridine dicarbonyl dichloride | | |
|---|---|---|
| Optimum Condition and % of Removal | Difenoconazole | Tetraconazole |
| Contact Time (minute)<br>% of Removal | 60<br>87.05% | 20<br>77.75% |
| pH value<br>% of Removal | 6<br>88.10% | 6<br>81.00% |
| Adsorbate Concentration(ppm)<br>% of Removal | 8<br>88.31% | 6<br>92.93% |
| Temperature (°C)<br>% of Removal | 20<br>88.49% | 25<br>92.98% |
| Adsorbent Dose (mg)<br>% of Removal | 15<br>94.65% | 15<br>94.88% |

**Table 3.6: Comparison for Difenoconazole or Tetraconazole pesticide removal by Cellulose Nanocrystalline, Cellulose functionalized with 2-furan carbonyl chloride (Cel-F) or Cellulose functionalized with 2,6-pyridine dicarbonyl dichloride (Cel-P).**

| Using the same adsorbate with different adsorbents | |
|---|---|
| Adsorption order for Difenoconazole | Cel-F > Cel-P > CNC |
| Adsorption order for Tetraconazole | Cel-F > Cel-P > CNC |
| Using the same adsorbent with different adsorbates | |
| Adsorption order for CNC | Difenoconazole > Tetraconazole |
| Adsorption order for Cel-F | Tetraconazole > Difenoconazole |
| Adsorption order for Cel-P | Tetraconazole > Difenoconazole |

## 3.4 Investigation of Adsorption Parameters

The adsorption efficiency was investigated for the removal of Difenoconazole or Tetraconazole pesticides on Cellulose nanocrystalline, Cellulose functionalized with 2-furan carbonyl chloride (Cel-F) or Cellulose functionalized with 2,6-pyridine dicarbonyl dichloride (Cel-P).

The optimum adsorption isotherm model was detected by studying Langmuir and Freundlich models. In addition, adsorption kinetics are also investigated using pseudo-first-order-kinetic, pseudo-second-order-kinetic and intra-particle-diffusion-adsorption-kinetic models. Moreover, for thermodynamic adsorption parameters, Van't Hoff plot was detected, and hence the enthalpy change, change in Gibbs free energy, and entropy change are calculated from the slope and y-intercept of the graph. These values will give information to determine if each adsorption is spontaneous or not, and if it is endothermic or exothermic one. This will also give a direct indication on how much each adsorption is a favorable or unfavorable process at the studied conditions.

### 3.4.1 Difenoconazole Adsorption by Cellulose Nanocrystalline

#### 3.4.1.1 Adsorption Isotherms

An investigation of the best adsorption isotherm for Difenoconazole pesticide on Cellulose nanocrystalline is determined according to the graphs for Freundlich and Langmuir isotherms. Adsorption isotherm parameters were calculated by plotting equation (1.1) that represents graph of $C_e/q_e$ on y-axis versus $C_e$ on x-axis for Langmuir adsorption isotherm, and equation (1.3) that represents plotting $\log q_e$ on y-axis versus $\log C_e$ on x-axis for Freundlich adsorption isotherm, as appears in (Figure 3.39) and (Figure 3.40) respectively.

##### 3.4.1.1.1 Langmuir Adsorption Isotherm

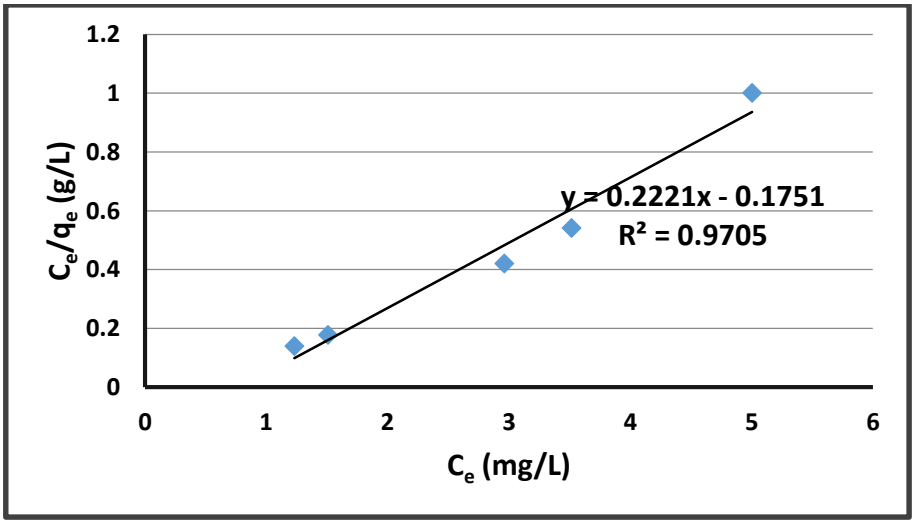


**Figure 3.39:** The plot of Langmuir Isotherm study for Difenoconazole removal by Cellulose Nanocrystalline, (pH = 7, temperature = 20 °C, adsorption time = 20 minute, nanopolymer dosage = 10 mg, reaction mixture volume = 10 mL).

### 3.4.1.1.2 Freundlich Adsorption Isotherm

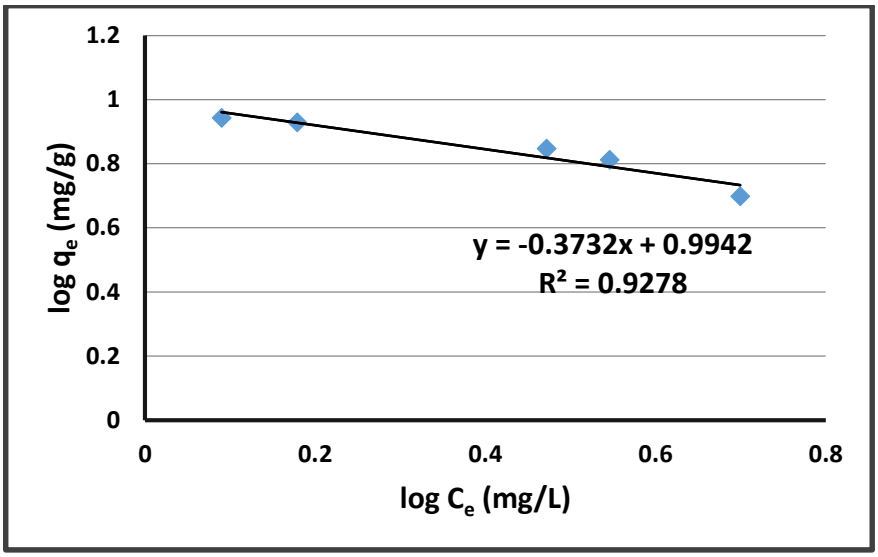


**Figure 3.40:** The plot of Freundlich Isotherm study for Difenoconazole removal by Cellulose Nanocrystalline, (pH = 7, temperature = 20 °C, adsorption time = 20 minute, nanopolymer dosage = 10 mg, reaction mixture volume = 10 mL).

The essential features of the Langmuir isotherm can be expressed in terms of a dimensionless constant separation factor $R_L$, which is given by the following equation :

$$R_L = \frac{1}{1 + b_{Co}} \qquad (3.2)$$

Value of $R_L$ indicates that the adsorption isotherm to be unfavorable if ($R_L$ > 1), Linear if ( $R_L$ = 1), favorable if (0 < $R_L$ < 1), or irreversible if ($R_L$ = 0) [120].

As shown from the previous figures, $R^2$ value using Langmuir adsorption isotherm equals 0.9705, while for Freundlich isotherm, $R^2$ is 0.9278. As well as, $R_L$ in Langmuir adsorption is 0.0731 that suggests that this adsorption is favorable according to Langmuir model. As a result of $R^2$ and $R_L$ values, we detect that the adsorption of Difenoconazole on Cellulose nanocrystalline

follows the Langmuir equation, and it represents chemical adsorption. These results are indicating into a strong evidence for the presence of real chemical bonds between difenoconazole and Cellulose nanocrystalline adsorbent.

The following table represents parameters of Freundlich and Langmuir isotherm adsorptions for Difenoconazole adsorption on Cellulose nanocrystalline.

**Table 3.7: Freundlich and Langmuir Isotherm Parameters for Difenoconazole removal by Cellulose Nanocrystalline Adsorbent.**

| Adsorption of Difenoconazole on Cellulose nanocrystalline | | | | | |
|---|---|---|---|---|---|
| Equilibrium Isotherm Models | | | | | |
| Langmuir Isotherm | | | Freundlich Isotherm | | |
| $Q_o$ (mg/g) | b (L/mg) | $R_L$ | $K_F$ (mg/g) | n (g/L) | 1/n (L/g) |
| 4.502 | 1.268 | 0.0731 | 9.867 | -2.679 | -0.373 |

### 3.4.1.2 Kinetics of Adsorption

In order to detect the adsorption mechanism, the experimental kinetic data for Difenoconazole adsorption on Cellulose nanocrystalline are fitted with intra-particle diffusion, pseudo-first-order and pseudo-second-order kinetic models

The kinetics parameters of adsorption and correlation coefficients have been calculated from the linear plots of equation (1.4) that represent plotting of $\log(q_e - q_t)$ versus time for pseudo-first-order-model, equation (1.5) that represents a graph of $(t/q_t)$ versus time for pseudo-second-order-model, and equation (1.6) by plotting $q_t$ versus $t^{0.5}$ for intra-particle-diffusion-kinetic-model, as appearing in (Figure 3.41–Figure 3.43).

### 3.4.1.2.1 Pseudo-First-Order-Kinetics

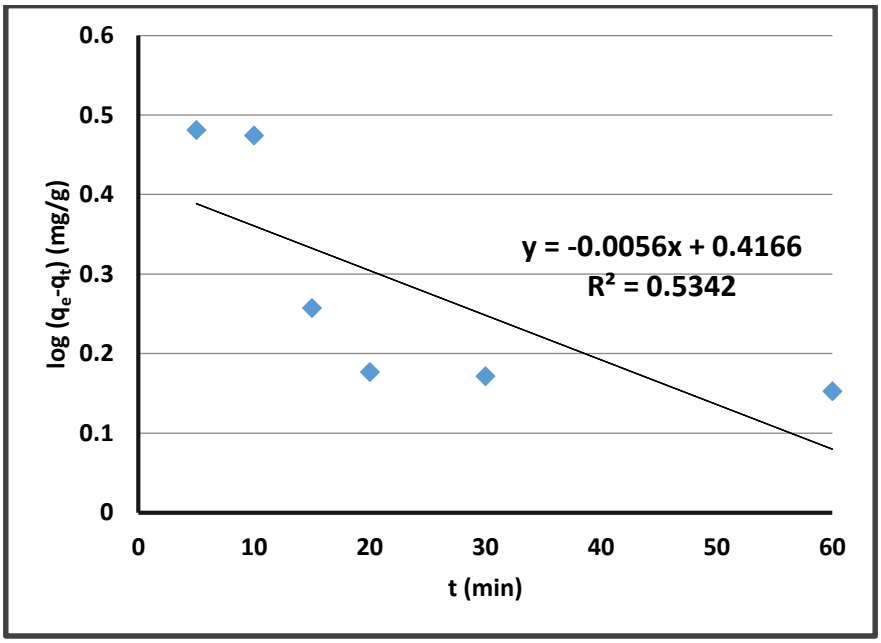


**Figure 3.41:** The plot of Pseudo-first-order-kinetic study for Difenoconazole removal by Cellulose Nanocrystalline, (nanopolymer dosage = 10 mg, initial concentration = 10 mg/L, reaction mixture volume = 10 mL, temperature = 20 °C, pH = 7).

### 3.4.1.2.2 Pseudo-Second-Order-Kinetics

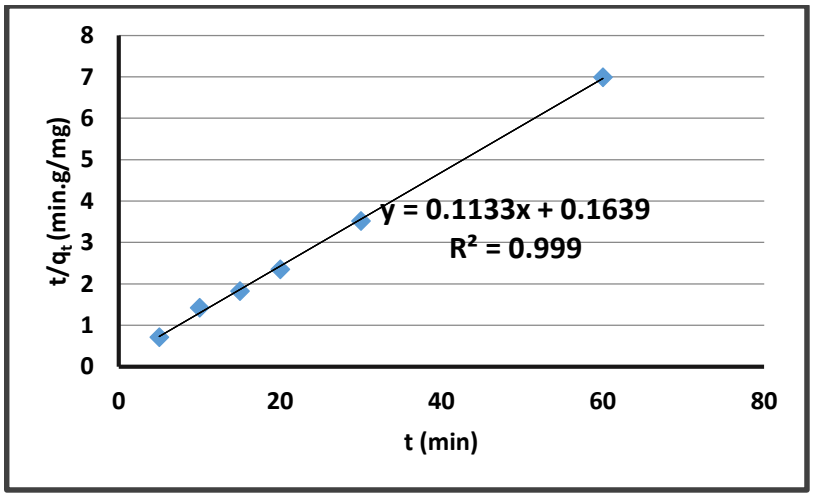


**Figure 3.42:** The plot of pseudo-second-order-kinetic study for Difenoconazole removal by Cellulose Nanocrystalline, (nanopolymer dosage = 10 mg, initial concentration = 10 mg/L, reaction mixture volume = 10 mL, temperature = 20 °C, pH = 7).

### 3.4.1.2.3 Intra-Particle-Diffusion-Kinetics

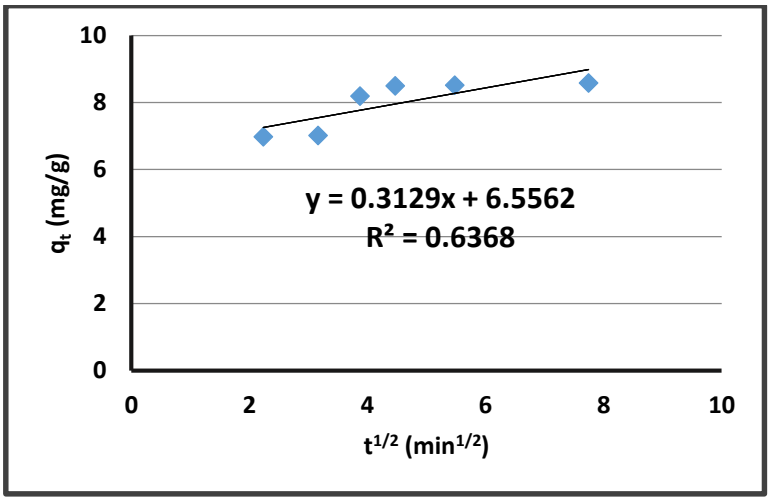


**Figure 3.43:** The plot of Intra-Particle-Diffusion-kinetic study for Difenoconazole removal by Cellulose Nanocrystalline, (nanopolymer dosage = 10 mg, initial concentration = 10 mg/L, reaction mixture volume = 10 mL, temperature = 20 °C, pH = 7).

By looking to the $R^2$ values using the studied kinetic models. The correlation coefficient for pseudo-second-order model was very close to one ($R^2$ = 0.999) comparing with pseudo-first-order ($R^2$ = 0.5342) and intra-particle diffusion ($R^2$ = 0.6368) models. As well as, the comparison between $q_e$ values that are calculated according to pseudo-first-order and pseudo-second-order adsorption kinetic models, value of $q_e$ via pseudo second-order kinetic model (that equals 8.826 mg/g) is very close to $q_e$ experimental (8.524 mg/g), in contrast of the calculated pseudo-first-order $q_e$ (2.609 mg/g) that is not close to the experimental one. These results showed that the adsorption of Difenoconazole on Cellulose nanocrystalline is fitted with pseudo-second-order adsorption kinetic mechanism.

The following table detects kinetic parameters of pseudo-first-order, pseudo-second-order and intra-particle diffusion models for Difenoconazole adsorption on Cellulose nanocrystalline.

**Table 3.8: The parameters for pseudo-first-order-kinetic, pseudo-second-order-kinetic and intra-particle-diffusion-kinetic models for Difenoconazole removal by Cellulose Nanocrystalline.**

| Adsorption of Difenoconazole on Cellulose nanocrystalline | | | | | | |
|---|---|---|---|---|---|---|
| Adsorption Kinetic Models | | | | | | |
| Pseudo First-Order Kinetics | | $q_{exp}$ (mg/g) | Pseudo Second-Order Kinetics | | Intra-Particle Diffusion Kinetics | |
| $q_e$ (mg/g) | $K_1$ ($mg.g^{-1}.min^{-1}$) | 8.524 | $q_e$ (mg/g) | $K_2$ ($g.mg^{-1}.min^{-1}$) | C (mg/g) | $K_p$ ($mg.g^{-1}.min^{-0.5}$) |
| 2.609 | 0.0128 | | 8.826 | 0.0783 | 6.5562 | 0.3129 |

### 3.4.1.3 Adsorption Thermodynamics

Depending on the thermodynamic relationship in Chapter one, equation (1.9), that represents the equation for Van't Hoff plot. The thermodynamic adsorption parameters including ($\Delta H$, $\Delta G$, $\Delta S$) for Difenoconazole adsorption on Cellulose nanocrystalline can be investigated from the slope which equals ($-\Delta H /R$) and y - intercept with a value of ($\Delta S/R$), for the graph ($\ln q_e/C_e$) versus ($1/T$) values, as appears in (Figure 3.44).

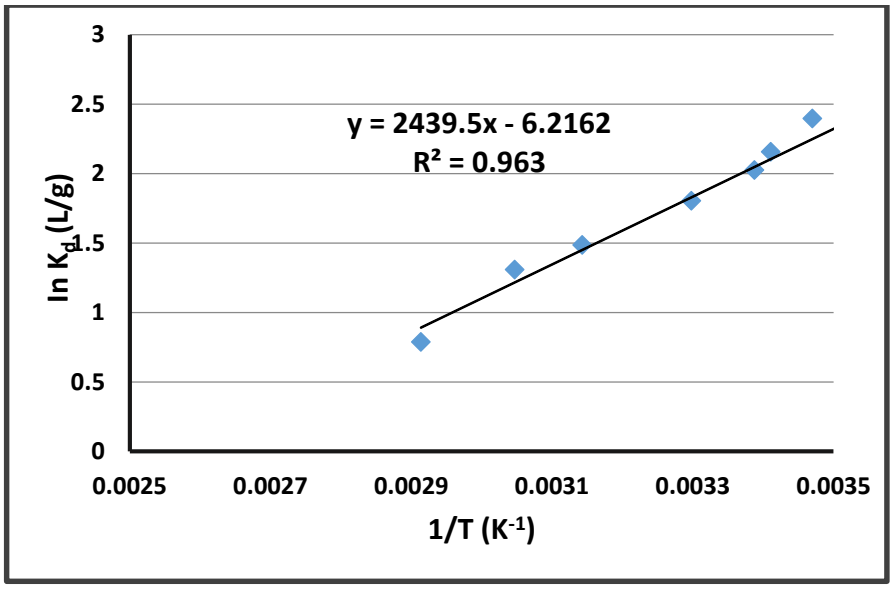


**Figure 3.44:** The plot of Van't Hoff Thermodynamic study for Difenoconazole removal by Cellulose Nanocrystalline, (initial concentration = 12 mg/L, pH = 7, adsorption time = 20 minute, nanopolymer dosage = 10 mg, reaction mixture volume= 10 mL).

The following table detects the adsorption thermodynamic parameters (ΔS, ΔG and ΔH) for Difenoconazole removal using Cellulose nanocrystalline.

**Table 3.9: The thermodynamic parameters for Difenoconazole removal by Cellulose Nanocrystalline.**

| Adsorption of Difenoconazole on Cellulose nanocrystalline | | |
|---|---|---|
| Adsorption Thermodynamics | | |
| ΔH (kJ) | Δ°G (kJ) | ΔS (J/K) |
| -20.282 | -5.132 | -51.681 |

The change in standard Gibbs free energy was calculated at the standard temperature (293.15 K), By looking to the (Δ°G = -5.132 kJ) value and change in enthalpy (ΔH = -20.282 kJ). This indicates that the adsorption process of Difenoconazole on Cellulose nanocrystalline is exothermic (ΔH < 0) and spontaneous (ΔG < 0).

The ΔS value for the adsorption process was negative indicating that the randomness at the solid/solution interface decreased during the adsorption

process. As well as negative change in Entropy value (-ΔS) indicated the presence of associative reaction mechanism in which absence of a significant change will occur in the internal structure of the cellulose nanocrystalline through the adsorption process.

### 3.4.2 Difenoconazole Adsorption by Cellulose functionalized with 2-furan carbonyl chloride

#### 3.4.2.1 Adsorption Isotherms

An investigation of the best isotherm for Difenoconazole adsorption on Cellulose Modified with 2-furan carbonyl chloride will be detected according to the plots for Freundlich and Langmuir isotherms. Adsorption isotherm parameters were calculated by plotting equation (1.1) that represents graph of $C_e/q_e$ on y-axis versus $C_e$ on x-axis for Langmuir adsorption isotherm, and equation (1.3) that represents $\log q_e$ on y-axis versus $\log C_e$ on x-axis for Freundlich adsorption isotherm as appearing in (Figure 3.45) and (Figure 3.46) respectively.

### 3.4.1.1.1 Langmuir Adsorption Isotherm

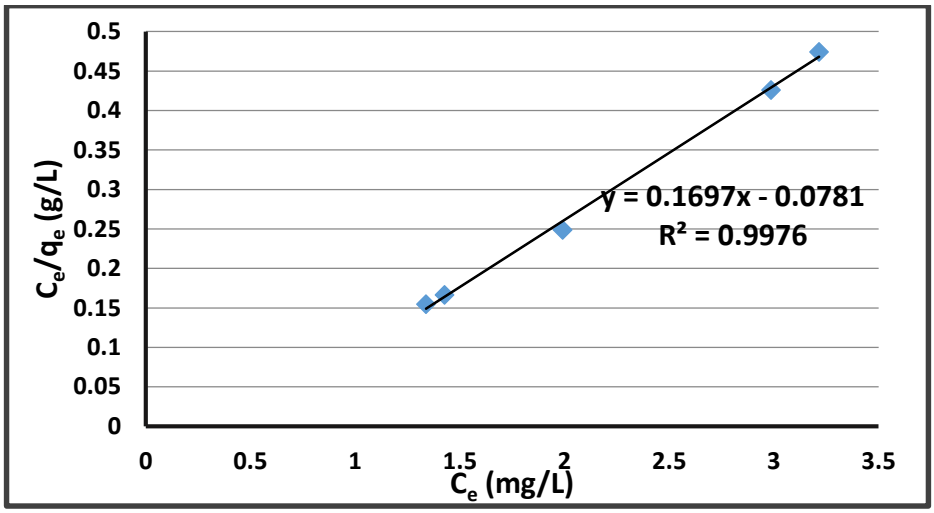


**Figure 3.45:** The plot of Langmuir Adsorption study for Difenoconazole removal by Cellulose functionalized with 2-furan carbonyl chloride, (pH = 8, temperature = 20 °C, adsorption time = 20 minute, nanopolymer dosage = 10 mg, reaction mixture volume= 10 mL).

### 3.4.2.1.2 Freundlich Adsorption Isotherm

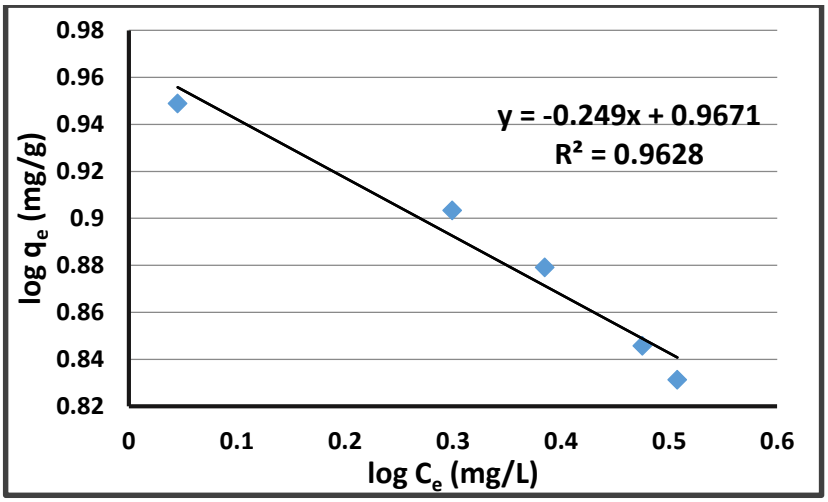


**Figure 3.46:** The plot of Freundlich Adsorption study for Difenoconazole removal by Cellulose functionalized with 2-furan carbonyl chloride, (pH = 7, temperature = 20 °C, adsorption time = 20 minute, nanopolymer dosage = 10 mg, reaction mixture volume = 10 mL).

As shown from the previous figures, $R^2$ value using Langmuir adsorption isotherm is 0.9976 (more close to 1 compared with $R^2$ for Freundlich model). As well as, $R_L$ in Langmuir adsorption is 0.0440 that suggests that this adsorption is favorable according to Langmuir model. As a result of $R^2$ and $R_L$ values, we detect that the adsorption of Difenoconazole on Cellulose Modified with 2-furan carbonyl chloride represents chemical adsorption and fitted with Langmuir equation. This is evidence on the presence of real chemical bonds between the Difenoconazole and the adsorbent Cellulose Modified with 2-furan carbonyl chloride.

The following table represents parameters of Freundlich and Langmuir isotherms for Difenoconazole removal on Cellulose Modified with 2-furan carbonyl chloride.

**Table 3.10: Freundlich and Langmuir Isotherm Parameters for Difenoconazole removal by Cellulose Functionalized with 2-furan carbonyl chloride.**

| Adsorption of Difenoconazole on Cellulose Modified with 2-furan carbonyl chloride | | | | | |
|---|---|---|---|---|---|
| Equilibrium Isotherm Models | | | | | |
| Langmuir Isotherm | | | Freundlich Isotherm | | |
| $Q_o$ (mg/g) | b (L/mg) | $R_L$ | $K_F$ (mg/g) | n (g/L) | 1/n (L/g) |
| 5.893 | 2.173 | 0.0440 | 9.270 | -4.016 | -0.249 |

### 3.4.2.2 Kinetics of Adsorption

In order to detect the adsorption mechanism, the experimental kinetic data for Difenoconazole adsorption on Cellulose Modified with 2-furan carbonyl chloride are fitted with intra-particle-diffusion-kinetic, pseudo-first-order-

kinetic and pseudo-second-order-kinetic models. The kinetics parameters of adsorption and correlation coefficients have been calculated from the linear plots of equation (1.4) that represent plotting of $\log(q_e - q_t)$ versus time for pseudo-first-order model, equation (1.5) that represents a graph of $(t/q_t)$ versus time for pseudo-second-order model, and equation (1.6) by plotting $q_t$ versus $t^{0.5}$ for intra-particle diffusion kinetic model, as appearing in (Figure 3.47–Figure 3.49).

### 3.4.2.2.1 Pseudo-First-Order-Kinetics

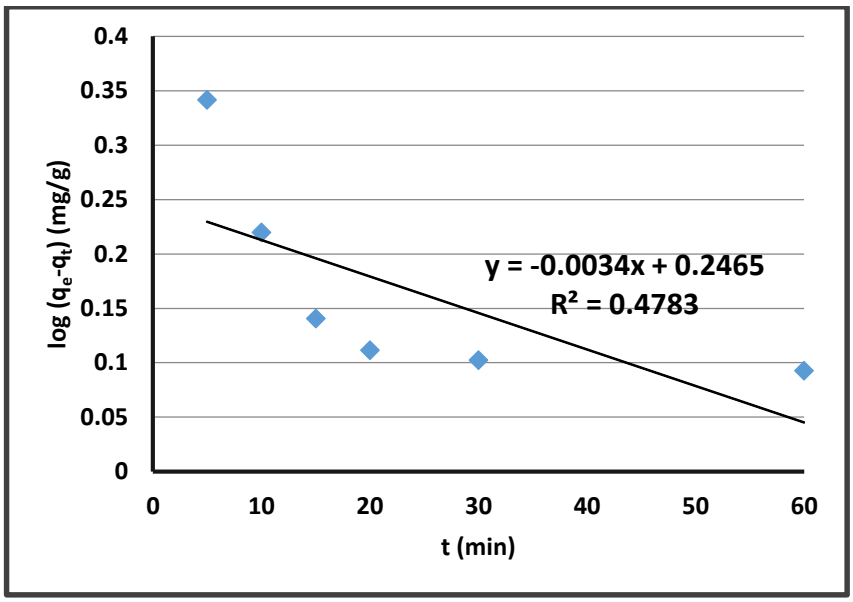


**Figure 3.47:** The plot of pseudo-first-order-kinetic study for Difenoconazole removal by Cellulose functionalized with 2-furan carbonyl chloride, (nanopolymer dosage = 10 mg, initial concentration = 10 mg/L, reaction mixture volume = 10 mL, temperature = 20 °C, pH = 7).

### 3.4.2.2.2 Pseudo-Second-Order-Kinetics

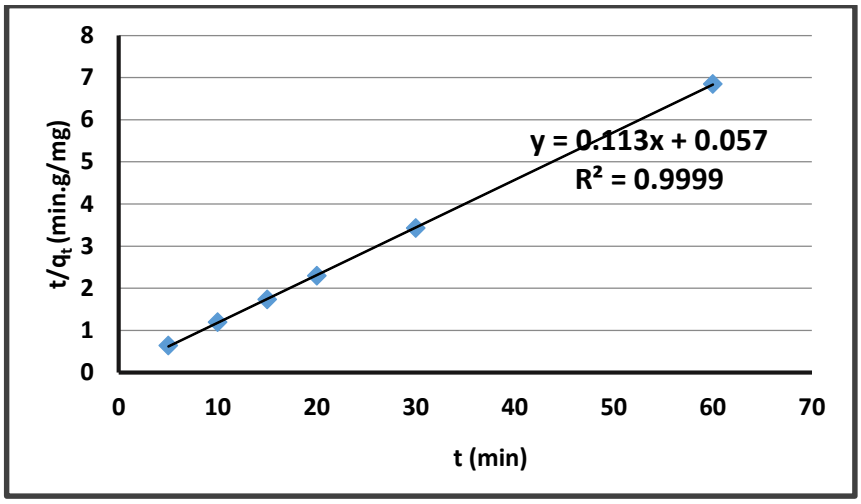


**Figure 3.48:** The plot of pseudo-second-order-kinetic study for Difenoconazole removal by Cellulose functionalized with 2-furan carbonyl chloride, (nanopolymer dosage = 10 mg, initial concentration = 10 mg/L, reaction mixture volume = 10 mL, temperature = 20 °C, pH = 7).

### 3.4.2.2.3 Intra-Particle-Diffusion-Kinetics

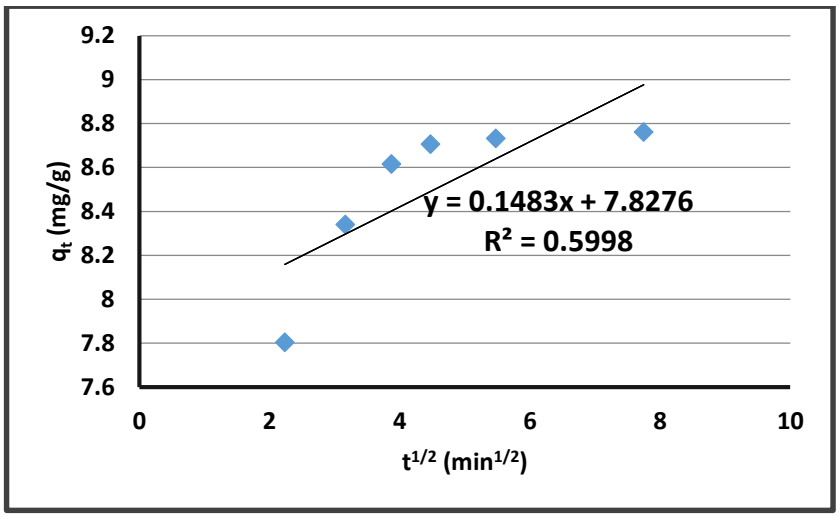


**Figure 3.49:** The plot of Intra-Particle-Diffusion-kinetic study for Difenoconazole removal by Cellulose functionalized with 2-furan carbonyl chloride, (nanopolymer dosage = 10 mg, initial concentration = 10 mg/L, reaction mixture volume = 10 mL, temperature = 20 °C, pH = 7).

Depending on the observed correlation coefficient ($R^2$) values in each studied kinetic model. As well as, the comparison between $q_e$ values that are detected according to pseudo-first-order and pseudo-second-order kinetic adsorptions, value of $q_e$ via pseudo-second-order kinetic adsorption model (that equals 8.849 mg/g) is very close to $q_e$ experimental (8.773 mg/g) in contrast of the calculated pseudo-first-order $q_e$ (1.764 mg/g) that is not close to the experimental one. These results showed that Difenoconazole removal on Cellulose Modified with 2-furan carbonyl chloride is fitted with the mechanism of pseudo-second-order kinetics.

The following table detects the kinetic parameters of pseudo-first-order-kinetic, pseudo-second-order-kinetic and intra-particle-diffusion models for Difenoconazole adsorption on Cellulose Modified with 2-furan carbonyl chloride.

**Table 3.11: The parameters for pseudo-first-order-kinetic, pseudo-second-order-kinetic and intra-particle-diffusion-kinetic models for Difenoconazole removal by Cellulose Functionalized with 2-furan carbonyl chloride.**

| Adsorption of Difenoconazole on Cellulose Modified with 2-furan carbonyl chloride | | | | | | |
|---|---|---|---|---|---|---|
| Adsorption Kinetic Models | | | | | | |
| Pseudo First-Order Kinetics | | $q_{exp}$ (mg/g) | Pseudo Second-Order Kinetics | | Intra-Particle Diffusion Kinetics | |
| $q_e$ (mg/g) | $K_1$ ($mg.g^{-1}.min^{-1}$) | 8.773 | $q_e$ (mg/g) | $K_2$ ($g.mg^{-1}.min^{-1}$) | C (mg/g) | $K_p$ ($mg.g^{-1}.min^{-0.5}$) |
| 1.764 | $7.83*10^{-3}$ | | 8.849 | 0.224 | 7.8276 | 0.1483 |

### 3.4.2.3 Adsorption Thermodynamics

According to the thermodynamic relationship in chapter one, equation (1.9); that represents Van't Hoff plot. The thermodynamic adsorption parameters for Difenoconazole adsorption by Cellulose functionalized with 2-furan carbonyl chloride can be investigated from the slope (-ΔH /R) and y-intercept (ΔS/R) for plotting ($\ln q_e/C_e$) versus (1/T) values, as appears in (Figure 3.50).

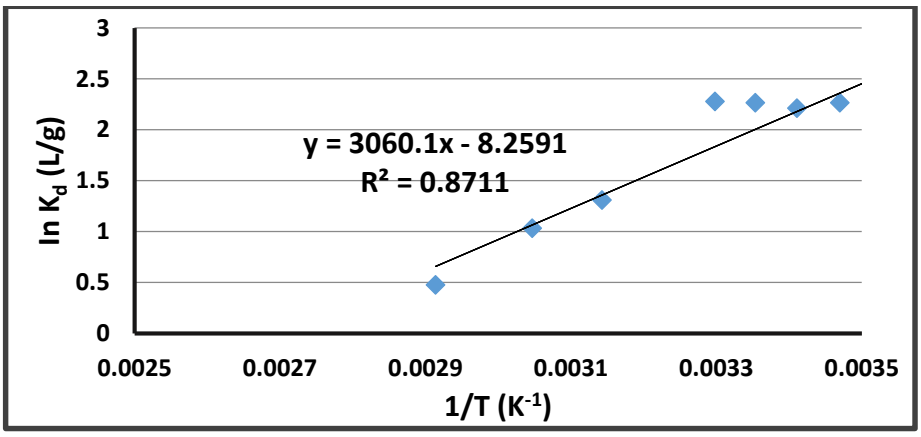


**Figure 3.50:** The plot of Van't Hoff Thermodynamic study for Difenoconazole removal by Cellulose functionalized with 2-furan carbonyl chloride, (initial concentration = 10 mg/L, pH = 8, adsorption time = 20 minute, nanopolymer dosage = 10 mg, reaction mixture volume = 10 mL).

The following table detects the adsorption thermodynamic parameters (ΔS, ΔG and ΔH) for Difenoconazole removal using Cellulose functionalized with 2-furan carbonyl chloride.

**Table 3.12: The thermodynamic parameters for Difenoconazole removal by Cellulose Functionalized with 2-furan carbonyl chloride.**

| Adsorption of Difenoconazole on Cellulose Modified with 2-furan carbonyl chloride | | |
|---|---|---|
| Adsorption Thermodynamics | | |
| ΔH (kJ) | Δ°G (kJ) | ΔS (J/K) |
| -25.442 | -5.322 | -68.667 |

The change in standard Gibbs free energy was calculated at the standard temperature (293.15 K), According to (Δ°G = -5.312 kJ) and (ΔH = -25.442 kJ) values. This indicates that the adsorption process of Difenoconazole on Cellulose Modified with Furan-2-carbonyl chloride is exothermic (ΔH < 0) and spontaneous (ΔG < 0). Negative change in Entropy indicates a presence of an associative mechanism in which absence of a significant change will occur in the internal structure of the Cellulose functionalized with 2-furan carbonyl chloride during the adsorption process.

### 3.4.3 Difenoconazole Adsorption by Cellulose functionalized with 2,6-pyridine dicarbonyl dichloride

#### 3.4.3.1 Adsorption Isotherms

An investigation of the best isotherm for Difenoconazole adsorption on Cellulose functionalized with 2,6-pyridine dicarbonyl dichloride will be determined according to the graphs for Freundlich and Langmuir isotherms. Adsorption isotherm parameters were calculated by plotting equation (1.1) that represents graph of $C_e/q_e$ versus $C_e$ for Langmuir adsorption isotherm, and equation (1.3) that represents $\log q_e$ versus $\log C_e$ for Freundlich adsorption isotherm, as appears in (Figure 3.51) and (Figure 3.52) respectively.

### 3.4.3.1.1 Langmuir Adsorption Isotherm

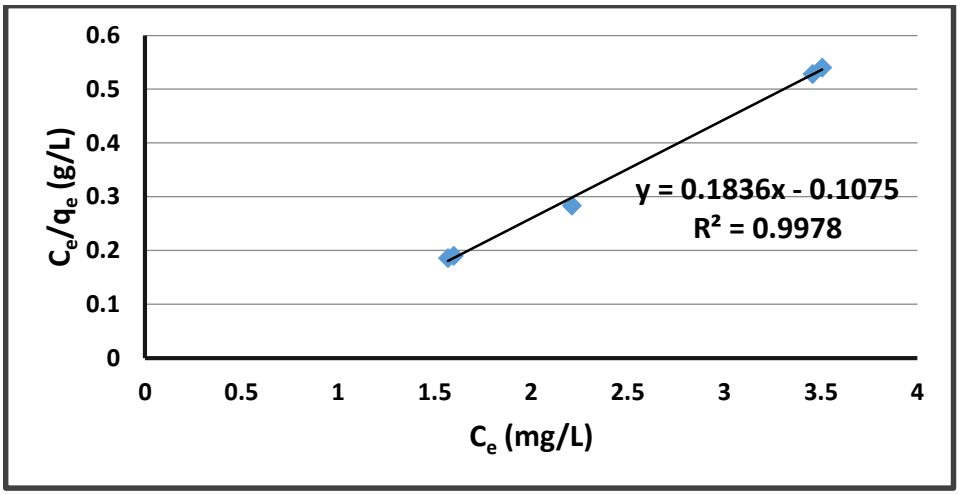


**Figure 3.51:** The plot of Langmuir Adsorption study for Difenoconazole removal by Cellulose functionalized with 2,6-pyridine dicarbonyl dichloride, (pH = 6, temperature = 20 °C, adsorption time = 60 minute, nanopolymer dosage = 10 mg, reaction mixture volume = 10 mL).

### 3.4.3.1.2 Freundlich Adsorption Isotherm

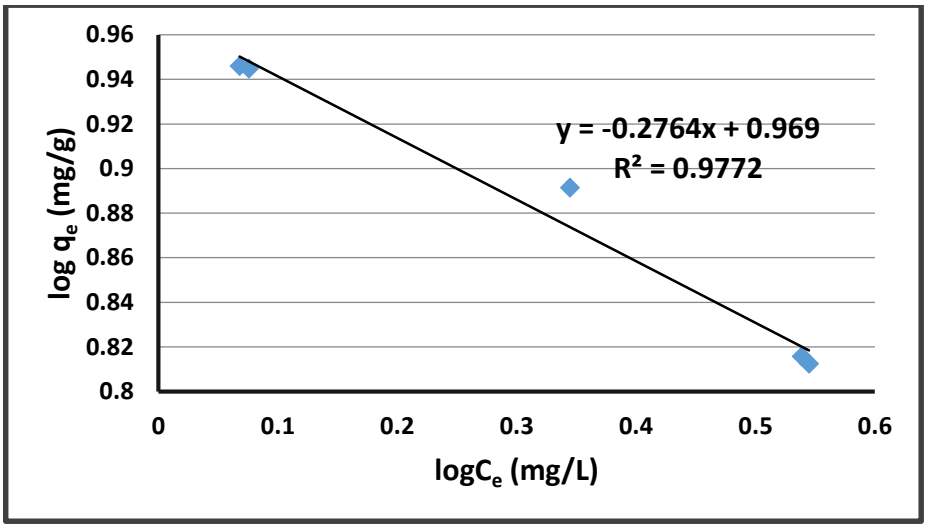


**Figure 3.52:** The plot of Freundlich Adsorption study for Difenoconazole removal by Cellulose functionalized with 2,6-pyridine dicarbonyl dichloride, (pH = 6, temperature = 20 °C, adsorption time = 60 minute, nanopolymer dosage = 10 mg, reaction mixture volume = 10 mL).

As shown from the previous figures, $R^2$ value using Langmuir adsorption isotherm is approximately 1. In addition, $R_L$ in Langmuir adsorption is 0.0553 which suggests that this adsorption is favorable according to Langmuir model. According to the detected $R^2$ and $R_L$ values, we conclude that the adsorption of Difenoconazole on Cellulose functionalized with 2,6-pyridine dicarbonyl dichloride is chemical adsorption and follows Langmuir equation. This is a strong evidence on the presence of real chemical bonds between the Difenoconazole pesticides and Cellulose Modified with 2,6-pyridine dicarbonyl dichloride.

The following table represents parameters of Freundlich and Langmuir isotherm adsorptions for Difenoconazole adsorption on Cellulose functionalized with 2,6-pyridine dicarbonyl dichloride.

**Table 3.13: Freundlich and Langmuir isotherm Parameters for Difenoconazole removal by Cellulose Functionalized with 2,6-pyridine dicarbonyl dichloride.**

| Adsorption of Difenoconazole on Cellulose Modified with 2,6-pyridine dicarbonyl dichloride | | | | | |
|---|---|---|---|---|---|
| Equilibrium Isotherm Models | | | | | |
| Langmuir Isotherm | | | Freundlich Isotherm | | |
| $Q_o$ (mg/g) | b (L/mg) | $R_L$ | $K_F$ (mg/g) | n (g/L) | 1/n (L/g) |
| 5.447 | 1.708 | 0.0553 | 9.311 | -3.618 | -0.276 |

### 3.4.3.2 Kinetics of Adsorption

In order to determine each adsorption mechanism, the experimental kinetic data for Difenoconazole adsorption on Cellulose functionalized with 2,6-pyridine dicarbonyl dichloride are fitted with intra-particle diffusion,

pseudo-first-order and pseudo-second-order kinetic models. The kinetics parameters of adsorption and correlation coefficients have been calculated from the linear plots of equation (1.4) that represent plotting of $\log(q_e - q_t)$ versus t for pseudo-first-order-model, equation (1.5) that represents a graph of $(t/q_t)$ versus t for pseudo-second-order-model, and equation (1.6) by plotting $q_t$ versus $t^{0.5}$ for intra-particle-diffusion-kinetic model, as appearing in (Figure 3.53–Figure 3.55).

### 3.4.3.2.1 Pseudo-First-Order-Kinetics

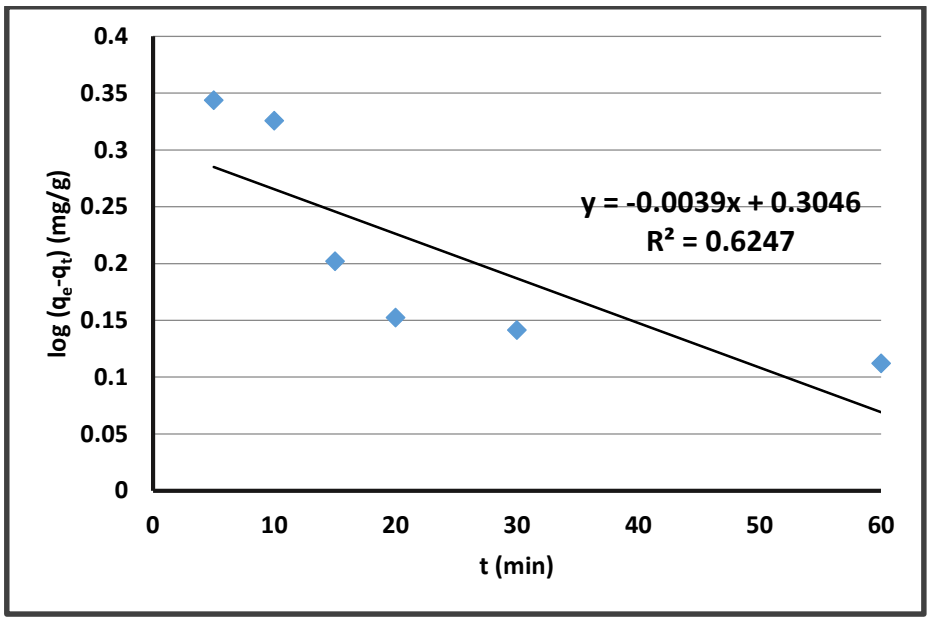


**Figure 3.53:** The plot of pseudo-first-order-kinetic study for Difenoconazole removal by Cellulose functionalized with 2,6-pyridine dicarbonyl dichloride, (nanopolymer dosage = 10 mg, initial concentration = 10 mg/L, reaction mixture volume = 10 mL, temperature = 20 °C, pH = 7).

### 3.4.3.2.2 Pseudo-Second-Order-Kinetics

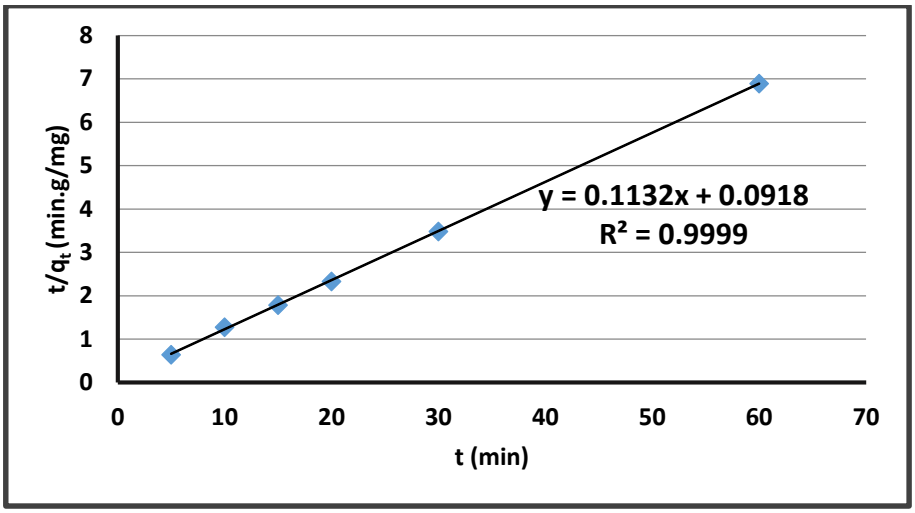


**Figure 3.54:** The plot of pseudo-second-order-kinetic study for Difenoconazole removal by Cellulose functionalized with 2,6-pyridine dicarbonyl dichloride, (nanopolymer dosage = 10 mg, initial concentration = 10 mg/L, reaction mixture volume = 10 mL, temperature = 20 °C, pH = 7).

### 3.4.3.2.3 Intra-Particle-Diffusion-Kinetics

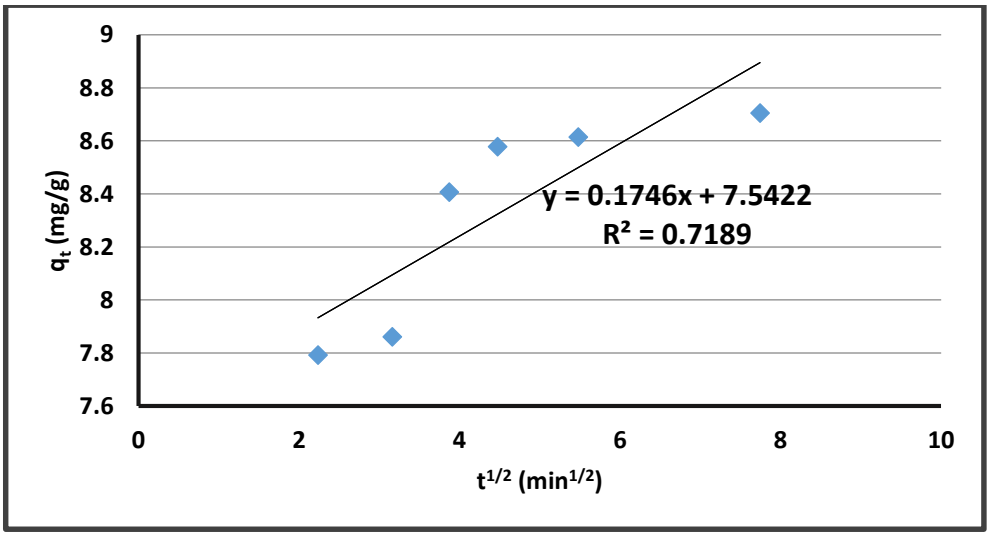


**Figure 3.55:** The plot of Intra-Particle-Diffusion-kinetic study for Difenoconazole removal by Cellulose functionalized with 2,6-pyridine dicarbonyl dichloride, (nanopolymer dosage = 10 mg, initial concentration = 10 mg/L, reaction mixture volume = 10 mL, temperature = 20 °C, pH = 7).

By looking to the $R^2$ values using the studied kinetic models. As well as, comparison between the values of $q_e$ that are calculated according to pseudo-first-order-kinetic and pseudo-second-order-kinetic models, value of $q_e$ via pseudo-second-order adsorption model (that equals 8.834 mg/g) is very close to $q_e$ experimental (8.745 mg/g) in contrast of the calculated pseudo-first-order $q_e$ (2.016 mg/g) that is not close to the experimental one. These results showed the adsorption of Difenoconazole on Cellulose functionalized with 2,6-pyridine dicarbonyl dichloride fitted with pseudo-second-order adsorption kinetics in which the value of $R^2$ for this kinetic model is 0.9999.

The following table investigates kinetic parameters of pseudo-first-order-kinetic, pseudo-second-order-kinetic and intra-particle-diffusion-models for Difenoconazole adsorption by Cellulose functionalized with 2,6-pyridine dicarbonyl dichloride.

**Table 3.14: The parameters for pseudo-first-order-kinetic, pseudo-second-order-kinetic and intra-particle-diffusion-kinetic models for Difenoconazole removal by Cellulose Functionalized with 2,6-pyridine dicarbonyl dichloride.**

| Adsorption of Difenoconazole on Cellulose Modified with 2,6-pyridine dicarbonyl dichloride | | | | | | |
|---|---|---|---|---|---|---|
| Adsorption Kinetic Models | | | | | | |
| Pseudo First-Order Kinetics | | $q_{exp}$ (mg/g) | Pseudo Second-Order Kinetics | | Intra-Particle Diffusion Kinetics | |
| $q_e$ (mg/g) | $K_1$ ($mg.g^{-1}.min^{-1}$) | 8.745 | $q_e$ (mg/g) | $K_2$ ($g.mg^{-1}.min^{-1}$) | C (mg/g) | $K_p$ ($mg.g^{-1}.min^{-0.5}$) |
| 2.016 | $8.982 * 10^{-3}$ | | 8.834 | 0.1396 | 7.5422 | 0.1746 |

### 3.4.3.3 Adsorption Thermodynamics

Depending on thermodynamic relationship in chapter one, equation (1.9), that represents Van't Hoff plot. The thermodynamic adsorption parameters including (ΔH, ΔG, ΔS) for Difenoconazole adsorption by Cellulose functionalized with 2,6-pyridine dicarbonyl dichloride can be investigated from the slope (-ΔH /R) and y-intercept (ΔS/R) for plotting (In $q_e/C_e$) versus (1/T) values, as appears in (Figure 3.56).

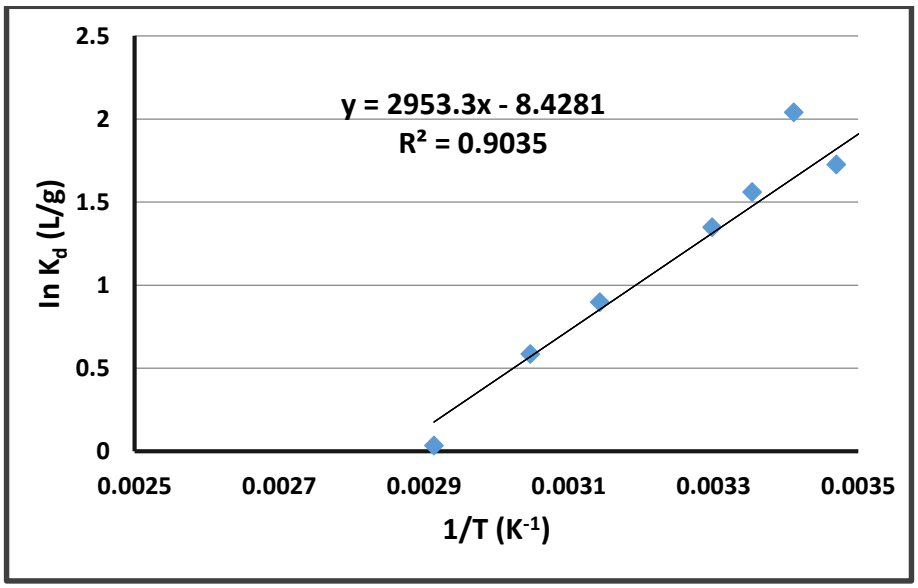


**Figure 3.56:** The plot of Van't Hoff Thermodynamic study for Difenoconazole removal by Cellulose functionalized with 2,6-pyridine dicarbonyl dichloride, (initial concentration = 8 mg/L, pH = 6, adsorption time = 60 minute, nanopolymer dosage = 10 mg, reaction mixture volume = 10 mL).

The following table represents the adsorption thermodynamic parameters (ΔS, ΔG and ΔH) for Difenoconazole removal using Cellulose functionalized with 2,6-pyridine dicarbonyl dichloride.

**Table 3.15: The thermodynamic parameters for Difenoconazole removal by Cellulose Functionalized with 2,6-pyridine dicarbonyl dichloride.**

| **Adsorption of Difenoconazole on Cellulose Modified with 2,6-pyridine dicarbonyl dichloride** | | |
|---|---|---|
| Adsorption Thermodynamics | | |
| ΔH (kJ) | Δ°G (kJ) | ΔS (J/K) |
| -24.554 | -4.013 | -70.071 |

The change in standard Gibbs free energy was calculated at the standard temperature (293.15 K), By considering the value of (Δ°G = -4.013 kJ) and value of change in enthalpy (ΔH = -24.554 kJ). This indicates that the adsorption process of Difenoconazole on Cellulose functionalized with 2,6-pyridine dicarbonyl dichloride is exothermic (ΔH < 0) and spontaneous (ΔG < 0).

The ΔS for the adsorption process was negative indicating that the randomness at the solid/solution interface decreased during the adsorption process. In addition, negative change in the Entropy (-ΔS) detects the existence of an associative reaction mechanism between the adsorbate and the nanopolymer, in which no significant change will appear in the internal structure for the Cellulose modified with 2,6-pyridine dicarbonyl dichloride during the adsorption process.

### 3.4.4 Tetraconazole Adsorption by Cellulose nanocrystalline

#### 3.4.4.1 Adsorption Isotherms

An investigation of the best isotherm for Tetraconazole adsorption on Cellulose nanocrystalline will be determined according to the graphs for

Freundlich and Langmuir isotherms. Adsorption isotherm parameters were calculated by plotting equation (1.1) that represents graph of $C_e/q_e$ versus $C_e$ for Langmuir adsorption isotherm, and equation (1.3) that represents $\log q_e$ versus $\log C_e$ for Freundlich adsorption isotherm, as appears in (Figure 3.57) and (Figure 3.58) respectively.

### 3.4.4.1.1 Langmuir Adsorption Isotherm

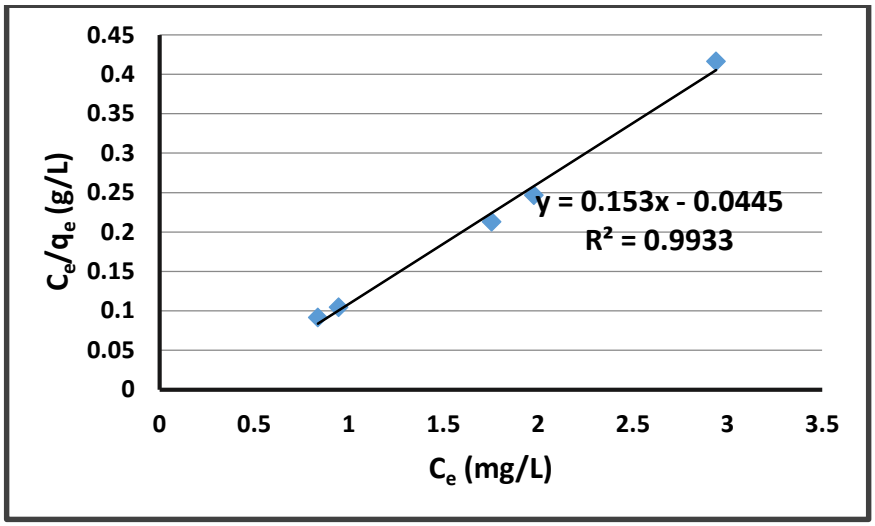


**Figure 3.57:** The plot of Langmuir Adsorption study for Tetraconazole removal by Cellulose Nanocrystalline, (pH = 4, temperature = 20 °C, adsorption time = 30 minute, nanopolymer dosage = 10 mg, reaction mixture volume = 10 mL).

### 3.4.4.1.2 Freundlich Adsorption Isotherm

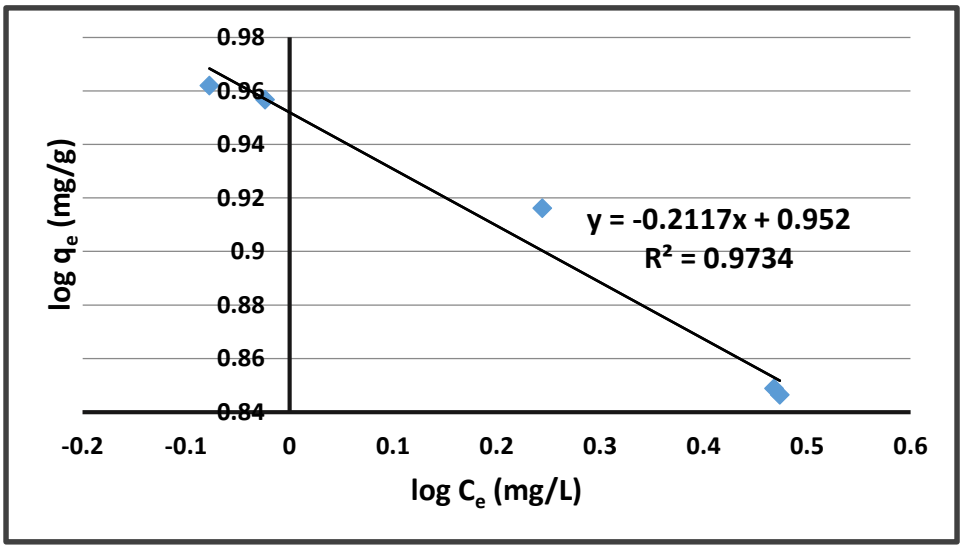


**Figure 3.58:** The plot of Freundlich Adsorption study for Tetraconazole removal by Cellulose Nanocrystalline, (pH = 4, temperature = 20 °C, adsorption time = 30 minute, nanopolymer dosage = 10 mg, reaction mixture volume = 10 mL).

As appearing in the previous figures, $R^2$ using Langmuir adsorption isotherm is 0.9933. In addition, $R_L$ in Langmuir adsorption is 0.0283 that suggests that this adsorption is favorable according to this adsorption model. As a result of $R^2$ and $R_L$ values, we investigate that the removal of Tetraconazole on Cellulose nanocrystalline represent a chemical adsorption and fitted with Langmuir equation which is an evidence for a presence of real chemical bonds between Tetraconazole and Cellulose nanocrystalline.

The following table represents parameters of Freundlich and Langmuir isotherm adsorptions for the adsorption of Tetraconazole by Cellulose nanocrystalline.

**Table 3.16: Freundlich and Langmuir isotherm Parameters for Tetraconazole removal by Cellulose Nanocrystalline Adsorbent.**

| Adsorption of Tetraconazole on Cellulose nanocrystalline | | | | | |
|---|---|---|---|---|---|
| Equilibrium Isotherm Models | | | | | |
| Langmuir Isotherm | | | Freundlich Isotherm | | |
| $Q_o$ (mg/g) | b (L/mg) | $R_L$ | $K_F$ (mg/g) | n (g/L) | 1/n (L/g) |
| 6.536 | 3.438 | 0.0283 | 8.954 | -4.724 | -0.212 |

### 3.4.4.2 Kinetics of Adsorption

In order to detect the adsorption mechanism, the experimental kinetic data for Tetraconazole adsorption on Cellulose nanocrystalline are fitted with intra-particle diffusion, pseudo-first-order and pseudo-second-order kinetic models

The kinetics parameters of adsorption and correlation coefficients have been calculated from the linear plots of equation (1.4) that represent plotting of $\log(q_e - q_t)$ versus time for pseudo-first-order-model, equation (1.5) that represents a graph of $(t/q_t)$ versus time for pseudo-second-order-model, and equation (1.6) by plotting $q_t$ versus $t^{0.5}$ for intra-particle-diffusion-kinetic model, as appearing in (Figure 3.59–Figure 3.61).

### 3.4.4.2.1 Pseudo-First-Order-Kinetics

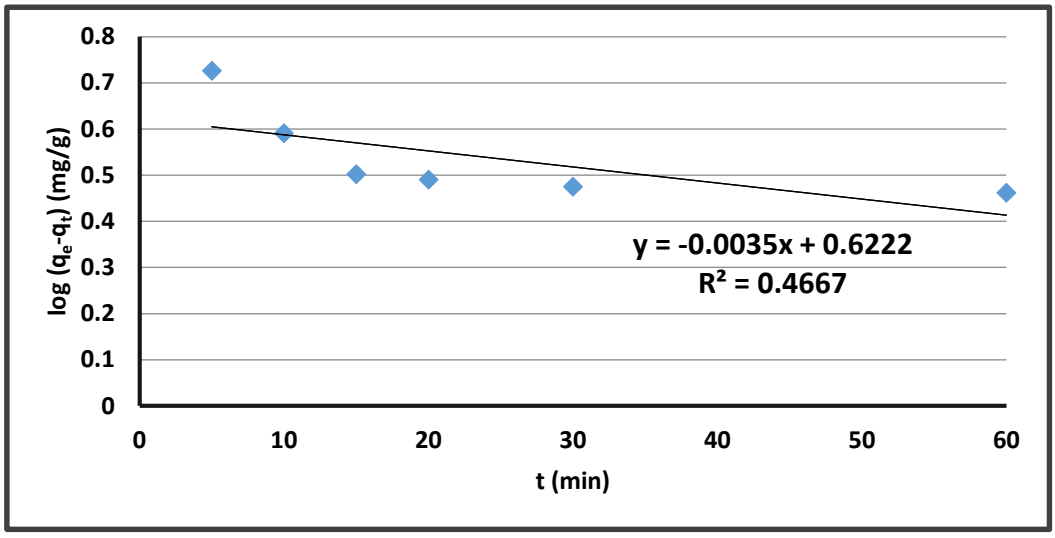


**Figure 3.59:** The plot of pseudo-first-order-kinetic study for Tetraconazole removal by Cellulose Nanocrystalline, (nanopolymer dosage = 10 mg, initial concentration = 10 mg/L, reaction mixture volume = 10 mL, temperature = 20 °C, pH = 7).

### 3.4.4.2.2 Pseudo-Second-Order-Kinetics

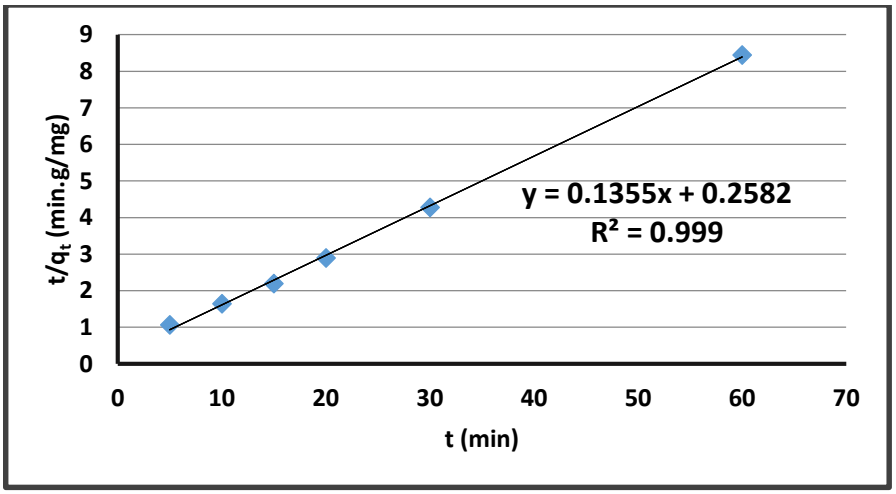


**Figure 3.60:** The plot of pseudo-second-order-kinetic study for Tetraconazole removal by Cellulose Nanocrystalline, (nanopolymer dosage = 10 mg, initial concentration = 10 mg/L, reaction mixture volume = 10 mL, temperature = 20 °C, pH = 7).

### 3.4.4.2.3 Intra-Particle-Diffusion Kinetics

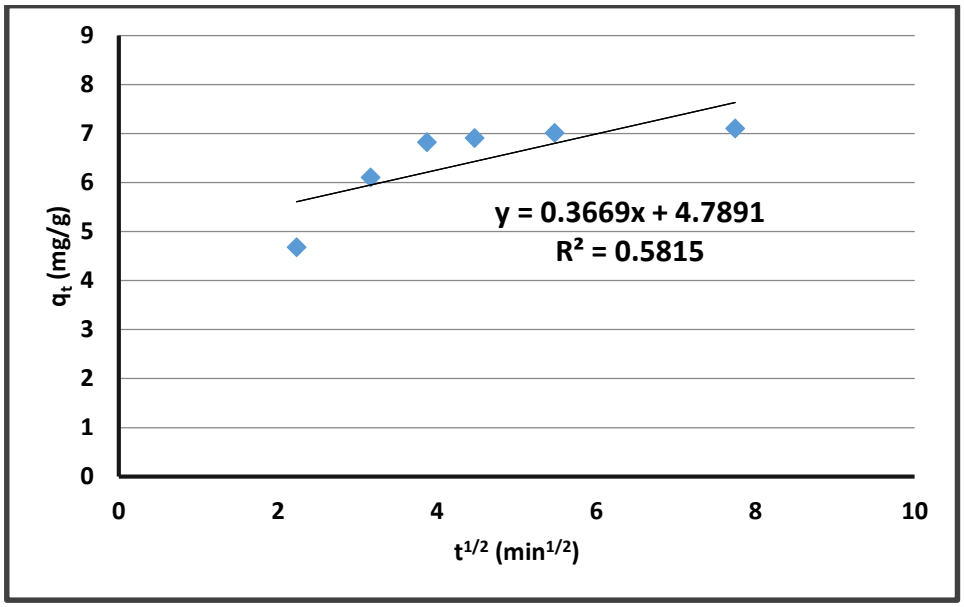


**Figure 3.61:** The plot of Intra-Particle-Diffusion-kinetic study for Tetraconazole removal by Cellulose Nanocrystalline, (nanopolymer dosage = 10 mg, initial concentration = 10 mg/L, reaction mixture volume = 10 mL, temperature = 20 °C, pH = 7).

By looking to the $R^2$ values using the studied kinetic models. The correlation coefficient for pseudo-second-order model was very close to one ($R^2$ = 0.999). As well as, the comparison between $q_e$ values that are calculated according to pseudo-first-order and pseudo-second-order adsorption kinetic models, value of $q_e$ via pseudo second-order kinetic model (that equals 7.380 mg/g) is very close to $q_e$ experimental (7.112 mg/g), in contrast to the calculated pseudo-first-order-model $q_e$ (4.189 mg/g) that is not close to the experimental value of $q_e$. These results showed that the adsorption of Tetraconazole on Cellulose nanocrystalline is fitted with pseudo-second-order adsorption kinetic mechanism

The following table detects the kinetic parameters of pseudo-first-order, pseudo-second-order and intra-particle diffusion models for Tetraconazole adsorption on Cellulose nanocrystalline.

**Table 3.17: The parameters for pseudo-first-order-kinetic, pseudo-second-order-kinetic and intra-particle-diffusion-kinetic models for Tetraconazole removal by Cellulose Nanocrystalline.**

| Adsorption Tetraconazole on Cellulose nanocrystalline | | | | | | |
|---|---|---|---|---|---|---|
| Adsorption Kinetic Models | | | | | | |
| Pseudo First-Order Kinetics | | $q_{exp}$ (mg/g) | Pseudo Second-Order Kinetics | | Intra-Particle Diffusion Kinetics | |
| $q_e$ (mg/g) | $K_1$ ($mg.g^{-1}.min^{-1}$) | 7.112 | $q_e$ (mg/g) | $K_2$ ($g.mg^{-1}.min^{-1}$) | C (mg/g) | $K_p$ ($mg.g^{-1}.min^{-0.5}$) |
| 4.189 | $8.06*10^{-3}$ | | 7.380 | 0.0711 | 4.7891 | 0.3669 |

### 3.4.4.3 Adsorption Thermodynamics

Depending on the thermodynamic relationship in chapter one, equation (1.9), that represents Van't Hoff plot. The thermodynamic adsorption parameters including (ΔH, ΔG, ΔS) for Tetraconazole adsorption on Cellulose nanocrystalline can be investigated from the slope ($-\Delta H/R$) and y-intercept ($\Delta S/R$) for the graph ($\ln q_e/C_e$) versus ($1/T$) values, as appears in (Figure 3.62).

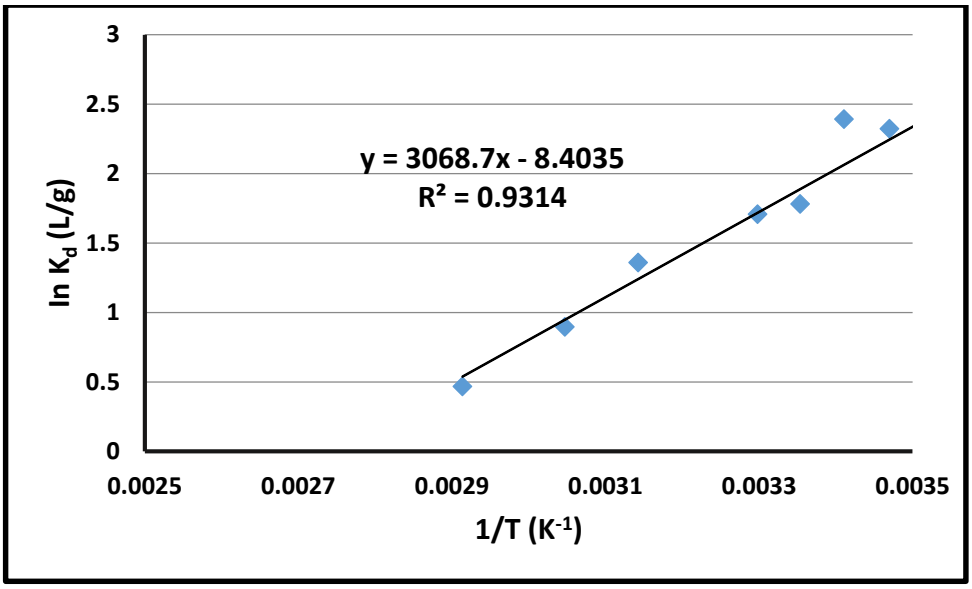


**Figure 3.62:** The plot of Van't Hoff Thermodynamic study for Tetraconazole removal by Cellulose Nanocrystalline, (initial concentration = 4 mg/L, pH = 4, adsorption time = 30 minute, nanopolymer dosage = 10 mg, reaction mixture volume = 10 mL).

The following table detects the adsorption thermodynamic parameters (ΔS, ΔG and ΔH) for Tetraconazole removal using Cellulose nanocrystalline.

**Table 3.18: The thermodynamic parameters for Tetraconazole removal by Cellulose Nanocrystalline.**

| Adsorption of Tetraconazole on Cellulose nanocrystalline | | |
|---|---|---|
| Adsorption Thermodynamics | | |
| ΔH (kJ) | Δ°G (kJ) | ΔS (J/K) |
| -25.513 | -5.031 | -69.867 |

The change in standard Gibbs free energy was calculated at the standard temperature (293.15 K), By looking to the (Δ°G = -5.031 kJ) value and change in enthalpy (ΔH = -25.513 kJ). This indicates that the adsorption process of Tetraconazole on Cellulose nanocrystalline is exothermic (ΔH < 0) and spontaneous (ΔG < 0).

The ΔS value for the adsorption process was negative indicating that the randomness at the solid/solution interface decreased during the adsorption

process. As well as, negative change in the Entropy (-ΔS) approved the existence of an associative reaction mechanism between the tetraconazole pesticide and the nanopolymer, in which no significant change will appear in the internal structure of Cellulose nanocrystalline during the adsorption process.

### 3.4.5 Tetraconazole Adsorption by Cellulose functionalized with 2-Furan carbonyl chloride

#### 3.4.5.1 Adsorption Isotherms

A detection of the best isotherm for Tetraconazole adsorption on Cellulose functionalized with 2-furan carbonyl chloride will be determined according to the graphs for Freundlich and Langmuir isotherms. Adsorption isotherm parameters were calculated by plotting equation (1.1) that represents a graph of $C_e/q_e$ on y-axis versus $C_e$ on x-axis for Langmuir adsorption isotherm, and equation (1.3) that represents $\log q_e$ on y-axis versus $\log C_e$ on x-axis for Freundlich adsorption isotherm, as appears in (Figure 3.63) and (Figure 3.64) respectively.

### 3.4.5.1.1 Langmuir Adsorption Isotherm

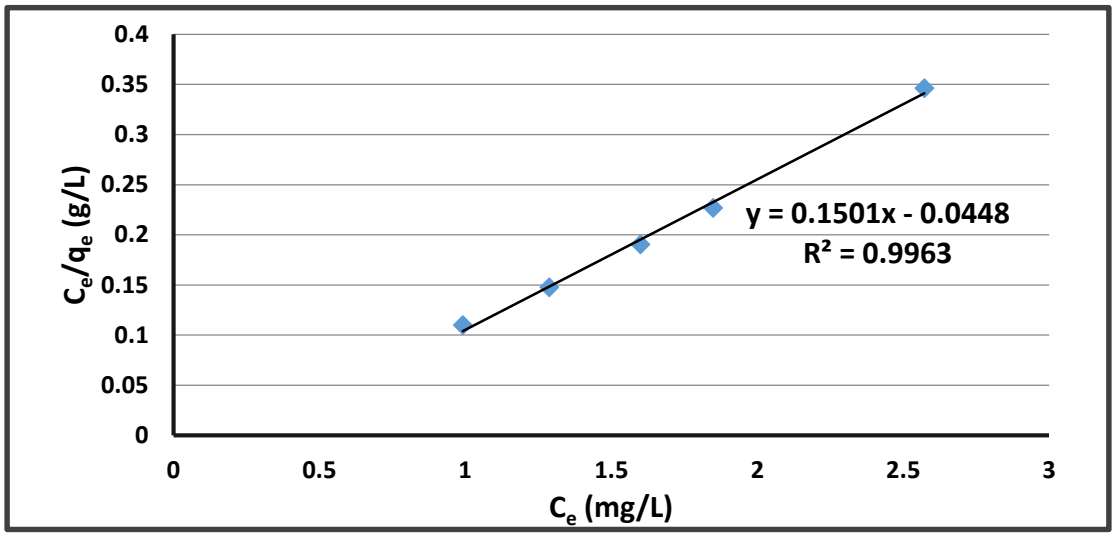


**Figure 3.63:** The plot of Langmuir Adsorption study for Tetraconazole removal by Cellulose functionalized with 2-furan carbonyl chloride, (pH = 4, temperature = 20 °C, adsorption time = 15 minute, nanopolymer dosage = 10 mg, reaction mixture volume = 10 mL).

### 3.4.5.1.2 Freundlich Adsorption Isotherm

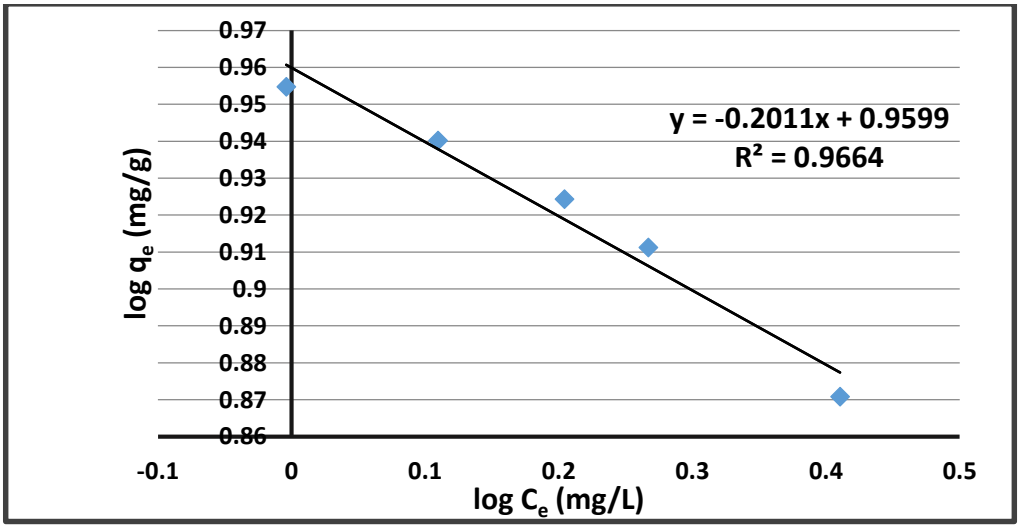


**Figure 3.64:** The plot of Freundlich study for Tetraconazole removal by Cellulose functionalized with 2-furan carbonyl chloride, (pH = 4, temperature = 20 °C, adsorption time = 15 minute, nanopolymer dosage = 10 mg, reaction mixture volume = 10 mL).

As shown from the previous figures, $R^2$ values using Langmuir adsorption isotherm is 0.9963 while for Freundlich isotherm, $R^2$ is 0.9664. As well as, $R_L$ in Langmuir adsorption is 0.0289 that suggests that this adsorption is favorable according to Langmuir model. As a result of $R^2$ and $R_L$ values, we detect that the adsorption of Tetraconazole on Cellulose functionalized with 2-furan carbonyl chloride follows the Langmuir equation and it represents chemical adsorption. These results are indicating a strong evidence for the presence of real chemical bonds between Tetraconazole and Cellulose Modified with 2-furan carbonyl chloride adsorbent.

The following table represents the parameters of Freundlich and Langmuir isotherm adsorptions for Tetraconazole on Cellulose functionalized with 2-furan carbonyl chloride.

**Table 3.19: Freundlich and Langmuir isotherm Parameters for Tetraconazole removal by Cellulose Functionalized with 2-furan carbonyl chloride.**

| Adsorption of Tetraconazole on Cellulose Modified with 2-furan carbonyl chloride | | | | | |
|---|---|---|---|---|---|
| Equilibrium Isotherm Models | | | | | |
| Langmuir Isotherm | | | Freundlich Isotherm | | |
| $Q_o$ (mg/g) | b (L/mg) | $R_L$ | $K_F$ (mg/g) | n (g/L) | 1/n (L/g) |
| 6.662 | 3.350 | 0.0289 | 9.118 | -4.973 | -0.201 |

### 3.4.5.2 Kinetics of Adsorption

In order to detect the adsorption mechanism, the experimental kinetic data for Tetraconazole adsorption by Cellulose functionalized with 2-furan carbonyl chloride are fitted with intra-particle diffusion, pseudo-first-order and pseudo-second-order kinetic models

The kinetics parameters of adsorption and correlation coefficients have been calculated from the linear plots of equation (1.4) that represent plotting of $\log(q_e - q_t)$ versus time for pseudo-first-order-model, equation (1.5) that represents a graph of $(t/q_t)$ versus time for pseudo-second-order-model, and equation (1.6) by plotting $q_t$ versus $t^{0.5}$ for intra-particle-diffusion-kinetic model, as appearing in (Figure 3.65–Figure 3.67).

### 3.4.5.2.1 Pseudo-First-Order-Kinetics

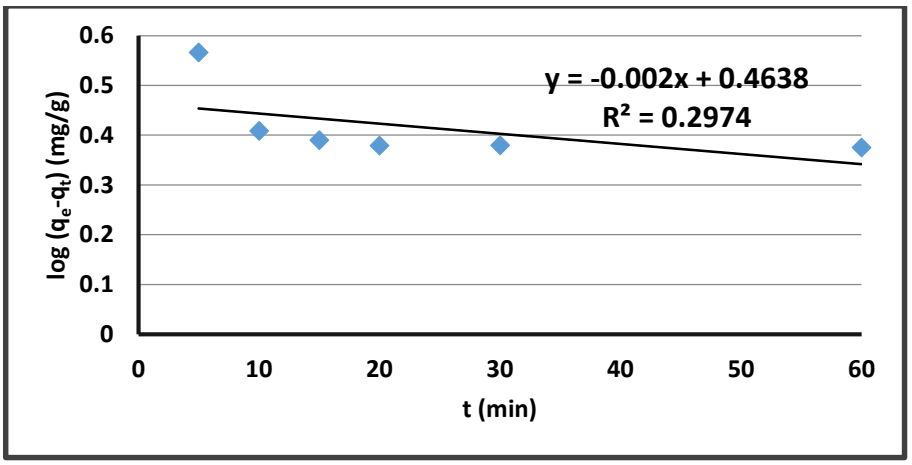


**Figure 3.65:** The plot of pseudo-first-order-kinetic study for Tetraconazole removal by Cellulose functionalized with 2-furan carbonyl chloride, (nanopolymer dosage = 10 mg, initial concentration = 10 mg/L, reaction mixture volume = 10 mL, temperature = 20 °C, pH = 7).

### 3.4.5.2.2 Pseudo-Second-Order-Kinetics

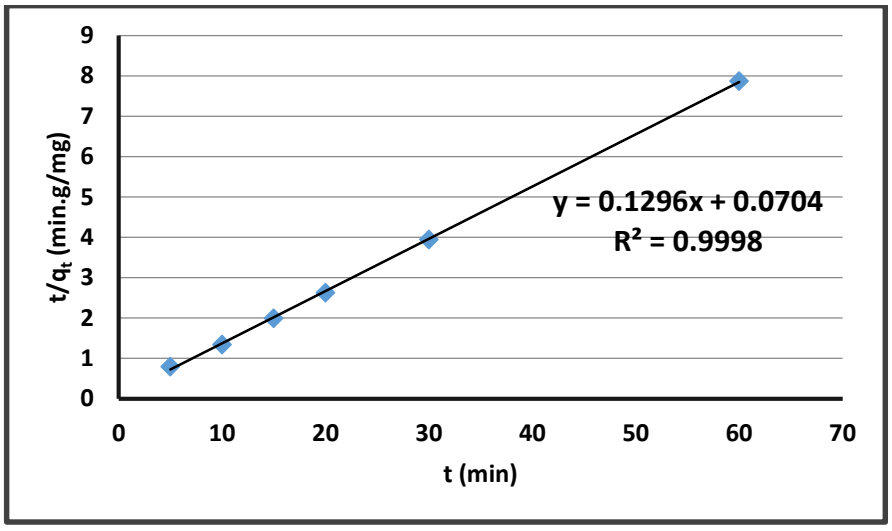


**Figure 3.66:** The plot of pseudo-second-order-kinetic study for Tetraconazole removal by Cellulose functionalized with 2-furan carbonyl chloride, (nanopolymer dosage = 10 mg, initial concentration = 10 mg/L, reaction mixture volume = 10 mL, temperature = 20 °C, pH = 7).

### 3.4.5.2.3 Intra-Particle-Diffusion-Kinetics

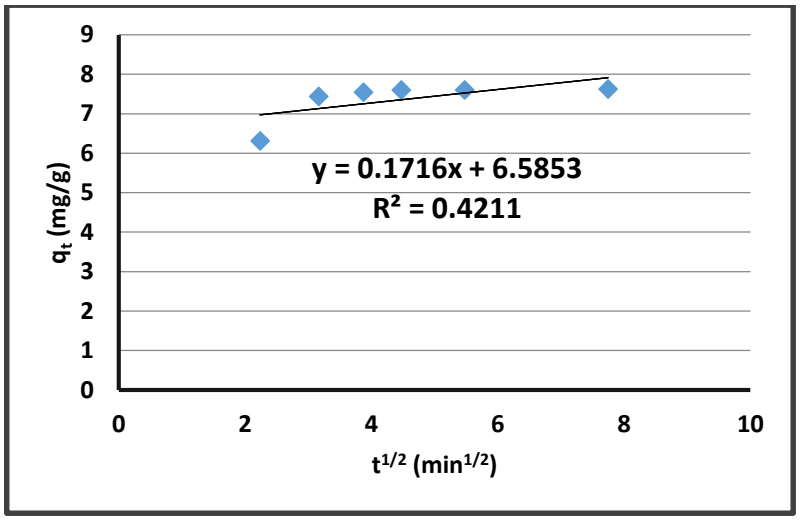


**Figure 3.67:** The plot of Intra-Particle-Diffusion-kinetic study for Tetraconazole removal by Cellulose functionalized with 2-furan carbonyl chloride, (nanopolymer dosage = 10 mg, initial concentration = 10 mg/L, reaction mixture volume = 10 mL, temperature = 20 °C, pH = 7).

By looking to the $R^2$ values using the studied kinetic models. The correlation coefficient for pseudo-second-order model was very close to one ($R^2$ = 0.9998) comparing with pseudo-first-order ($R^2$ = 0.2974) and intra-particle diffusion ($R^2$ = 0.4211) models. As well as, the comparison between $q_e$ values that are calculated according to pseudo-first-order and pseudo-second-order adsorption kinetic models, value of $q_e$ via pseudo second-order kinetic model (that equals 7.716 mg/g) is very close to $q_e$ experimental (7.619 mg/g), in contrast of the calculated pseudo-first-order $q_e$ (17.95 mg/g) that is not close to the experimental value of $q_e$. These results showed that the adsorption of Tetraconazole on Cellulose functionalized with 2-furan carbonyl chloride is fitted with pseudo-second-order adsorption kinetic mechanism.

The following table detects the kinetic parameters of pseudo-first-order, pseudo-second-order and intra-particle diffusion models for Tetraconazole on Cellulose functionalized with 2-furan carbonyl chloride.

**Table 3.20: The parameters for pseudo-first-order-kinetic, pseudo-second-order-kinetic and intra-particle-diffusion-kinetic models for Tetraconazole Adsorption by Cellulose Functionalized with 2-furan carbonyl chloride.**

| Adsorption of Tetraconazole on Cellulose Modified with 2-furan carbonyl chloride | | | | | | |
|---|---|---|---|---|---|---|
| Adsorption Kinetic Models | | | | | | |
| Pseudo First-Order Kinetics | | $q_{exp}$ (mg/g) | Pseudo Second-Order Kinetics | | Intra-Particle Diffusion Kinetics | |
| $q_e$ (mg/g) | $K_1$ ($mg.g^{-1}.min^{-1}$) | 7.619 | $q_e$ (mg/g) | $K_2$ ($g.mg^{-1}.min^{-1}$) | C (mg/g) | $K_p$ ($mg.g^{-1}.min^{-0.5}$) |
| 2.909 | $4.61 * 10^{-3}$ | | 7.716 | 0.238 | 6.5853 | 0.1716 |

### 3.4.5.3 Adsorption Thermodynamics

Depending on the thermodynamic relationship in chapter one, equation (1.9), that represents Van't Hoff plot. The thermodynamic adsorption parameters including (ΔH, ΔG, ΔS) for Tetraconazole adsorption on Cellulose Modified with 2-furan carbonyl chloride can be investigated from the slope (-ΔH /R) and y-intercept (ΔS/R) for plotting (In $q_e/C_e$) versus (1/T) values, as appears in (Figure 3.68).

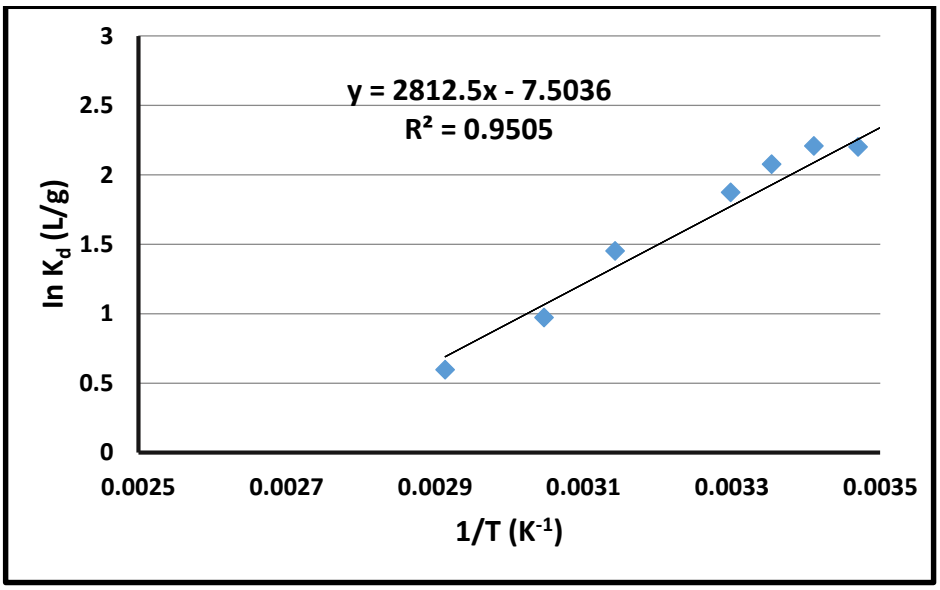


**Figure 3.68:** The plot of Van't Hoff Thermodynamic study for Tetraconazole removal by Cellulose functionalized with 2-furan carbonyl chloride, (initial concentration = 8 mg/L, pH = 4, adsorption time = 15 minute, nanopolymer dosage = 10 mg, reaction mixture volume = 10 mL).

The following table detects the adsorption thermodynamic parameters (ΔS, ΔG and ΔH) for Tetraconazole removal on Cellulose functionalized with 2-furan carbonyl chloride.

**Table 3.21: The thermodynamic parameters for Tetraconazole removal by Cellulose Functionalized with 2-furan carbonyl chloride.**

| Adsorption of Tetraconazole on Cellulose Modified with 2-furan carbonyl chloride | | |
|---|---|---|
| Adsorption Thermodynamics | | |
| ΔH (kJ) | Δ°G (kJ) | ΔS (J/K) |
| -23.383 | -5.095 | -62.385 |

The change in standard Gibbs free energy was calculated at the standard temperature (293.15 K), By looking to the (Δ°G = -5.095 kJ) value and change in enthalpy (ΔH = -23.383 kJ). This indicates that the adsorption process of Tetraconazole on Cellulose functionalized with 2-furan carbonyl chloride is exothermic (ΔH < 0) and spontaneous (ΔG < 0).

The ΔS for the adsorption process was negative detecting that the randomness at the solid/solution interface decreased during the adsorption process. As well as, negative change in Entropy detects the existence of an associative reaction mechanism between the pesticide and the nanopolymer, in which no significant change will appear in the internal structure of the adsorbent during the adsorption process.

### 3.4.6 Tetraconazole Adsorption by Cellulose functionalized with 2,6-pyridine dicarbonyl dichloride

#### 3.4.6.1 Adsorption Isotherms

An investigation of the best isotherm for Tetraconazole on Cellulose functionalized with 2,6-pyridine dicarbonyl dichloride will be determined according to the graphs for Freundlich and Langmuir isotherms. Adsorption isotherm parameters were calculated by plotting equation (1.1)

that represents graph of $C_e/q_e$ on y-axis versus $C_e$ on x-axis for Langmuir adsorption isotherm, and equation (1.3) that represents $\log q_e$ on y-axis versus $\log C_e$ on x-axis for Freundlich adsorption isotherm, as appears in (Figure 3.69) and (Figure 3.70) respectively.

### 3.4.6.1.1 Langmuir Adsorption Isotherm

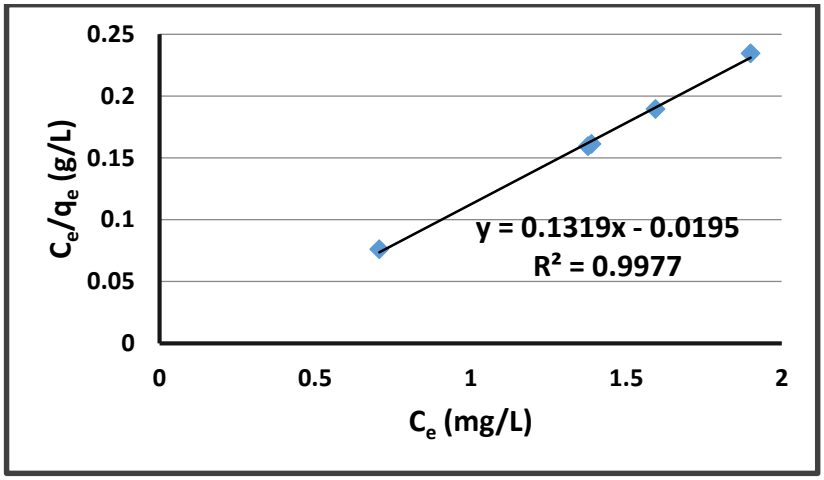


**Figure 3.69:** The plot of Langmuir Adsorption study for Tetraconazole removal by Cellulose functionalized with 2,6-pyridine dicarbonyl dichloride, (pH = 6, temperature = 20 °C, adsorption time = 20 minute, nanopolymer dosage = 10 mg, reaction mixture volume = 10 mL).

### 3.4.6.1.2 Freundlich Adsorption Isotherm

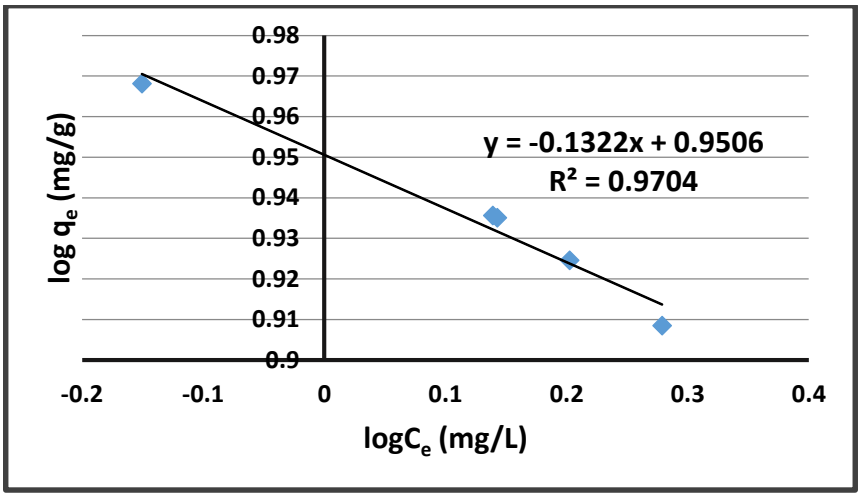


**Figure 3.70:** The plot of Freundlich Adsorption study for Tetraconazole removal by Cellulose functionalized with 2,6-pyridine dicarbonyl dichloride, (pH = 6, temperature = 20 °C, adsorption time = 20 minute, nanopolymer dosage = 10 mg, reaction mixture volume = 10 mL).

As shown from the previous figures, $R^2$ values using Langmuir adsorption isotherm is 0.9977 while for Freundlich isotherm, $R^2$ is 0.9704. As well as, $R_L$ in Langmuir adsorption is 0.0145 that suggests that this adsorption is favorable according to Langmuir model. As a result of $R^2$ and $R_L$ values, we conclude that the adsorption of Tetraconazole on Cellulose functionalized with 2,6-pyridine dicarbonyl dichloride follows the Langmuir equation and it represents chemical adsorption. These results are indicating a strong evidence for the presence of real chemical bonds between Tetraconazole and Cellulose functionalized with 2,6-pyridine dicarbonyl dichloride adsorbent.

The following table represents parameters of Freundlich and Langmuir isotherm adsorptions for Tetraconazole adsorption on Cellulose functionalized with 2,6-pyridine dicarbonyl dichloride.

**Table 3.22: Freundlich and Langmuir Isotherm Parameters for Tetraconazole removal by Cellulose Functionalized with 2,6-pyridine dicarbonyl dichloride.**

| Adsorption of Tetraconazole on Cellulose Modified with 2,6-pyridine dicarbonyl dichloride | | | | | |
|---|---|---|---|---|---|
| Equilibrium Isotherm Models | | | | | |
| Langmuir Isotherm | | | Freundlich Isotherm | | |
| $Q_o$ (mg/g) | b (L/mg) | $R_L$ | $K_F$ (mg/g) | n (g/L) | 1/n (L/g) |
| 7.582 | 6.764 | 0.0145 | 8.925 | -7.564 | -0.132 |

### 3.4.6.2 Kinetics of Adsorption

In order to detect the adsorption mechanism, the experimental kinetic data for Tetraconazole on Cellulose functionalized with 2,6-pyridine dicarbonyl dichloride are fitted with intra-particle diffusion, pseudo-first-order and pseudo-second-order kinetic models

The kinetics parameters of adsorption and correlation coefficients have been calculated from the linear plots of equation (1.4) that represent plotting of $\log(q_e - q_t)$ versus time for pseudo-first-order-model, equation (1.5) that represents a graph of $(t/q_t)$ versus time for pseudo-second-order-model, and equation (1.6) by plotting $q_t$ versus $t^{0.5}$ for intra-particle-diffusion-kinetic model, as appearing in (Figure 3.71–Figure 3.73).

### 3.4.6.2.1 Pseudo-First-Order-Kinetics

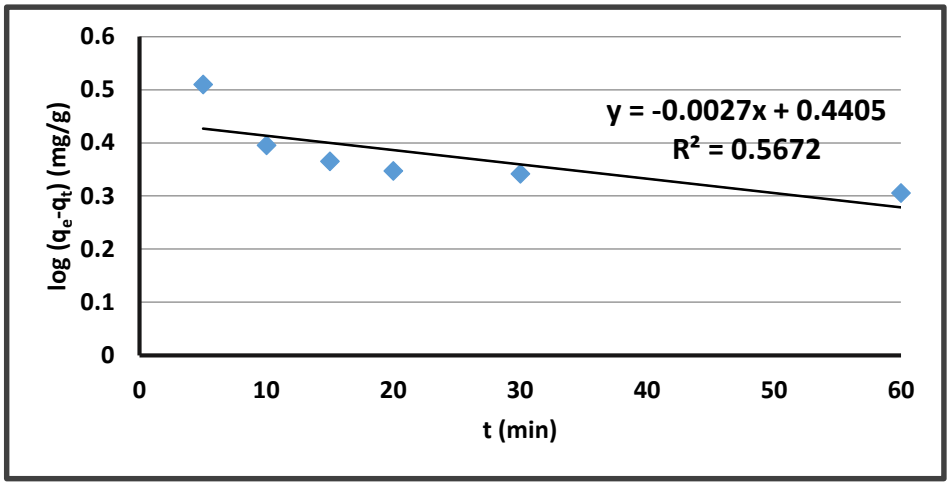


**Figure 3.71:** The plot of pseudo-first-order-kinetic study for Tetraconazole removal by Cellulose functionalized with 2,6-pyridine dicarbonyl dichloride, (pH = 7, nanopolymer dosage = 10 mg, reaction mixture volume = 10 mL, initial concentration = 10 mg/L, temperature = 20 °C).

### 3.4.6.2.2 Pseudo-Second-Order-Kinetics

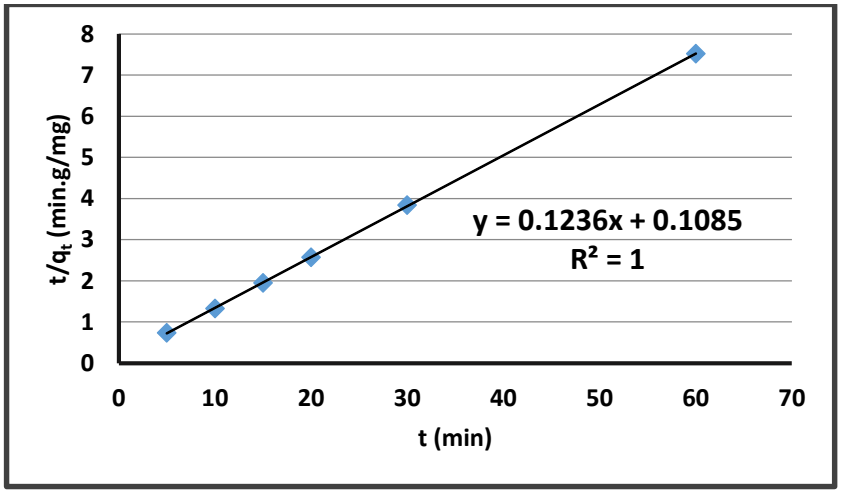


**Figure 3.72:** The plot of pseudo-second-order-kinetic study for Tetraconazole removal by Cellulose functionalized with 2,6-pyridine dicarbonyl dichloride, (pH = 7, nanopolymer dosage = 10 mg, reaction mixture volume = 10 mL, initial concentration = 10 mg/L, temperature = 20 °C).

### 3.4.6.2.3 Intra-Particle-Diffusion-Kinetics

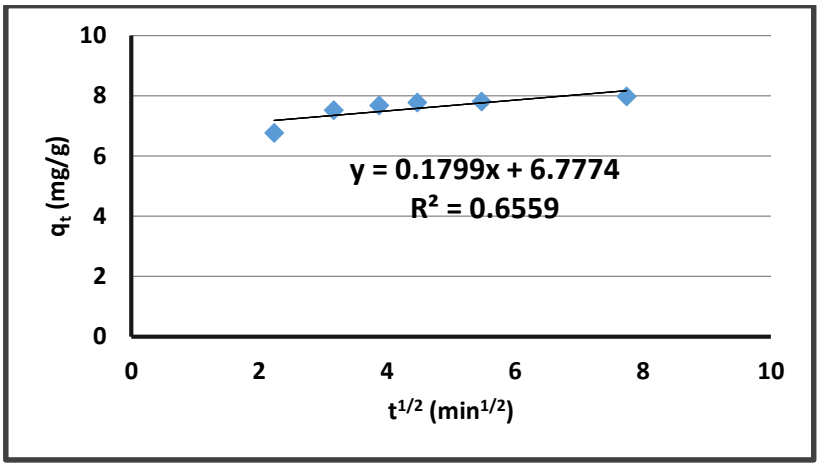


**Figure 3.73:** The plot of Intra-Particle-Diffusion-Kinetics study for Tetraconazole removal by Cellulose functionalized with 2,6-pyridine dicarbonyl dichloride, (pH = 7, nanopolymer dosage = 10 mg, reaction mixture volume = 10 mL, initial concentration = 10 mg/L, temperature = 20 °C).

By looking to the $R^2$ values using the studied kinetic models. The correlation coefficient for pseudo-second-order model was one comparing with pseudo-first-order ($R^2$ = 0.5672) and intra-particle diffusion ($R^2$ = 0.6559) models. As well as, the comparison between $q_e$ values that are calculated according to pseudo-first-order and pseudo-second-order adsorption kinetic models, value of $q_e$ via pseudo second-order kinetic model (that equals 8.091 mg/g) is very close to $q_e$ experimental (7.992 mg/g), in contrast to the calculated pseudo- first-order $q_e$ (2.757 mg/g) that is not close to the experimental one. These results showed that the adsorption of Tetraconazole on Cellulose functionalized with 2,6-pyridine dicarbonyl dichloride is fitted with pseudo-second-order adsorption kinetic mechanism

The following table detects the kinetic parameters of pseudo-first-order-kinetic, pseudo-second-order-kinetic and intra-particle-diffusion-kinetic

models for Tetraconazole adsorption on Cellulose functionalized with 2,6-pyridine dicarbonyl dichloride.

**Table 3.23: The parameters for pseudo-first-order-kinetic, pseudo-second-order kinetic and intra-particle-diffusion-kinetic models for Tetraconazole removal by Cellulose Functionalized with 2,6-pyridine dicarbonyl dichloride.**

| Adsorption of Tetraconazole on Cellulose Modified with 2,6-pyridine dicarbonyl dichloride | | | | | | |
|---|---|---|---|---|---|---|
| Adsorption Kinetic Models | | | | | | |
| Pseudo First-Order Kinetics | | $q_{exp}$ (mg/g) | Pseudo Second-Order Kinetics | | Intra-Particle Diffusion Kinetics | |
| $q_e$ (mg/g) | $K_1$ ($mg.g^{-1}.min^{-1}$) | 7.992 | $q_e$ (mg/g) | $K_2$ ($g.mg^{-1}.min^{-1}$) | C (mg/g) | $K_p$ ($mg.g^{-1}.min^{-0.5}$) |
| 2.757 | $6.218 * 10^{-3}$ | | 8.091 | 0.141 | 6.7774 | 0.1799 |

### 3.4.6.3 Adsorption Thermodynamics

By using the thermodynamic relation of Van't Hoff plot (equation 1.9). The thermodynamic adsorption parameters (ΔH, ΔG and ΔS) for Tetraconazole on Cellulose functionalized with 2,6-pyridine dicarbonyl dichloride can be measured from the slope and y-intercept of the graph of In $K_d$ versus (1/T), as appears in (Figure 3.74).

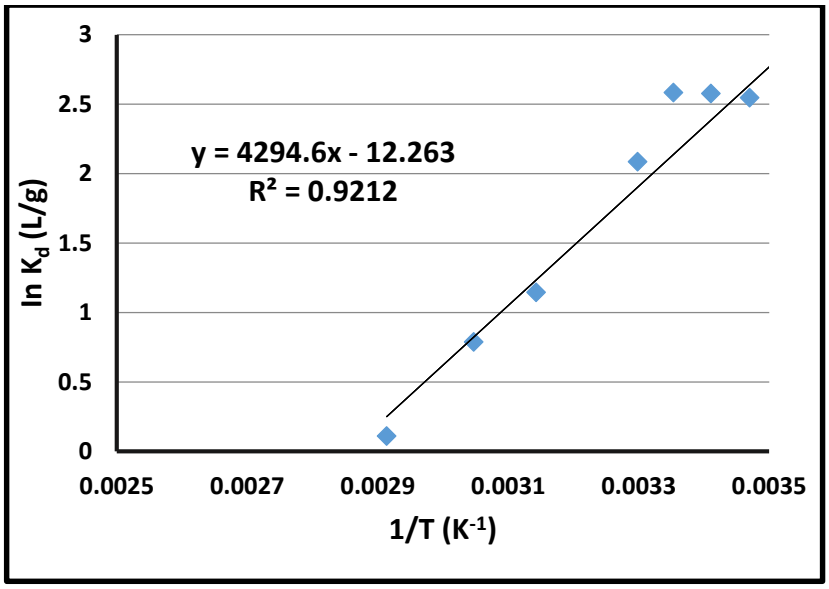


**Figure 3.74:** The plot of Van't Hoff Thermodynamics study for Tetraconazole removal by Cellulose functionalized with 2,6-pyridine dicarbonyl dichloride, (pH = 6, initial concentration = 6 mg/L, adsorption time = 20 minute, nanopolymer dosage = 10 mg, reaction mixture volume = 10 mL).

The following table detects the adsorption thermodynamic parameters (ΔS, ΔG and ΔH) for Tetraconazole pesticide on Cellulose Modified with 2,6-pyridine dicarbonyl dichloride.

**Table 3.24: The thermodynamic parameters for Tetraconazole removal by Cellulose Functionalized with 2,6-pyridine dicarbonyl dichloride.**

| Adsorption of Tetraconazole on Cellulose Modified with 2,6-pyridine dicarbonyl dichloride | | |
|---|---|---|
| Adsorption Thermodynamics | | |
| ΔH (kJ) | Δ°G (kJ) | ΔS (J/K) |
| -35.705 | -5.817 | -101.954 |

The change in standard Gibbs free energy was calculated at the standard temperature (293.15 K), Δ°G equals -5.817 kJ, and enthalpy change ΔH value equals -35.705 kJ. These negative values detect that the adsorption process of Tetraconazole on Cellulose Modified with 2,6-pyridine

dicarbonyl dichloride is feasible and exothermic one ($\Delta H < 0$), as well as, the process is spontaneous ($\Delta G < 0$).

$\Delta S$ of this adsorption process was negative detecting that the randomness at the solid/solution interface decreased during the adsorption reaction. As well as, negative change in the Entropy ($-\Delta S$) detects an existence of an associative reaction mechanism between adsorbate and nanopolymer, such that, no significant change will appear in the internal structure of this adsorbent during adsorption.

### 3.5 Adsorption of Pesticide Mixture

HPLC instrument was used to measure the remained amount for a mixture of total volume 20 mL, containing 10 ppm concentration of Difenoconazole, 10 mL solution, with 10 ppm of Tetraconazole, 10 mL solution, pH of the mixture equals 7, temperature 20 °C and adsorbent dose equals 20 mg using the three adsorbents. The results showed that Tetraconazole showed higher percentages of removal than difenoconazole for the three adsorbent as shown in Table 3.25.

**Table 3.25: Adsorption Results for Difenoconazole and Tetraconazole mixture using CNC, Cel-F and Cel-P adsorbents.**

| Adsorbent | Difenoconazole Percentage removal in the mixture | Tetraconazole Percentage removal in the mixture |
|---|---|---|
| **CNC** | 92.43% | 93.59% |
| **Cel-F** | 93.25% | 95.19% |
| **Cel-P** | 91.25% | 92.76% |

## 3.6 Adsorbents Regeneration

(Figure 3.75) and (Figure 3.76) show the effect of adsorbent recovery for the adsorption of Difenoconazole or Tetraconazole pesticides on Cellulose functionalized with 2-furan carbonyl chloride (Cel-F) or Cellulose functionalized with 2,6-pyridine dicarbonyl dichloride (Cel-P). As shown in the figures, the difference between percentages of pesticides removal after the first and second regeneration of each synthesized cellulose derivative is very low. This is a strong evidence that the synthesized adsorbents can be recycled, and hence be used efficiently for several times.

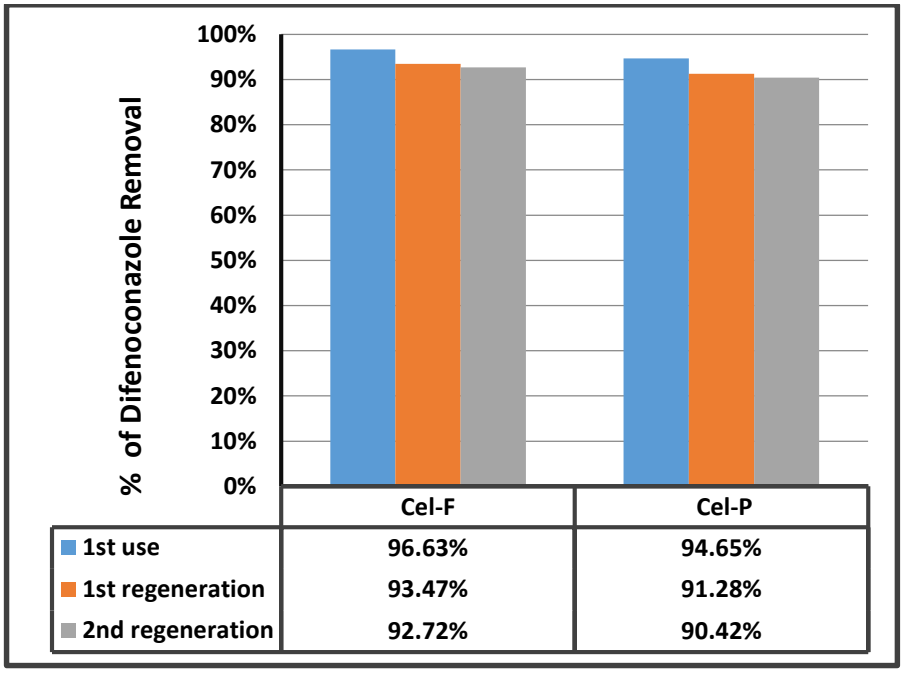


**Figure 3.75:** Nanopolymers Reuse Effect of Difenoconazole pesticide removal by Cellulose functionalized with 2-furan carbonyl chloride (Cel-F) or Cellulose functionalized with 2,6-pyridine dicarbonyl dichloride (Cel-P), (reaction mixture volume = 10 mL).

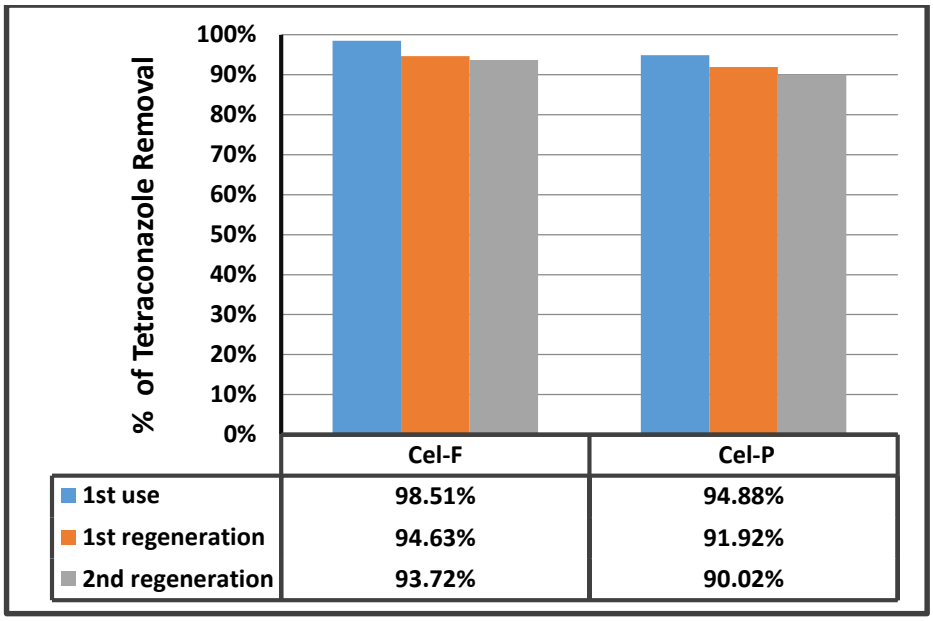


**Figure 3.76:** Nanopolymers Reuse Effect of Tetraconazole pesticide removal by Cellulose functionalized with 2-furan carbonyl chloride (Cel-F) or Cellulose functionalized with 2,6-pyridine dicarbonyl dichloride (Cel-P), (reaction mixture volume = 10 mL).

# CHAPTER FOUR

# CONCLUSION AND RECOMMENDATIONS

## 4.1 Conclusion

Organic pesticides can cause many health and environmental problems due to their excessive toxic properties and poor biodegradability. In this work, novel cellulose-based derivatives modified with different suitable chemical reagents were synthesized, characterized using different analytical instruments including SEM, TGA, $H^1$ NMR and FT-IR spectrometer, and then used for pesticides removal from water.

Synthesis and characterization of the new synthesized adsorbents including "cellulose nanocrystalline, cellulose modified with 2-furan carbonyl chloride and cellulose modified with 2,6-pyridine dicarbonyl dichloride", detect that all adsorbents have promising chemical and thermal stabilities at the studied temperatures. The results indicate that the synthesized compounds behave as perfect adsorbents for difenoconazole and tetraconazole extraction from water to a drinkable degree.

The observed results for this project include:

1. Maximum extent of adsorption was for cellulose modified with 2-furan carbonyl chloride adsorbent in the presence of tetraconazole pesticide with 98.51% as percentage removal. For difenoconazole pesticide, the maximum percent of removal was 96.63% in the presence of the same adsorbent. In case of using cellulose modified

with 2,6-pyridine dicarbonyl dichloride as an adsorbent, the maximum percentage of removal was approximately 95% for both difenoconazole and tetraconazole. While using cellulose nanocrystalline has resulted in percent's of removal of 93.08% and 91.73% for difenoconazole and tetraconazole, respectively.

2. The results detect that adsorption reactions fitted with the Langmuir isotherm of adsorption. Moreover, all the mechanisms were fitted with pseudo-second-order adsorption kinetic model.

3. Novel synthesized cellulose derivatives have promising adsorption efficiencies; as well as, results suggest strong complexation properties between adsorbents and pesticides.

4. Thermodynamic parameters proved that all adsorptions in this project are spontaneous ($\Delta G < 0$) and exothermic processes ($\Delta H < 0$).

5. The regenerated cellulose derivative adsorbents showed very good adsorption capacities and a small effect on percentages of removal for difenoconazole and tetraconazole was detected after multiple reuses.

## 4.2 Recommendations for Future work

- Using the new synthesized cellulose-based derivatives for removing several non-persistent, moderately and persistent pesticides from water.
- Using the novel adsorbents for water purification on a commercial scale in Palestine in the future.
- Using the synthesized adsorbents for removing pesticides from different types of soils in Palestine.
- Adsorption studies of several water organic pollutants on the new synthesized cellulose nanoparticles.
- Preparation of new cellulose nanomembranes modified with different chemical reagents for water treatment.
- Distribution study of pesticides in the soil and water at Jenin city.
- Studying the exposure extent of the Palestinian farmers to toxic pesticides.

# REFERENCES

[1] D. Guha-Sapir, F. Vos, R. Below, S. Ponserre. **Annual Disaster Statistical Review 2013: The Numbers and Trends**. Centre for Research on the Epidemiology of Disasters (CRED), Institute of Health and Society (IRSS), Université Catholique de Louvain, Brussels, 2014, 1–50.

[2] A. Rieu-Clarke, A. Allan, S. Hendry. **Routledge Handbook of Water Law and Policy**, 2017.

[3] **Environmental Outlook to 2050: The Consequences of Inaction**. OECD, 2012.

[4] J. Petersen-Perlman, J. Veilleux, A. Wolf. **International water conflict and cooperation: challenges and opportunities**. Water International 42(2), 2017, 105–120.

[5] **Safe Drinking Water is Essential - Why is Safe Water Essential**, 2016.

[6] **Drinking contaminated water can lead to waterborne diseases**. [Internet]. Vestergaard.com, 2016.

[7] P. Leonard, S. Hearty, J. Brennan, et al. **Advances in biosensors for detection of pathogens in food and water**. Enzyme Microb. Technol. 32(1), 2003, 3–13.

[8] M. Arias-Estévez, E. López-Periago, E. Martínez-Carballo, J. Simal-Gándara, J. Mejuto, L. García-Río. **The mobility and degradation of**

**pesticides in soils and the pollution of groundwater resources**. Agric. Ecosyst. Environ. 123, 2008, 247–260.

[9] P. Hazell, S. Wood. **Drivers of change in global agriculture**. Philos. Trans. R. Soc. Lond. B Biol. Sci. 363, 2008, 495–515.

[10] B. Lin. **Resilience in agriculture through crop diversification: adaptive management for environmental change**. BioScience 61(3), 2013, 183–193.

[11] S. Baker, C. Wilkenson. **The effects of pesticides on human health.** Princeton Sci. Pub., Princeton, 1990.

[12] J. Bumpus, M. Tien, D. Wright, S. Aust. **Oxidation of persistent environmental pollutants by a white rot fungus**. Science 228, 1985, 1434–1436.

[13] J. Bear. **Hydraulics of Groundwater**. Courier Corporation, 2012.

[14] M. Stoytcheva, R. Zlatev. **Pesticides in the Modern World – Trends in Pesticides Analysis**. InTech, Croacia, 2011, 143–164.

[15] Z. Aksu. **Application of Biosorption for the Removal of Organic Pollutants: A review**. Process Biochem. 40, 2005, 997–1026.

[16] H. Fiedler. **Release inventories of polychlorinated dibenzo-p-dioxins and polychlorinated dibenzofurans**. Handbook of Environmental Chemistry (Springer, Berlin Heidelberg), 2016, 1–28.

[17] F. Wania, D. MacKa. **Peer reviewed: Tracking the distribution of persistent organic pollutants**. Environ. Sci. Technol. 30, 1996, 390A–396A.

[18] S. M. Harmon. **The Toxicity of Persistent Organic Pollutants to Aquatic Organisms**. Compr. Anal. Chem., 2015, 587–613.

[19] M. Bigot, D. Muir, D. Hawker, et al. **BengtsonNash, S. Air–seawater exchange of organochlorine pesticides in the southern ocean between australia and antarctica**. Environ. Sci. Technol. 50, 2016, 8001–8009.

[20] S. Lari, N. Khan, et al. **Comparison of pesticide residues in surface water and ground water of agriculture intensive areas**. J. Environ. Health Sci. Eng. 12, 2014, 11–19

[21] P. Prasertsup, N. Ariyakanon. **Removal of chlorpyrifos by water lettuce (Pistia stratiotes L.) and duckweed (Lemna minor L.)**. Int. J. Phytorem. 13, 2011, 383–395.

[22] A. Affam, S. Kutty, M. Chaudhuri. **Solar photo-Fenton induced degradation of combined chlorpyrifos, cypermethrin and chlorothalonil pesticides in aqueous solution**. World Acad. Sci. Eng. Technol. 6(2), 2012, 70–76.

[23] R. Bhagobaty, A. Malik. **Utilization of chlorpyrifos as a sole sources of carbon by bacteria isolated from wastewater irrigated agriculture soils in an industrial area of western Uttar Pradesh, India**. Res. J. Microbiol. 3(5), 2008, 293–307.

[24] R. Agudelo, M. Jaramillo, G. Penuela. **Comparison of the removal of chlorpyrifos and dissolved organic carbon in horizontal sub-surface and surface flow wetlands**. Sci. Total Environ. 431, 2012, 271–277.

[25] J. Bloomfield, R. Williams, D. Gooddy. **Impacts of climate change on the fate and behavior of pesticides in surface and groundwater-a UK perspection**. Sci. Total. Environ. 369(1-3), 2006, 163–177.

[26] M. Gavrilescu. **Fate of pesticides in the environment and its bioremediation**. Eng. Life Sci. 5(6), 2005, 497–526.

[27] S. Batista, E. Silva, S. Galhardo. **Evaluation of pesticide contamination of ground water in two agricultural areas of Portugal.** Int. J. Environ. Anal. Chem. 82 (8), 2002, 601–609.

[28] J. Dunlop, et al. **Options for characterising pesticide risk in the Great Barrier Reef catchments**, 2008, 1–35.

[29] A. Saleh, F. Neiroukh, O. Ayyash, S. Gasteyer. **Pesticide usage in the West Bank.** Applied Research Institute-Jerusalem (ARIJ), 1995, 22.

[30] C. Damalas and S. Koutroubas. **Farmers exposure to pesticides: toxicity types and ways of prevention**. Toxics 4(1), 2016, 1–10.

[31] Z. Zhang, W. Jiang, Q. Jian, et al. **Residues and dissipation kinetics of triazole fungicides difenoconazole and propiconazole in wheat and soil in Chinese fields**. Food Chem., 168, 2015, 396–403.

[32] Z. Wang, T. Yang, D. Qin, Y. Gong, Y. Ji. **Determination and dynamics of difenoconazole residues in Chinese cabbage and soil**. Chinese Chemical Letters 19(8), 2008, 969–972.

[33] F. Dong, et al. **Chiral triazole fungicide difenoconazole: absolute stereochemistry, stereoselective bioactivity, aquatic toxicity, and environmental behavior in vegetables and soil**. Environ. Sci. Technol. 47, 2013, 3386–3394.

[34] G. Crini , A. Saintemarie, S. Rocchi, M. Fourmentin, A. Jeanvoine, L. Millon, N. Morin-Crini. **Simultaneous removal of five triazole fungicides from synthetic solutions on activated carbons and cyclodextrin-based adsorbents.** Heliyon 3(8), 2017, e00380.

[35] I. Saleh, N. Zouari, M. Al-Ghouti. **Removal of pesticides from water and wastewater: Chemical, physical and biological treatment approaches.** Environ. Technol. Innov., 2020, 101026.

[36] F. Suo, X. Liu, C. Li, M. Yuan, B. Zhang, J. Wang, M. Ji. **Mesoporous activated carbon from starch for superior rapid pesticides removal.** Int. J. Biol. Macromol., 121, 2019, 806–813.

[37] G. Ma, M. Zhang, L. Zhu, H. Chen, X. Liu, C. Lu. **Facile synthesis of amine-functional reduced graphene oxides as modified quick, easy, cheap, effective, rugged and safe adsorbent for multi-pesticide residues analysis of tea.** J. Chromatogr. A, 1531, 2018, 22–31.

[38] M. Nazir, Z. Tahir, et al. **Remediation of Pesticide in Water.** In Sustainable Agriculture Reviews 47 Springer, Cham, 2021, 271–307.

[39] S. Menkissoglu, et al. **Dissipation of the fungicide tetraconazole from field-sprayed sugar beets**. J. Agric. Food Chem. 46(12), 1998, 5342–5346.

[40] S. Khalfallah, et al. **Dissipation study of the fungicide tetraconazole in greenhouse-grown cucumbers**. J. Agric. Food Chem. 46(4), 1998, 1614–1617.

[41] Council Directive (2009) Council Directive 2009/82/EC of 13 July 2009 amending directive 91/414/EEC to include tetraconazole as an active substance. Off J. Eur. Union 196, 2009, 10–13.

[42] EFSA (2008). **Conclusion regarding the peer review of the pesticide risk assessment of the active substance tetraconazole**. EFSA Sci. Rep. 2007, 1–86.

[43] W. Zhang, et al. **Effect of tetraconazole application on the soil microbial community**. Environ. Sci. Pollut. Res. 21, 2014, 8323–8332.

[44] A. Mukherjee, et al. **Removal of pesticide residues by mesoporous alumina from water.** IJCS, 7(3), 2019, 1719–1725 .

[45] J. Socorro, et al. **Light induced heterogeneous ozone processing on the pesticides adsorbed on silica particles.** AGUFM, 2013, A51C-0033.

[46] Z. Li, M. Hou, S. Bai, C. Wang, Z. Wang. **Extraction of imide fungicides in water and juice samples using magnetic graphene nanoparticles as adsorbent followed by their determination with gas chromatography and electron capture detection.** Analytical Sciences, 29(3), 2013, 325–331.

[47] C. Masselon, G. Krier, J. Muller, S. Nelieu, J. Einhorn. **Laser desorption Fourier transformation cyclotron resonance mass spectrometry of selected pesticides extracted on C18 silica solid-phase extraction membranes**. Analyst. 121, 1996, 1429–1433.

[48] M. Mahalakshmi, B. Arabindoo, M. Palanichamy, V. Murugesan. **Photocatalytic degradation of carbofuran using semiconductor oxides**. J Hazard. Mater. 143, 2007, 240–245.

[49] M. Maldonado, S. Malato, L. Perez-Estrada, W. Gernjak, I. Oller, Dom´enech X, Peral J. **Partial degradation of five pesticides and an industrial pollutant by ozonation in a pilot-plant scale reactor**. J. Hazard. Mater. 38, 2006, 363–369.

[50] Mart´ın MMB, S´anchez P´erez JA, S´anchez JLG, Montes de Oca L, Casas L´opez JL, Oller I, Rodr´ıguez SM. **Degradation of Alachlor and pyrimethanil by combined photo-fenton and biological oxidation**. J Hazard Mater. 155, 2008, 342–349.

[51] P. Saritha, C. Aparna, V. Himabindu, Y. Anjaneyulu. **Comparison of various advanced oxidation processes for the degradation of 4-chloro-2 nitrophenol**. J. Hazard. Mater. 149, 2007, 609–614.

[52] A. Lagadec, D. Miller, A. Lilke, S. Hawthorne. **Pilot-scale subcritical water remediation of polycyclic aromatic hydrocarbons- and pesticide-contaminated soil**. Environ. Sci. Technol. 34, 2000, 1542–1548.

[53] H. Rajashekara, H. Manonmani. **Aerobic degradation of technical hexachlorocyclohexane by a defined microbial consortium**. J. Hazard. Mater. 149, 2007, 18–25.

[54] A. Ahmad, L. Tan, S. Shukor. **Dimethoate and atrazine retention from aqueous solution by nanofiltration membranes**. J. Hazard. Mater.151, 2008, 71–77.

[55] Z. Jia, Y. Li, S. Lu, H. Peng, J. Ge, S. Chen. **Treatment of organophosphate contaminated waste water by acidic hydrolysis and precipitation**. J. Hazard. Mater. 129, 2006, 234–238.

[56] M. Danish, O. Sulaiman, M. Rafatullah, R. Hashim, A. Ahmad. **Kinetics for the removal of paraquat dichloride from aqueous solution by activated date (Phoenix dactylifera) stone carbon**. J. Disp. Sci. Tech. 31, 2010, 248–259.

[57] I. Ali, V. Gupta. **Advances in water treatment by adsorption technology**. Nat. Protoc. 1, 2006, 2661–2667.

[58] B. Srivastava, V. Jhelum, D. Basu, P. Patanjali. **Adsorbents for pesticide uptake from contaminated water: a review**. J. Sci. Ind. Res. 68, 2009, 839–850.

[59] **Status of the Environment in the State of Palestine – 2015**. Applied Research Institute-Jerusalem (ARIJ), 2015.

[60] Amnesty International, Troubled Waters. **West Bank and Gaza - Assessment of restrictions on Palestinian water sector development**. 2009, 17.

[61] Palestinian Water Authority. **Palestine: The Right to Water**, 2011, 4.

[62] S. Samhan. **Obstacles to enhance groundwater aquifer by reclaimed water using artificial recharge as a reuse option in West Bank, Palestine**. In: Proc. INNOVA-MED Workshop on New Technologies of non-Conventional Water Recycling and New Challenges for Arid and Semi - Arid Areas. Agadir, Morocco, 2008.

[63] A. Pier, D. Consonni, S. Bachetti, M. Rubagotti, A. Baccarelli, C. Zocchetti, A. Pesatori. **Health Eff ects of Dioxin Exposure: A 20-Year Mortality Study**. American J. Epidem 153(11), 2001, 1031–1044.

[64]M. Yassin, T. Abu Mourad, J. Safi. **Knowledge, attitude, practice, and toxicity symptoms associated with pesticide use among farm workers in the Gaza Strip**. Occup. Environ. Med. 59, 2002, 387–393.

[65] J. Piccin, et al. **Adsorption Isotherms and Thermochemical Data of FD&C RED N° 40 Binding by Chitosan.** Braz. J. Chem. Eng. 28(2), 2011, 295–304.

[66] M. Ghiaci, A. Abbaspur, R. Kia, F. Seyedeyn-Azad. **Equilibrium isotherm studies for the sorption of benzene, toluene, and phenol onto Organozeolites and as-synthesized MCM-41**. Sep. Purif. Technol. 40, 2004, 217–229.

[67] M. Ncibi. **Applicability of some statistical tools to predict optimum adsorption isotherm after linear and non-linear regression analysis,** J. Hazard. Mater. 153, 2008, 207–212.

[68] O. Sylvester, et al. **Proposing a new empirical adsorption isotherm known as Adejo-Ekwenchi isotherm**. J. Appl. Chem., 2014, 66–71.

[69] K. Foo and B. Hameed. **Insights into the modeling of adsorption isotherm systems**. Chem. Eng. J. 156, 2010, 2–10.

[70] H. Qiu, L. Lv, B. Pan, Q. Zhang, W. Zhang, Q. Zhang. **Critical Review in Adsorption Kinetic Models**. J. Zhejiang Univ. Sci. A 10, 2009, 716–724.

[71] J. He, S. Hong, L. Zhang, F. Gan, Y. Ho. **Equilibrium and Thermodynamic Parameters of Adsorption of Methylene Blue onto Rectorite**. Fresenius Environ. Bull. 19, 2010, 2651–2656.

[72] D. Sridev, K. Rajendran. **Synthesis and Optical Characteristics of ZnO Nanocrystals**. Bull. Mater. Sci. 32, 2009, 165–168.

[73] L. Ferrari and et al. **Interaction of cement model systems with super plasticizers investigated by atomic force microscopy, zeta potential, and adsorption measurements**. J. Colloid Interface Sci., 2010, 15–24.

[74] Y. Bai, et al. **Removal of Cadmium from wastewater using ion exchange resin amberjet 1200H columns**. Pol. J. Environ. Stud. 18, 2009, 1191.

[75] A. Agrawal, K. Sahu. **Kinetics and isotherm studies of cadmium adsorption on manganese nodule residue**. J. Hazard. Mater. 137, 2009, 915–924.

[76] Y. Li, S. Wang, Z. Luan, J. Ding, C. Xu, D. Wu. **Adsorption of Cadmium (II) from aqueous solution by surface oxidized carbon Nanotubes**. J. of Elsevier. 41, 2003, 1057–1062.

[77] I. Tan, B. Hameed, A. Ahmad. **Equilibrium and Kinetic studies on basic dye adsorption by oil palm fiber activated carbon**. J. Chem. Eng. 127, 2007, 111–119.

[78] J. Lin, L. Wang. **Comparison between linear and non-linear forms of pseudo-first-order and pseudo-second-order adsorption kinetic models for the removal of Methylene blue by activated carbon**. J. of Environ. Sci. Engin. 83, 2009, 11–17.

[79] S. Ardizzone, F. Dioguardi, T. Mussini, P. Mussini, S. Rondini, B. Vercelli, A. Vertova. Cellulose 5, 1999, 57.

[80] L. Hakka, D. Brown. **Recovery and Recycling of $SO_2$ in A Sulfite Pulp Mill**. Sulphur 98, 1998, 1–4.

[81] P. Loureiro, M. Dominguesc, A. Fernandesd, M. Grac, V. Carvalho, D. Evtuguina. **Discriminating The Brightness Stability of Cellulosic**

**Pulp In Relation To The Final Bleaching Stage.** Carbohydrate Polymers 88, 2012, 726–733.

[82] A. Shatalov, H. Pereira. **Polysaccharide Degradation During Ozone-Based TCF Bleaching of Non-Wood Organosolv Pulps**. Carbohydrate Polymers 67, 2007, 275–328.

[83] O. Hamed, S. Jodeh, N. Al-Hajj, A. Abo-Obeid, E. Hamed, Y. Fouad. **Cellulose acetate from biomass waste of olive industry.** J. WOOD Sci. 61(1), 2015, 45–52.

[84] M. Achor, Y. Oyeniyi, A. Yahaya. **Extraction and characterization of microcrystalline cellulose obtained from the back of the fruit of Lageriana siceraria (water gourd)**. J. Appl. Pharma. Sci. 4(1), 2014, 57–60.

[85] S. Yuldoshov, A. Sarymsakov, N. Ashurov, et al. **Kinetics of solid-phase carboxymetyllation of cotton and microcrystalline cellulose**. Macromol. Ind. J. 10(2), 2014, 69–72.

[86] M. Ioelovich, A. Leykin. **Microcrystalline cellulose: nanostructure formation**. Cellulose Chem. Technol. 40, 2006, 313–317.

[87] L. Qingqing. **Nanocellulose: Preparation, characterization, supramolecular modeling, and its life cycle assessment**. A Dissertation submitted to the Faculty of Virginia Polytechnic Institute and State University in Partial Fulfillment of the Requirements for the Degree of Doctor of Philosophy in Forest Products, Blacksburg, Virginia, 2012.

[88] M. Ioelovich. **Cellulose as a nanostructured polymer**. Bio Res. 3(4), 2008, 1403–1418.

[89] B. Braun, J. Dorgan. **Single Step Method for the Isolation and Surface Functionalisation of Cellulosic Nanowhiskers.** Biomacromol. 10(2), 2009, 334–341.

[90] M. Ioelovich, O. Figovsky, A. Leykin**. Nano cellulose and its applications.** Proceedings of 7th World Congress Nano composite-2007; 2007 Sep 05-07; Las Vegas, USA.

[91] J. Cuculo, C. Smith, U. Sangwatanaroj, E. Stejskal, S. Sankar. **A study on the mechanism of dissolution of the cellulose/$NH_3$/$NH_4SCN$ system**. I. J Polym Sci, Part A: Polym. Chem. 32, 1994, 229–239.

[92] H. Jin, C. Zha, L. Gu. **Direct dissolution of cellulose in NaOH/thiourea/urea aqueous solution**. Carbohydr. Res. 342, 2007, 851–858.

[93] A. El-Kafrawy. **Investigation of the cellulose/LiCl/dimethylacetamide and cellulose/LiCl/N-methyl-2-pyrrolidinone solutions by 13C NMR spectroscopy**. J. Appl. Polym. Sci. 27, 2010, 2435–2443.

[94] T. Belousova, M. Shablygin, Y. Belousov, L. Golova, S. Papkov. **Spectral features of the N-methylmorpholine-N-oxide-water-cellulose system**. Polym. Sci. USSR 28, 1986, 1115–1122.

[95] M. Isik, H. Sardon, D. Mecerreyes. **Ionic liquids and cellulose: dissolution, chemical modification and preparation of new cellulosic materials**. Int. J. Mol. Sci. 15, 2014, 11922–11940

[96] C. Zhang, R. Liu, J. Xiang, H. Kang, Z. Liu, Y. Huang. **Dissolution mechanism of cellulose in N,N-Dimethylacetamide/ lithium chloride: revisiting through molecular interactions**. J. Phys. Chem. B 118, 2014, 9507–9514.

[97] Y. Wei, F. Cheng. **Effect of solvent exchange on the structure and rheological properties of cellulose in LiCl/ DMAc**. J. Appl. Polym. Sci. 106, 2007, 3624–3630.

[98] W. Wang, Y. Li, W. Li, B. Zhang, Y. Liu. **Effect of solvent pre-treatment on the structures and dissolution of microcrystalline cellulose in lithium chloride/dimethylacetamide.** Cellulose 26(5), 2019, 3095–3109.

[99] A. Potthast, et al. **Comparison testing of methods for gel permeation chromatography of cellulose: coming closer to a standard protocol**. Cellulose 22, 2015, 1591–1613.

[100] B. Lindman, B. Medronho, L. Alves, C. Costa, H. Edlund, M. Norgren. **The relevance of structural features of cellulose and its interactions to dissolution, regeneration, gelation and plasticization phenomena**. Chem. Phys. 19, 2017, 23704–23718.

[101] D. Ishii, D. Tatsumi, T. Matsumoto. **Effect of solvent exchange on the supramolecular structure, the molecular mobility and the**

**dissolution behavior of cellulose in LiCl/DMAc**. Carbohydr Res 343, 2008, 919–928.

[102] S. Chrapava, D. Touraud, T. Rosenau, A. Potthast, W. Kunz. **The investigation of the influence of water and temperature on the LiCl/DMAc/cellulose system**. Phys. Chem.5, 2003, 1842–1847.

[103] W. Coffey. **Finite integral representation of characteristic times of orientational relaxation processes: Application to the uniform bias force effect in relaxation in bistable potentials**. Adv Chem Phys. 103, 1998, 259–333.

[104] M. de Souza Lima, R. Borsali. **Cellulose Microcrystals: Structure, Properties, and Applications**. Macromol Rapid Commun. 25(7), 2004, 771–787.

[105] M. Mariño, L. Lopes da Silva, N. Nelson Durán, L. Tasic. **Enhanced Materials from Nature: Nanocellulose from Citrus Waste**. Molecules 20 2015, 5908–5923.

[106] M. Granström. **Cellulose Derivatives: Synthesis, Properties and Applications**, 2009.

[107] R. Moon, A. Martini, J. Nairn, J. Simonsen. **Cellulose nanomaterials review: structure, properties and nanocomposites**. Chem. Soc. Rev. 40, 2011, 3941–3994.

[108] W. Haoran, R. Katia, R. Scott, J. Peter. **Environmental science and engineering applications of NanoCellulose-based nanocomposites.** Environ. Sci. Nano 1, 2014, 302–316.

[109] Ch. Hayashi, R. Uyeda, A. Tasaki. **Ultra-fine Particles: Exploratory Science and Technology**. Exploratory science and technology, 1997.

[110] C. Salas, T. Nypelö, C. Rodriguez-Abreu, C. Carrillo, O. Rojas. **Nanocellulose: Properties and Applications in Colloids and Interfaces**. Curr. Opin. Colloid Interface Sci. 19 (5), 2014, 383–396.

[111] C. Chirayil, L. Mathew, S. Thomas. **Review of Recent Research in Nano Cellulose Preparation From Different Lignocellulosic Fibers**. Rev .Adv. Mater. Sci. 37: 2014, 20–28.

[112] M. Rashed. **Adsorption Technique for the Removal of Organic Pollutants from Water and Wastewater**. Organic Pollutants Monitoring, Risk and Treatment, 2013, 167–194.

[113] A. Dąbrowski. **Adsorption—From Theory to Practice.** Colloid Interface Sci. 93, 2001, 135–224.

[114] Y. Salameh. **Methods for extracting Cellulose material from Olive Pulp**. MSc Thesis, An-Najah National University, 2009.

[115] M. Ugurlu, A. Gurses, M. Acıkyıldız. **Comparison of textile dyeing effluent adsorption on commercial activated carbon and activated carbon prepared from olive stone by $ZnCl_2$ activation**. Microporous Mesoporous Mater. 111, 2008, 228–235.

[116] B. Medronho, B. Lindman. **Competing forces during cellulose dissolution: from solvents to mechanisms**. Curr Opin Colloid Interface Sci. 19, 2014, 32–40.

[117] L. Ramos, D. Morgado, F. Gessner, et al. **A physical organic chemistry approach to dissolution of cellulose: effects of cellulose mercerization on its properties and on the kinetics of its decrystallization**. Arkivoc 7, 2011, 416–425.

[118] K. Kowsaka, K. Okajima, K. Kamide. **Two-dimensional nuclear magneticresonance spectra of cellulose and cellulose triacetate.** Polym. J. 20(12), 1988, 1091–1099.

[119] A. Isogai. **NMR analysis of cellulose dissolved in aqueous NaOH solutions**. Cellulose, 4(2), 1997, 99–107.

[120] D. Sridev, K. Rajendran. **Synthesis and Optical Characteristics of ZnO Nanocrystals**. Bull. Mater. Sci. 32, 2009, 165–168.

جامعة النجاح الوطنية

كلية الدراسات العليا

# تنقية المياه في فلسطين من المبيدات الزراعية الثابتة بواسطة جسيمات سليولوز نانونية حديثة التحضير

إعداد

بيان محمد محمود خلف

إشراف

أ.د. شحدة جودة

أ.د. عثمان حامد

قدمت هذه الأطروحة استكمالاً لمتطلبات الحصول على درجة الدكتوراة في الكيمياء بكلية الدراسات العليا في جامعة النجاح الوطنية، نابلس، فلسطين.

2021

**تنقية المياه في فلسطين من المبيدات الزراعية الثابتة بواسطة جسيمات سليولوز نانونية حديثة التحضير**

**إعداد**

**بيان محمد محمود خلف**

**إشراف**

**أ.د. شحدة جودة**

**أ.د. عثمان حامد**

## الملخص

في هذا البحث تم استخدام السليلوز المستخلص من الجفت الناتج بكميات هائلة من مخلفات معاصر الزيتون في فلسطين و كذلك جزيئات النانوسليلوز المحضرة من السليلوز، و من ثم تطوير العديد من المواد المازة الجديدة المركبة من مشتقات السليلوز و المعدّلة بمركبات كيميائية مناسبة ، من أجل تنقية المياه من المبيدات السامة و هي ديفينوكونازول و تتراكونازول ، بحيث نحصل على مياه نظيفة صالحة للشرب.

تم فحص المركبات التي تم تحضيرها باستخدام أجهزة تحليلية متقدمة في مركز أبحاث يوليش في ألمانيا و جامعة النجاح الوطنية في فلسطين من أجل تحديد ثباتيتها الكيميائية والحرارية. و من ثم تحديد الظروف المثالية بحيث نحصل على أقصى نسبة مئوية للتنقية ، كذلك تحديد الخواص الحركية للتفاعلات ومعاملات الديناميكيا الحرارية. ويمتاز هذا البحث بأن المواد المحضرة للتنقية رخيصة التكلفة و فعاليتها كبيرة بحيث يمكن تطبيقها على المستوى المحلي لتنقية المياه.

في البداية تم تحضير محاليل معيارية معروفة التراكيز من دافينوكونازول و تتراكونازول، و بعدها تمت إزالة هذه العناصر السامّة بالإعتماد على طريقة الإمتزاز ، حيث حُضّرت ثلاثة مركبات ذات خصائص سطحية ممتازة و هذه المواد هي:

Cellulose Nanocrystalline, Cellulose modified with 2-furan carbonyl chloride and Cellulose modified with 2,6-pyridine dicarbonyl dichloride

، و من ثُمّ تمّ فحص صفات هذه المركبات و ثباتية كلٍ منها كيميائياً و حرارياً باستخدام تقنيات و أجهزة عديدة أثبتت أنّ هذه المركبات المصنعة ذات قدرة كبيرة على إزالة المبيدات السامة من المياه ، مما يعني كفاءتها كمواد مازة.

تم اختبار العديد من الظروف المختلفة مثل: زمن التحريك، درجة الحرارة، درجة الحموضة، التركيز الإبتدائي للمادة المُمتزة، و كمية المادة المازة، و ذلك من أجل معرفة الظروف المثالية التي تؤدي إلى أكبر نسبة إزالة للمبيدات بطريقة فعالة.

أشارت النتائج أنّ عملية الإمتزاز كانت أفضل عند درجات الحرارة المنخفضة حيث أنّ درجة الحرارة المثالية لأغلب عمليات الإمتزاز كانت عند درجة حرارة الغرفة أو أقل من ذلك؛ و بالنسبة لدرجة الحموضة المثالية فكانت تتراوح بشكل عام ما بين 4 و8؛ أما بالنسبة لوقت الإتصال الأمثل ما بين المادة المازة و المُمتزة فكان قليل جداً لأغلب العمليات، و كان الوقت الأطول هو 60 دقيقة و ذلك عند استخدام الدافينوكونازول مع مادة Cellulose functionalized with 2,6-pyridine dicarbonyl dichloride

أشارت النتائج النهائية أنّ أعلى نسبة إزالة للدافينوكونازول كانت بقيمة 96.63 % وذلك بوجود المادة المازة Cellulose functionalized with 2-furan carbonyl chloride ، أما بالنسبة لازالة مبيد التتراكونازول فكانت النسبة 98.51% وذلك باستخدام نفس المادة المازة.

بعد ذلك، تم تطبيق عمليات الإمتزاز المختلفة على نماذج الإمتزاز ثابتة الحرارة

(Langmuir and Freundlich Isotherms) ، حيث تم ملاحظة أنّ كل عمليات الإمتزاز كانت تابعة لنموذج (Langmuir) و بالتالي فهي إمتزازات كيميائية، مما يدل على وجود روابط كيميائية حقيقية ما بين كل من المادة المازة و المُمتزة.

من أجل معرفة ميكانيكية كل من تفاعلات الإمتزاز ؛ تم تطبيق هذه العمليات على نماذج الإمتزاز الحركية و هي:

“Pseudo-first-order adsorption kinetic model, pseudo-second-order adsorption kinetic adsorption and intra-particle diffusion adsorption kinetic model”

و بالإعتماد على قيمة معامل الإرتباط لكل عملية إمتزاز ؛ كانت النتائج تشير أنّ كل تفاعلات الإمتزاز في البحث تابعة لنموذج (Pseudo second-order kinetics).

و أيضاً تم رسم مخطط (Van’t Hoff plot) من أجل معرفة دلائل الديناميكا الحرارية لعمليات الإمتزاز المختلفة ، و أشارت النتائج أنّ جميع هذه العمليات باعثة للحرارة ($\Delta H < 0$) و تحدث بصورة تلقائية ($\Delta G < 0$) عند درجة حرارة الغرفة. في النهاية تم إعادة استخدام المواد المازة مرة أخرى من أجل معرفة أثر ذلك على نسبة المبيدات الزراعية. بشكل عام ؛ أشارت نتائج هذا البحث أنّ المواد المازة التي تم تحضيرها كانت فعالة جداً في إزالة مبيدات الدافينوكونازول و التتراكونازول من المياه.